AD A090778

Low Drag Airfoil Design Utilizing Passive Laminar Flow and Coupled Diffusion Control Techniques

R. L. Mask

Vought Corporation Advanced Technology Center
Dallas, Texas 75266

September 1980

Final Report for Period September 1977 – December 1979

Approved for public release, distribution unlimited

Prepared for:

Department of the Navy
Naval Air Development Center
Warminster, Pennsylvania 18974

VOUGHT CORPORATION
advanced technology center

80 10 16 057

14 ATC-R-11100/9CR-71

REPORT DOCUMENTATION PAGE	READ INSTRUCTIONS BEFORE COMPLETING FORM

1. REPORT NUMBER	2. GOVT ACCESSION NO.	3. RECIPIENT'S CATALOG NUMBER
NADC 79119-60	AD-A090778	

4. TITLE (and Subtitle)
LOW DRAG AIRFOIL DESIGN UTILIZING PASSIVE LAMINAR FLOW AND COUPLED DIFFUSION CONTROL TECHNIQUES

5. TYPE OF REPORT & PERIOD COVERED
FINAL REPORT.
30 Sep 1977 - 1 Dec 1979

6. PERFORMING ORG. REPORT NUMBER
R-91100/9CR-71

7. AUTHOR(s)
B. L. Mask

8. CONTRACT OR GRANT NUMBER(s)
N62269-77-C-0442
N62269-79-C-0277

9. PERFORMING ORGANIZATION NAME AND ADDRESS
VOUGHT CORPORATION ADVANCED TECHNOLOGY CENTER
P. O. BOX 226144
DALLAS, TEXAS 75266

10. PROGRAM ELEMENT, PROJECT, TASK AREA & WORK UNIT NUMBERS
84

11. CONTROLLING OFFICE NAME AND ADDRESS
NAVAL AIR DEVELOPMENT CENTER
CODE 6053
WARMINSTER, PENNSYLVANIA 18974

12. REPORT DATE
SEPTEMBER 1980

13. NUMBER OF PAGES
83

14. MONITORING AGENCY NAME & ADDRESS(if different from Controlling Office)

15. SECURITY CLASS. (of this report)
UNCLASSIFIED

15a. DECLASSIFICATION/DOWNGRADING SCHEDULE

16. DISTRIBUTION STATEMENT (of this Report)

This document has been approved for public release and sale; its distribution is unlimited.

17. DISTRIBUTION STATEMENT (of the abstract entered in Block 20, if different from Report)

18. SUPPLEMENTARY NOTES

19. KEY WORDS (Continue on reverse side if necessary and identify by block number)
Natural/Passive Laminar Flow Wing, Laminar Flow Stabilization, Passive/Active Boundary Layer Control, Low Drag Airfoil, Airfoil/Wing, Aerodynamics, Energy Efficient Wing, High Reynolds Number Laminar Flow, Laminar Flow

20. ABSTRACT (Continue on reverse side if necessary and identify by block number)
A two-dimensional high chord Reynolds number passive laminar airfoil was designed for a $C_l = 0.73$ at a $M_\infty = 0.6$ and $Re_c = 4 \times 10^7$ providing an extremely high $L/D = 240$. This laminar airfoil design concept integrates passive laminar flow stabilization, by pressure gradient shaping, with active diffusion control techniques on the airfoil trailing edge. A discussion of the airfoil design concept and the predicted performance is presented. Full scale Reynolds number passive laminar flow/transition experiments defining maximum transition →next page

DD FORM 1473 EDITION OF 1 NOV 68 IS OBSOLETE
1 JAN 73
S/N 0102-014-6601

SECURITY CLASSIFICATION OF THIS PAGE(When Data Entered)

Reynolds number and real flow environment influence on transition are presented. Examination of wind tunnel scaling influences and real flow environment effects on the ATC/laminar airfoil performance are discussed and summarized for typical low turbulence tunnels, (e.g., the NASA-Ames 12 foot pressure tunnel).

FOREWORD

This investigation was performed by Vought Corporation Advanced Technology Center, Dallas, Texas for the Naval Air Development Center (Contracts No. N62269-77-C-0442 and N62269-79-C-0277) under the auspices of the Naval Air Systems Command. The NADC contract monitor was Dr. K. T. Yen and the NASC administration was performed by Mr. R. F. Siewert and Mr. D. Kirkpatrick.

\

ii

TABLE OF CONTENTS

LIST OF FIGURES

NOMENCLATURE

a	Amplification ratio
C	Chord length
C_d	Drag coefficient
C_ℓ	Lift coefficient
C_p	Pressure coefficient
C_μ	Blowing jet momentum coefficient
K	Roughness height/width
L	Air Boundary Layer Channel length (304.5 inches)
L/D	Lift to drag ratio
M	Mach number
Re	Reynolds number
s	Surface arc length
T	Turbulence intensity
U	Velocity
ω	Non-dimensional frequency
X	Distance
β	Hartree parameter
ν	Kinematic viscosity

Subscripts:

c	Evaluated for chord length
crit	Evaluated at the critical value
K	Evaluated at the roughness element
tran	Evaluated at transition
∞	Freestream conditions

1.0 INTRODUCTION

In recent years, increased attention has been given to the stabilization of laminar flow on wings and bodies because of the resultant benefits of drag reduction and improvements in energy efficiency. The benefits associated with laminar flow stabilization have been widely acknowledged as the most promising concept for achievement of high energy efficiency. This concept has been of particular interest for advanced subsonic military/commercial aircraft missions requiring long-range or high endurance with heavy loads. Two fundamental concepts currently being considered for new-technology laminar flow wing design are: (1) a passive concept utilizing pressure gradient shaping, and (2) an active concept consisting of distributed and discrete suction. The primary design objectives of an advanced laminar airfoil design are to maintain large regions of laminar flow at high chord Reynolds numbers (high transition Reynolds numbers) and to diffuse the flow to the trailing edge pressure without separation. To maintain laminar flow passively at high chord Reynolds numbers of $25-40 \times 10^6$, large favorable forward pressure gradients are required, which in turn increase the trailing edge pressure recovery and flow separation problems. In view of this design constraint, conventional applications of passive stabilization of laminar flow have been limited to transition Reynolds numbers less than 15×10^6 and maximum transition locations less than 60 percent chord. To utilize the passive concept at higher Reynolds numbers, trailing edge pressure recovery requirements necessitate some form of trailing edge boundary layer control (BLC). In the absence of an efficient discrete method to rapidly diffuse the trailing edge flow, existing approaches to laminar flow control at high Re_c have emphasized designs compatible with distributed and discrete suction wing technology design.[1,2] An inherent problem in this approach is the highly complex skin/ducting suction system that is required. The present approach which combines the full potential of passive laminar flow contouring with unique active diffusion control methods for rapid efficient trailing edge pressure recovery is an appealing alternative. The basic device utilized for active diffusion control is the Antiseparation Tailored Contour (ATC).

This report covers the work performed under two successive contract phases preparing the technology for follow-on tunnel/flight validation of the ATC/laminar airfoil design concept. The objectives of these efforts were:

1

Phase I - Contract No, N62269-77-C-0442

Design of a low drag high Reynolds number airfoil utilizing passive
laminar flow and coupled diffusion control techniques to obtain
improved lift-to-drag ratios for advanced subsonic aircraft application.
Perform full scale Reynolds number laminar/transition flow experiments
to validate the passive laminar flow stabilization concept including a
limited assessment of real flow disturbance effects.

Phase II - Contract No. N62269-79-C-0277

Define wind tunnel real flow environment interaction with full scale
Reynolds number passive laminar flow stabilization and identify the
ATC/laminar airfoil validation envelopes. The contract scope included:
limited test facility/configuration evaluation (candidate tunnel-NASA-Ames
12 foot pressure tunnel), tunnel scaling influences (freestream turbulence,
unit Reynolds number, surface perturbation, model/freestream temperature),
preliminary model design, definition of validation objectives/plans, and
crossflow stability assessment.

This report discusses the ATC/laminar airfoil concept design and perfor-
mance, presents full scale Reynolds number laminar/transition flow simulation
experimental results for the design point configuration, examines validation
environment influences on the design/off design performance, identifies valida-
tion potential for candidate tunnels, defines preliminary model design/fabrica-
tion tolerances, and addresses crossflow degradation.

2.0 ATC/LAMINAR AIRFOIL

2.1 CONCEPT

The ATC/laminar airfoil concept is an integration of passive laminar flow
stabilization with active diffusion boundary layer control to provide a high
Reynolds number low drag airfoil design. The low drag benefits associated
with a stable laminar boundary layer are illustrated in Figure 2-1, identifying
flat plate drag reductions. For example, laminar flow over 80 percent of the
chord length, defined by $X/C_{tran} = 0.8$, provides a 60 percent reduction in
drag at $Re_c = 10^7$, with reference to a fully turbulent flat plate. Because
the drag reduction is not linear with transition location, the percent of
performance improvements for a delta improvement in X/C_{tran} is larger with
increasing X/C_{tran} values. Note also for a fixed transition location the
drag improvement increases slightly with increasing Re_c. The ATC/laminar
airfoil concept maximizes the low drag benefits at high Reynolds numbers by
tailoring the pressure gradient to obtain large regions of stable laminar
boundary layer growth. Maximization of the airfoil design/off-design performance
is permitted by the relaxed trailing edge pressure recovery constraints obtained
by the integration of an active diffusion boundary layer control concept, which
couples a wall jet with surface/pressure-gradient shaping, Figure 2-2. The
active diffusion control concept is based on the hypothesis that by properly
energizing the mainstream boundary layer existing at the wall jet, significant
diffusion over a short distance is possible.[3] This permits flexibility in the
design for large regions of stable laminar flow. A key characteristic of the
ATC device is the low auxiliary blowing rate (or engine bleed) required for full
BLC. This permits the use of relatively low pressure fan air for bleed without
having prohibitive mass flow requirements. Validation of the active diffusion
control concept, denoted as an Anti-separation Tailored Contour (ATC), has been
obtained experimentally for several subsonic STOL and supercritical cruise/
maneuvering wing designs, demonstrating efficient boundary layer energization.[4-6]

2.2 DESIGN

A high chord Reynolds number ATC/laminar airfoil geometry was defined using
the passive laminar flow stabilization concept coupled with active diffusion
trailing edge boundary layer control. The airfoil design objective was directed
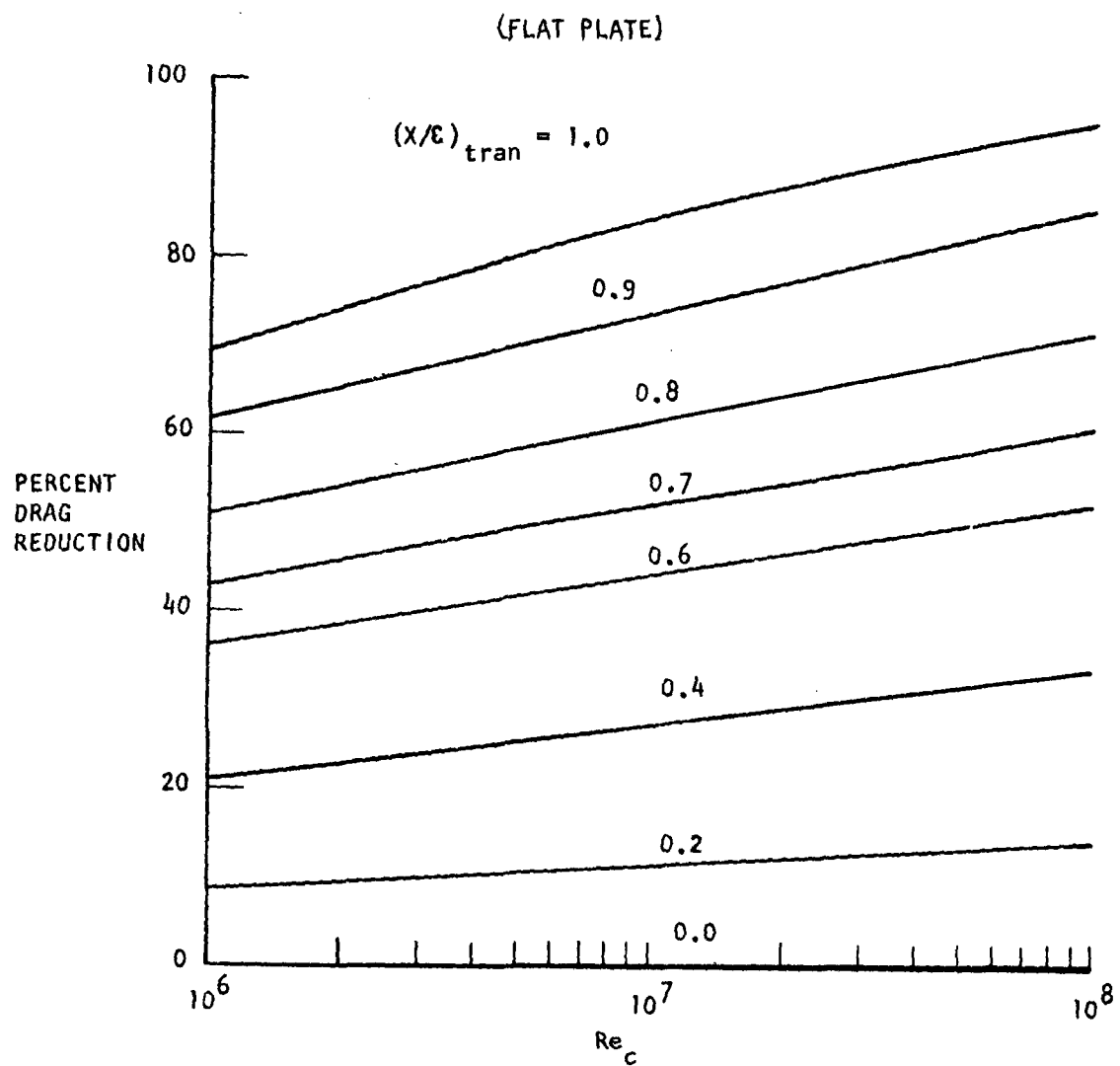at maximizing the L/D performance of a high Reynolds number airfoil for a cruise

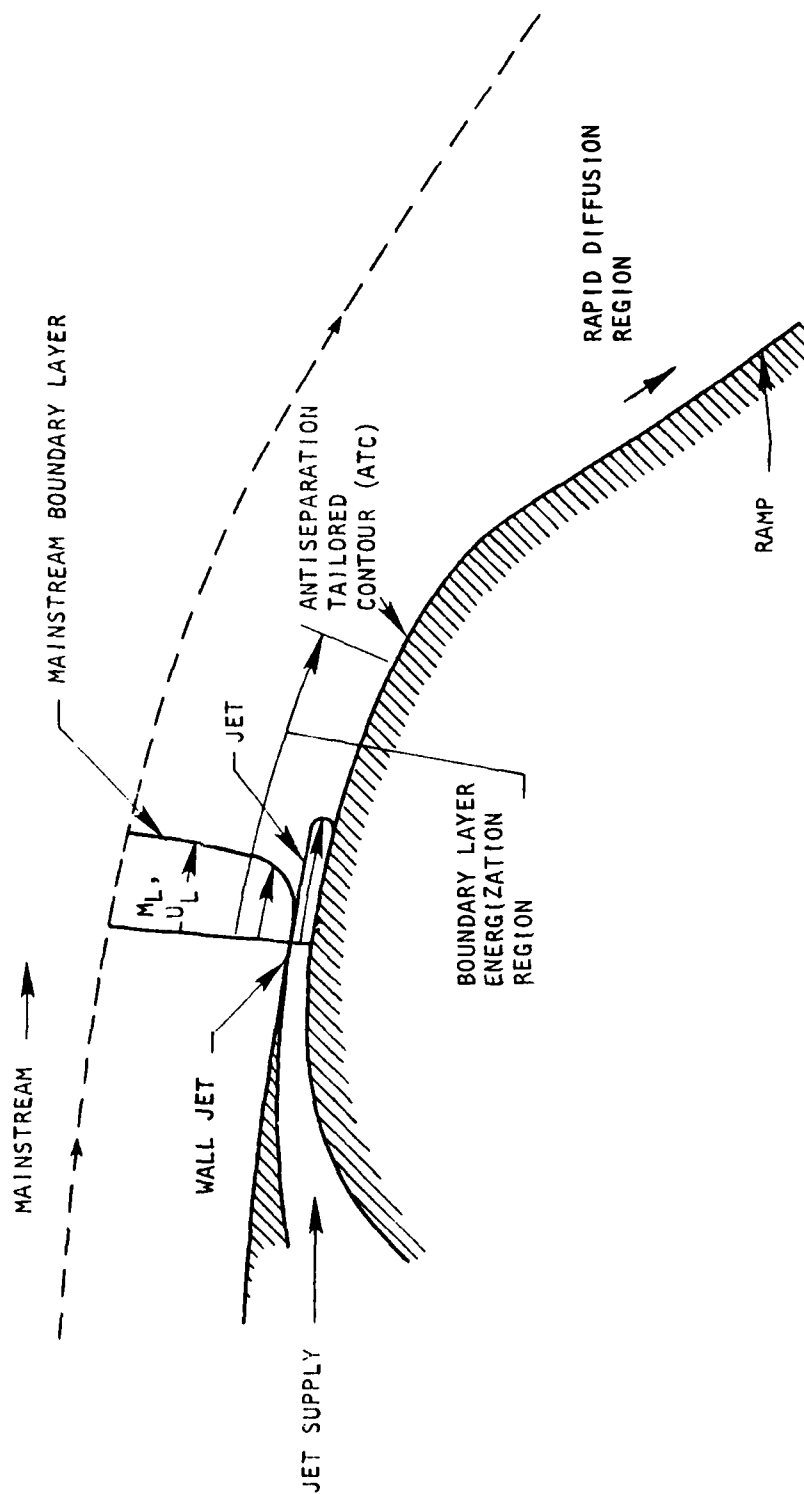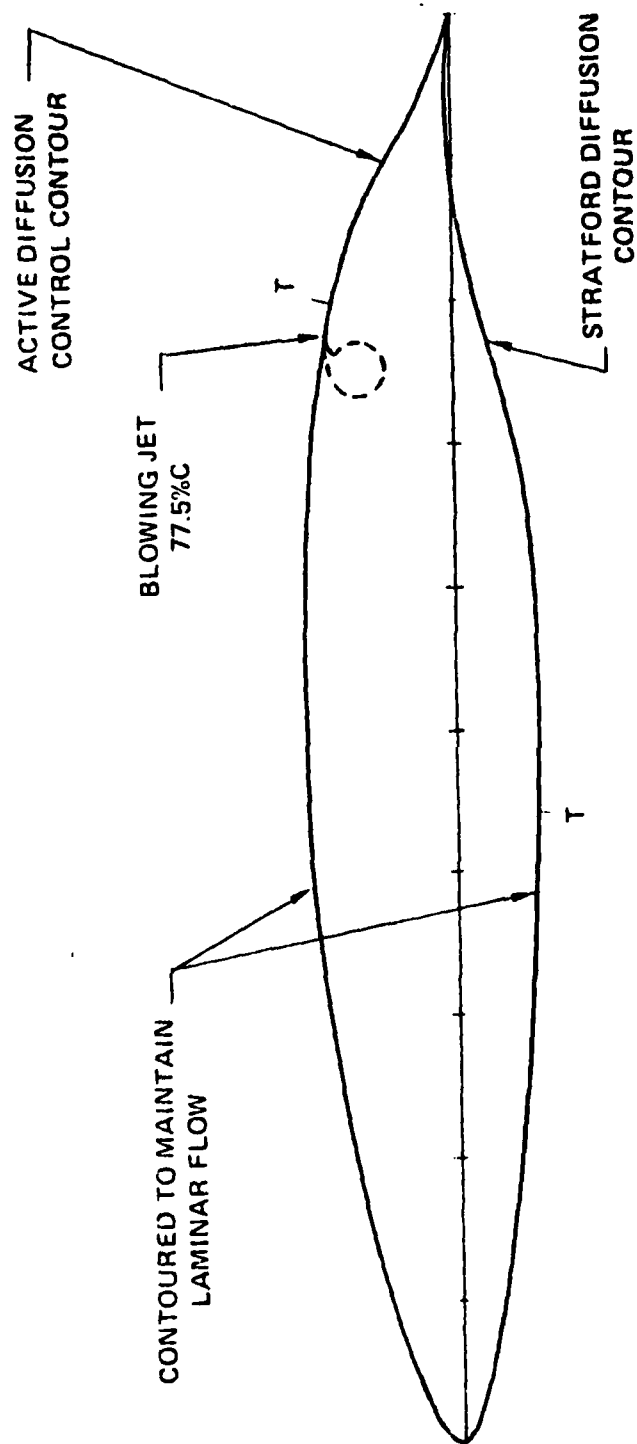FIGURE 2-1   DRAG REDUCTION FOR DIFFERENT TRANSITION LOCATIONS

FIGURE 2-2 SCHEMATIC OF ATC ACTIVE DIFFUSION CONTROL DEVICE

5

C_ℓ and M_∞ typical of a subsonic patrol/multi-purpose Naval aircraft. A large chord Reynolds number, $Re_c = 4 \times 10^7$, passive laminar flow ATC airfoil was designed at a high subcritical Mach number ($M_\infty = 0.6$) and $C_\ell = 0.73$, Figure 2-3. The design point $C_\ell(0.73)$ pressure distribution is illustrated in Figure 2-4. The airfoil pressure gradient tailoring was performed with both direct and indirect airfoil design codes.[7,8] Three major pressure gradient design areas are illustrated in the design point $C_\ell(0.73)$ pressure distribution and are related to specific contours in the airfoil geometry. These three design areas define the passive laminar flow stabilization region, transition stabilization zone, and trailing edge diffusion.

Two design areas essential to passive stabilization of laminar flow are leading edge radius and favorable pressure gradient. It was determined that by varying the size of the leading edge radius, the neutral stability point could be moved forward or aft affecting the upper and lower surface flow stability. The smaller radii stabilized the flow by moving the neutral stability point aft. Reference 27 also confirms that the smaller leading edge radius moves the neutral stability location aft by reducing the growth of the Tollmien-Schlichting instabilities. The selected radius for the ATC/laminar airfoil design produces a far aft neutral stability point location on both upper and lower surfaces, $X/C = 0.14$ and 0.04, respectively, Figure 2-4. To prevent rapid growth of the Tollmien Schlichting instabilities aft of the neutral stability point, a strong favorable pressure gradient was required for the passive stabilization of the laminar flow at the design Re_c (4×10^7). The growth of these instabilities were predicted with the Transition Analysis Program System (TAPS) and definition of transition onset was identified by the e^9 transition correlation.[9,10] For the design Re_c, the predicted upper and lower surface transition locations are at $X/C = 0.8$ and 0.44, respectively. The stability analysis corresponding to the upper surface transition prediction is illustrated in Figure 2-5. The maximum spatial amplification ratio, $\ln(a)$, at the wall jet location $X/C = 0.775$ ($S/C = 0.8$) is 4.5, well below the transition onset criteria of 9, predicting a very stable high Reynolds number passive laminar flow design.[10] Aft of the wall jet location the amplification ratio grows rapidly predicting transition within the transition stabilization zone, Figure 2-4. Because the flow was so stable a stability analysis was also performed for a larger Re_c (6×10^7) to determine the extent of maximum Re_c capability for the ATC/laminar airfoil design point configuration. For this larger Re_c (6×10^7), Figure 2-6, the maximum spatial amplification ratio at wall jet location increased from 4.5 to 8. However, this is still below the transition onset criteria of 9. Hence, passive laminar flow stabilization at Re_c slightly greater than 6×10^7 is predicted for the selected configuration. These

ACTIVE DIFFUSION CONTROL CONTOUR

STRATFORD DIFFUSION CONTOUR

BLOWING JET 77.5%C

CONTOURED TO MAINTAIN LAMINAR FLOW

τ

T

DESIGN POINT

C_ℓ = 0.73 Re_c = 40 × 10^6

C_d = 0.00303 $M\infty$ = 0.6

t/c = 0.165   T = Transition

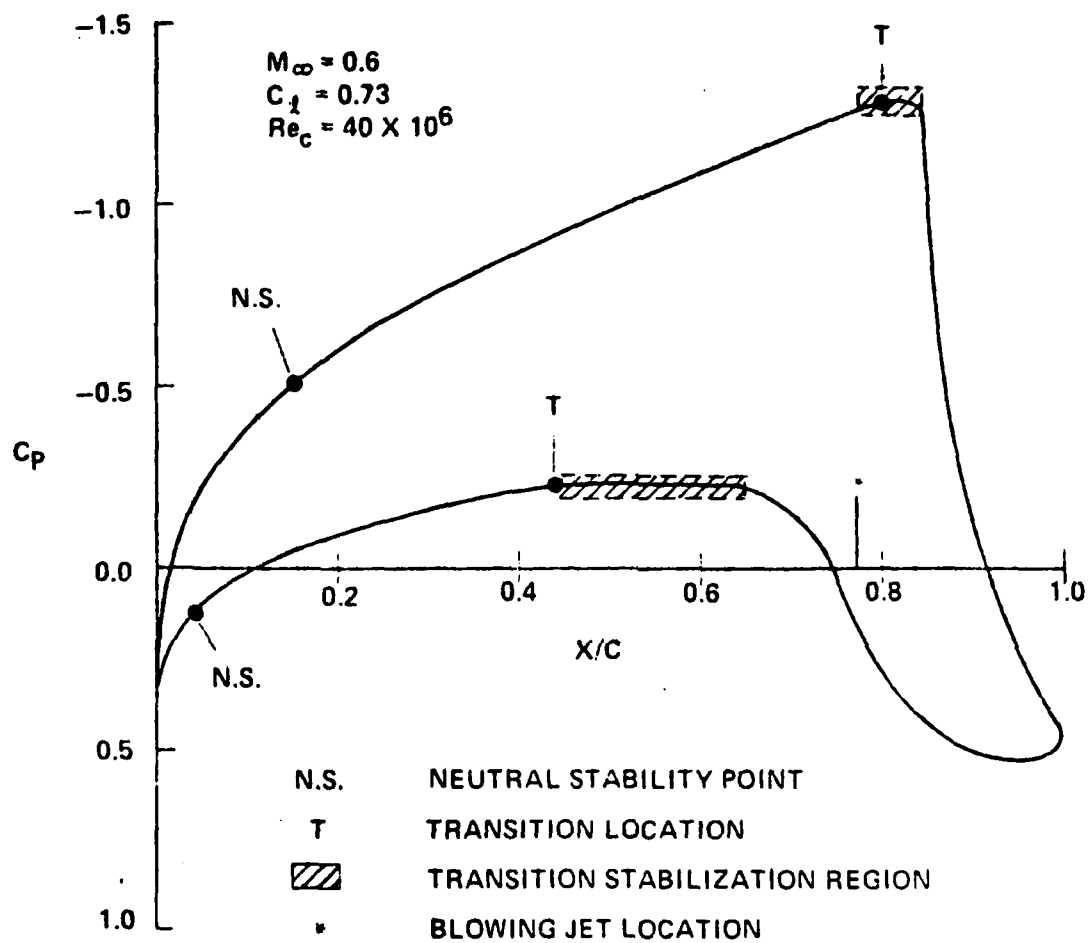FIGURE 2-3   ATC/LAMINAR AIRFOIL DESIGN

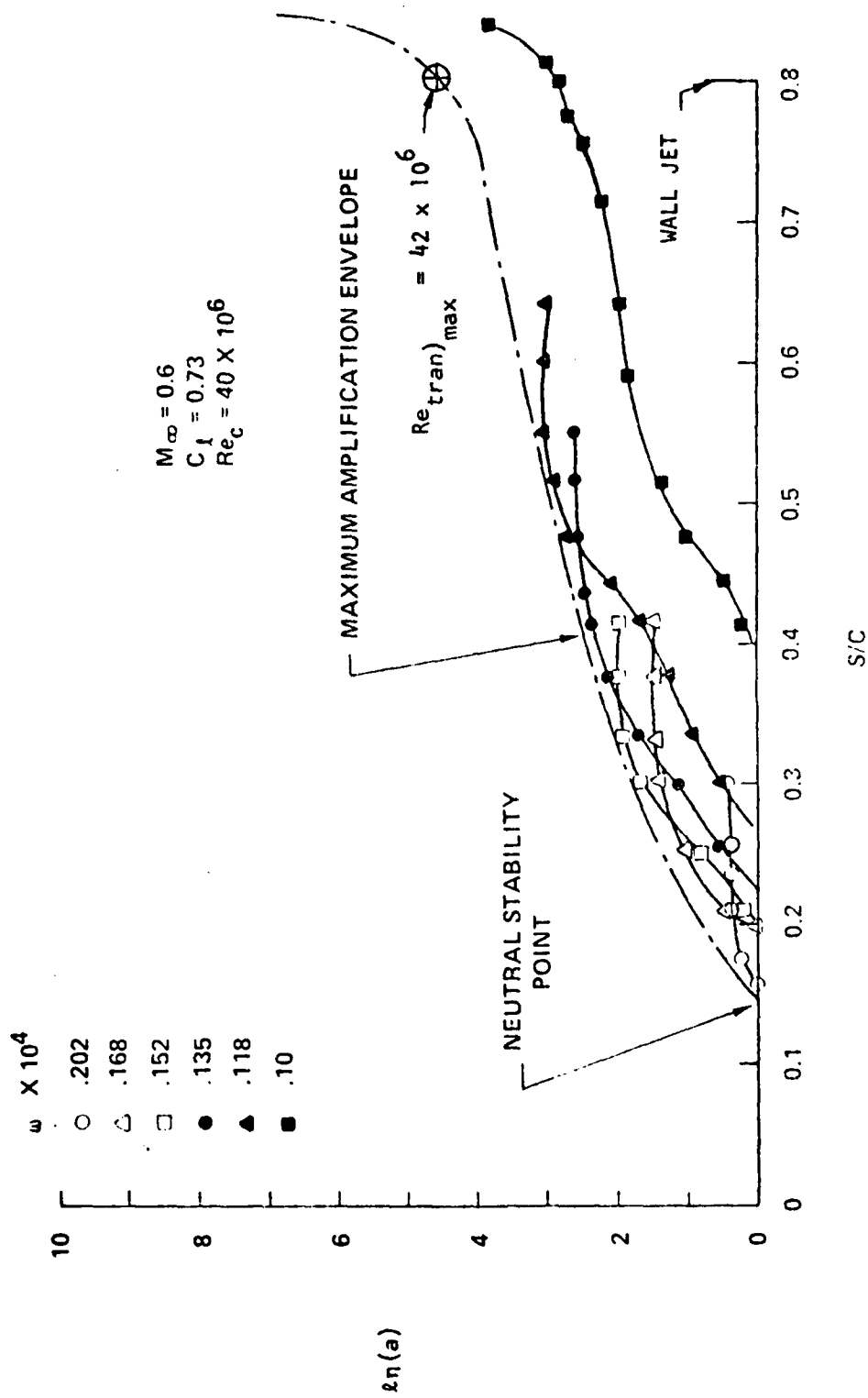FIGURE 2-4   ATC/LAMINAR AIRFOIL DESIGN PRESSURE DISTRIBUTION

FIGURE 2-5 ATC/LAMINAR AIRFOIL UPPER SURFACE STABILITY ANALYSIS $C_\ell = 0.73$, $Re_c = 4 \times 10^7$.

9
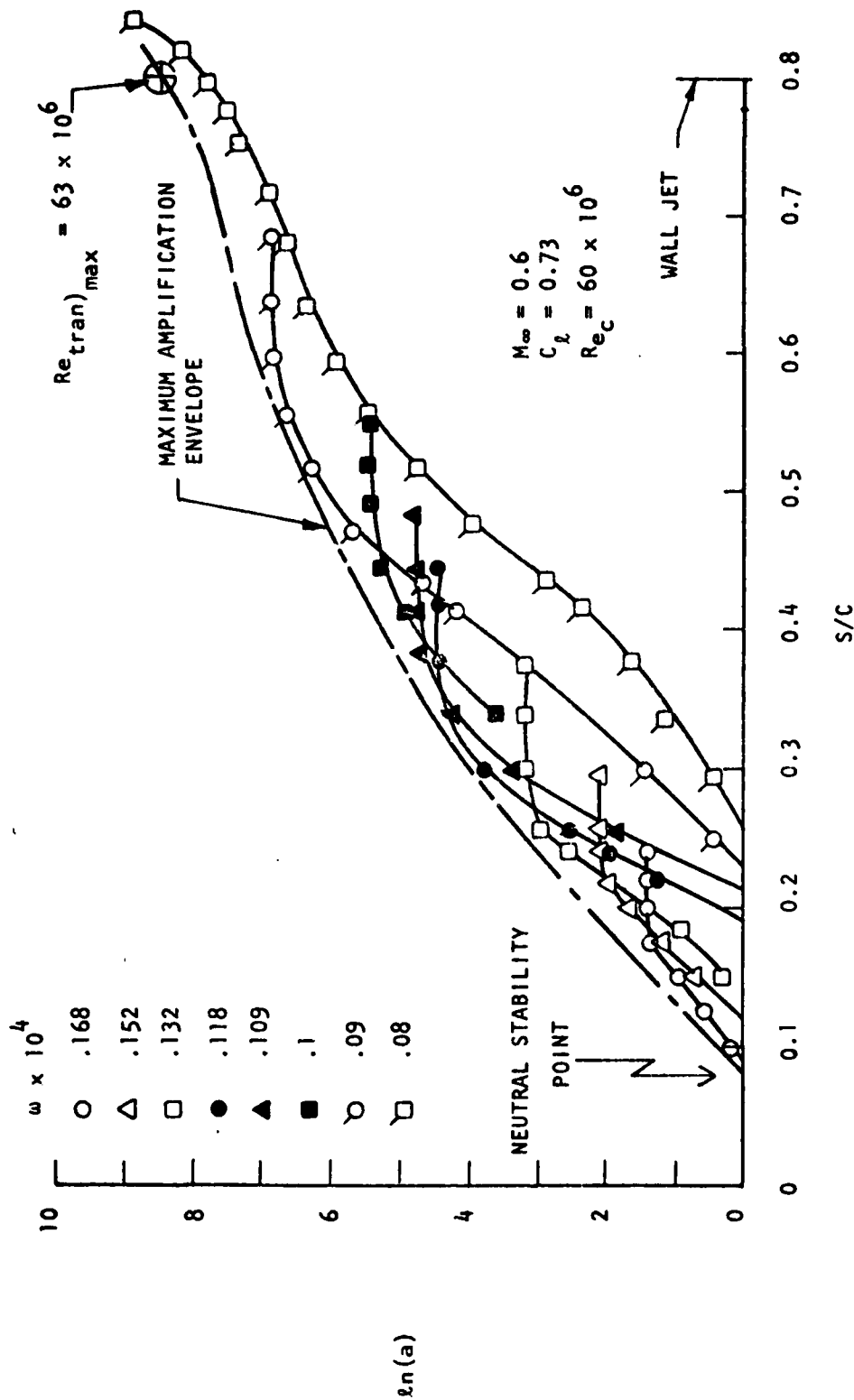
FIGURE 2-6 ATC/LAMINAR AIRFOIL UPPER SURFACE STABILITY ANALYSIS, C_ℓ = 0.73, Re_c = 6 × 10⁷.

10

specific calculations illustrate the potentials for extremely high Reynolds number passive laminar flow airfoil designs.

Following the upper and lower surface favorable pressure gradients are the transition stabilization zones, Figure 2-4. These zones are a near zero pressure gradient design, preventing laminar/turbulent boundary layer separation and insuring a stable turbulent boundary layer development. The minimal lengths of these zones were defined by a delta momentum Reynolds number growth of 500. Located within the upper surface zone is the wall jet, at $X/C = 0.775$, utilizing the short region of constant pressure aft of the jet to provide efficient jet mixing prior to the rapid diffusion to the trailing edge. Details of the active diffusion concept are discussed in Reference 3. The larger lower surface transition stabilization zone is designed for off-design conditions and is followed by a Stratford diffusion type design to achieve lower surface trailing edge pressure recovery.[11,12]

2.3 PERFORMANCE

An analysis of the ATC/laminar airfoil performance was made for two Re_c's (4×10^7 and 6×10^7) at $M_\infty = 0.6$ covering the design/off-design C_ℓ range establishing passive lamimar flow technology potentials. The airfoil performance was established from transition information derived from the TAPS program and used as input into a compressible laminar/turbulent boundary layer program to identify the section drag characteristics.[9,13,14] For conditions when upper surface trailing edge diffusion was not achieved due to separation, the BLC (C_μ) requirements to achieve the diffusion were predicted with a compressible active diffusion prediction method.[5]

At the design point (C_ℓ (0.73) and Re_c (4×10^7)) the predicted $C_d \approx 0.00303$ required no BLC ($C_\mu = 0$) to achieve trailing edge diffusion, thus generating an extremely high $L/D = 240$. In addition to this high energy efficient design potential, the passive laminar flow stability analysis, Figure 2-5, illustrates a large safety margin against transition onset forward of $S/C = 0.8$. This large margin, defined by the difference between the predicted maximum amplification envelope and the transition onset criteria of $\ln(a) = 9$, could maintain potentially some protection against flow disturbances. Examination of this potential with reference to freestream turbulence is discussed in section 4.3.

For the off design C_ℓ's, analysis of the passive laminar flow stability identified airfoil pressure distribution influence on transition location and the resulting performance. The movement of the transition location, illustrated

11

In Figure 2-7, is shown for two Re_c's (4×10^7 and 6×10^7) covering a C_ℓ range from 0.73 to 1.3. As expected, with increasing C_ℓ, the transition location moves forward on the upper surface from $X/C = 0.8$ toward the leading edge. The lower surface transition location, however, moves aft decreasing the lower surface section drag. As the upper surface transition location moves forward, the length of the turbulent boundary layer growth becomes much larger, increasing the boundary layer momentum deficit at the onset of the trailing edge diffusion, causing the flow to separate on the diffusion ramp. For these specific off-design cases, BLC is required to maximize performance.

Using the transition location information defined in Figure 2-7, drag polars with and without BLC were predicted for both $Re_c = 4 \times 10^7$ and 6×10^7, and are shown in Figure 2-8. The no BLC case ($C_\mu = 0$) is represented by the dashed line. For this case, the drag bucket extends up to a $C_\ell = 0.85$, generating an extremely high $L/D = 280$. These curves, represented by $C_\mu = 0$, identify cruise type C_ℓ operation for maximum L/D performance. For $C_\ell > 0.85$, an abrupt stall is predicted resulting from trailing edge stall/separation. By controlling the upper surface trailing edge boundary layer, off-design high maneuvering C_ℓ potentials can be shown. The solid curves correspond to the *full BLC case and represent the* C_μ equivalent to full energization of the local boundary layer at the jet location. Note however that the full BLC predictions have not been optimized for minimum $(C_d + C_\mu)$, and therefore include some overblowing penalty. At the lower design $C_\ell = 0.73$, full BLC C_μ is 0.001; at $C_\ell > 1.1$ full BLC C_μ approaches a near constant value of 0.01 until stall occurs forward of the blowing jet. For stall to occur, an adverse gradient would have to occur forward of the wall jet location, thus $C_\ell > 1.5$ could be realized at $M_\infty = 0.6$. The ATC/laminar airfoil design concept potentially provides the "best of two worlds": (1) laminar flow at cruise C_ℓ (0.73) with an extremely high $L/D = 240$ for a $Re_c = 4 \times 10^7$, and (2) high maneuvering C_ℓ's at low drag levels associated with C_p roof-top loading and BLC.
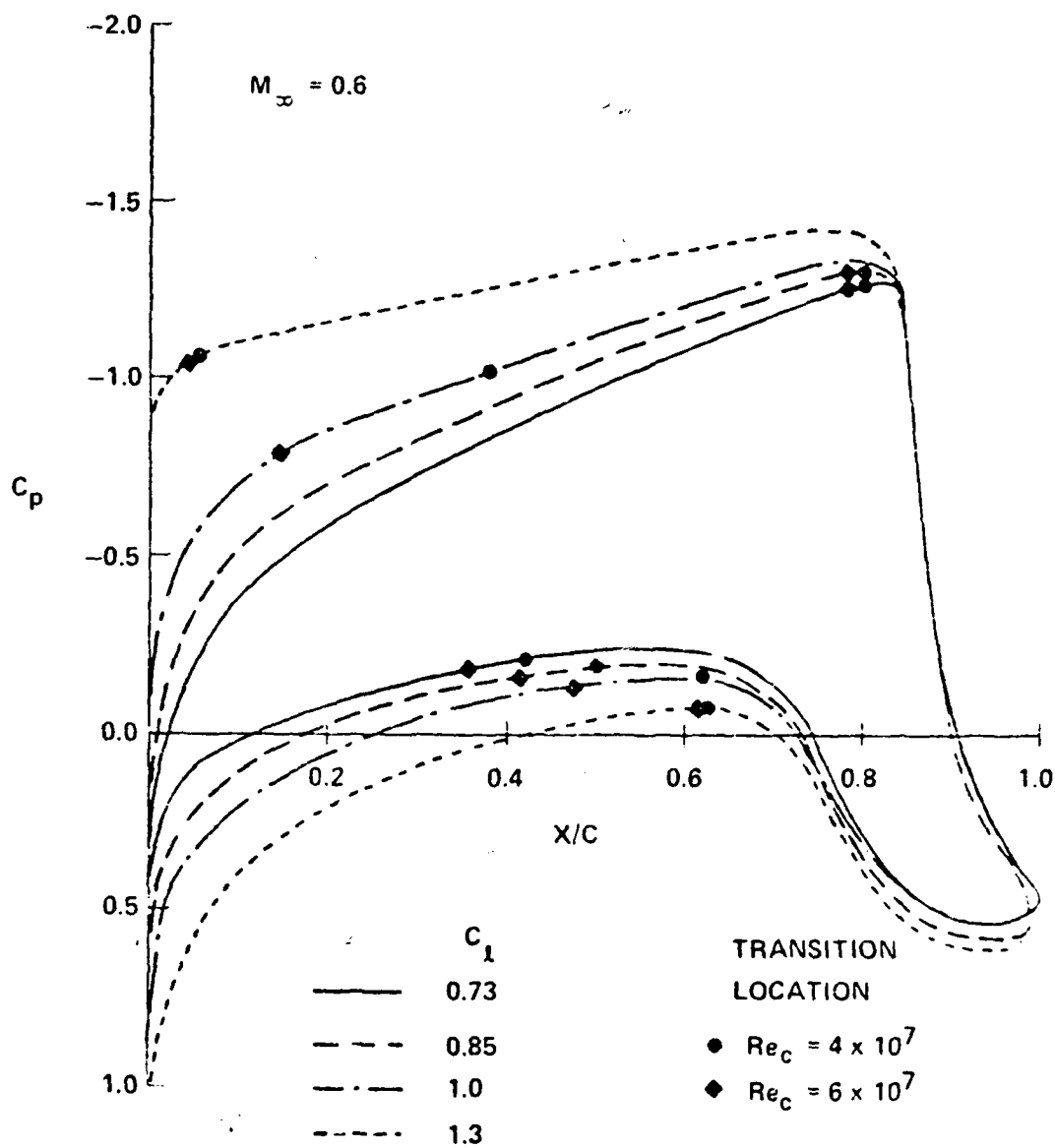
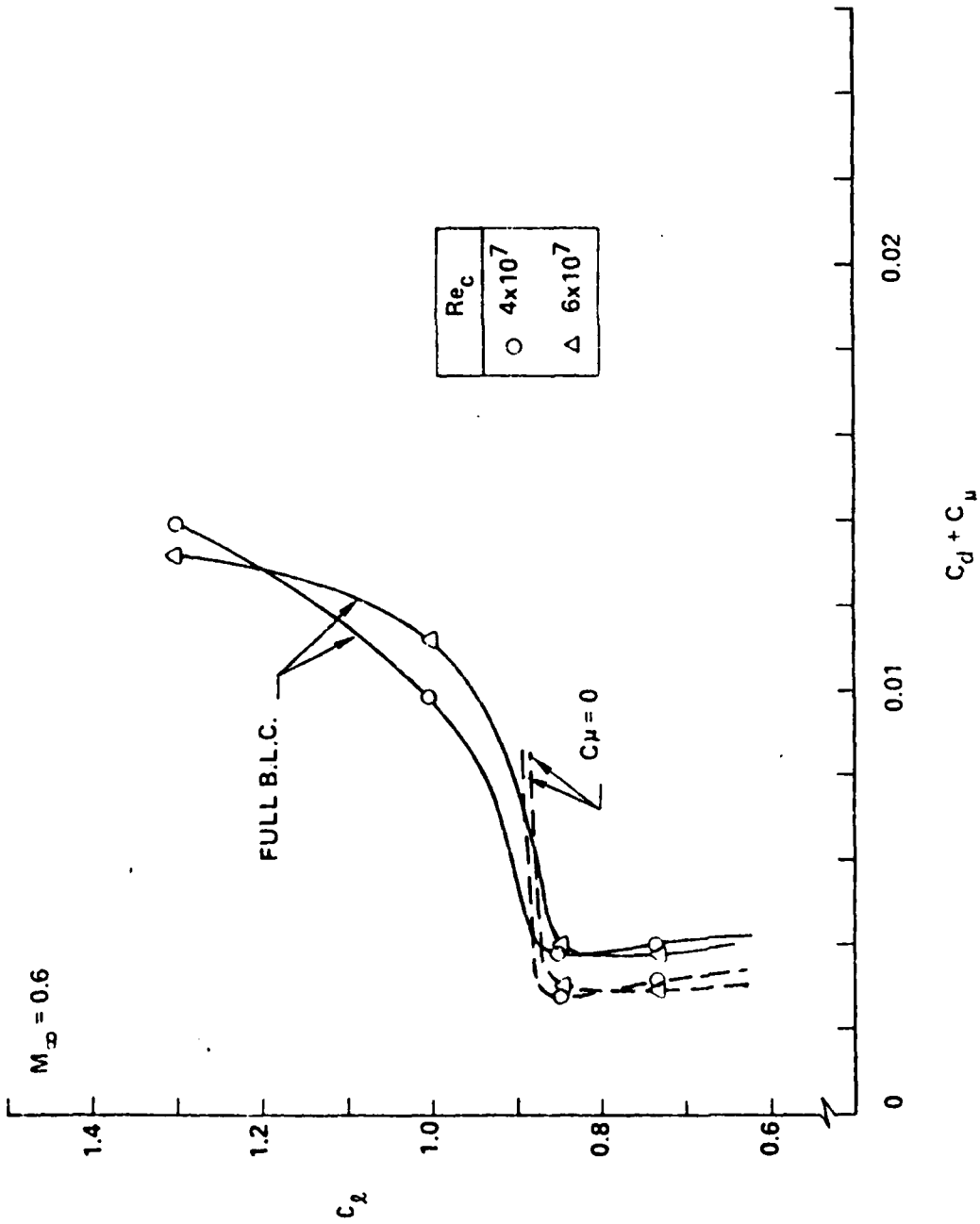FIGURE 2-7   TRANSITION LOCATION FOR DESIGN/OFF-DESIGN C_{ℓ}.

FIGURE 2-8   ATC/LAMINAR AIRFOIL DRAG POLAR PREDICTION.

14

3.0 PASSIVE LAMINAR FLOW STABILIZATION EXPERIMENTS

The major validation problem of any laminar flow design is the strong influence of real flow freestream turbulence degradation on laminar boundary layer stability. The major consideration in any tunnel validation of a laminar flow design concept is the inherent high levels of turbulence intensity. The lowest turbulence intensities in some of the best designed low turbulence tunnels have documented levels 2 or 3 times larger than that in the flight environment, Figure 3-1.[15-17] The level of tunnel turbulence intensity tends to increase with both unit Reynolds number and Mach number. In addition to this known test environment characteristic, the problem is compounded by the lack of an analytical method which one could apply to a design to identify the real flow environment effects. Hence experimental examination of the ATC/laminar airfoil concept in a real flow environment was essential because of the limitations of the theory. Also, the assumption that e^9, established for low to moderate Reynolds numbers, applies to extremely high transition Reynolds numbers, needs some justification.[10] The questions to be answered experimentally are; can the theory predict high transition Reynolds number laminar flow using e^9 as a transition correlation for an ideal flow environment, what is the magnitude of real flow turbulence intensity influence on maximum transition Reynolds number, and what are the critical fabrication tolerances for the ATC/laminar airfoil? To identify these unknowns, full scale Reynolds number experiments, simulating the ATC/laminar airfoil design point $C_\ell (0.73)$, were performed in the Vought Air Boundary Layer Channel (ABLC) facility, Figure 3-2. These experiments were aimed at the examination of the high Reynolds number passive laminar flow concept by simulating the first 80 percent of the airfoil upper surface design point C_ℓ (0.73) velocity distribution, Figure 2.4.

3.1 TEST FACILITY

The Air Boundary Layer Channel (ABLC) is a low turbulence/acoustic facility, Figure 3-2, uniquely designed for passive laminar flow stabilization/transition boundary layer research. Two previous experiments, a near flat plate and pressure gradient simulation, performed in the ABLC have demonstrated and validated passive laminar flow stabilization potentials at low to moderate Reynolds numbers.[18,19] Test results from the near flat plate simulation, a constant diameter section, demonstrated Re_{tran} as high as 5.1×10^6. For the pressure gradient simulation, a Mangler transformed simulation of an axisymmetric laminar flow body, a maximum $Re_{tran} = 27 \times 10^6$

FIGURE 3-1 TUNNEL TURBULENCE INTENSITY

16

DAMPING SECTION

ACOUSTIC PLENUM

20:1 CONTRACTION

BOUNDARY LAYER BLEED
(4:1 CONTRACTION)

PLEXIGLAS TEST SECTION

AXIAL
LIGHTING
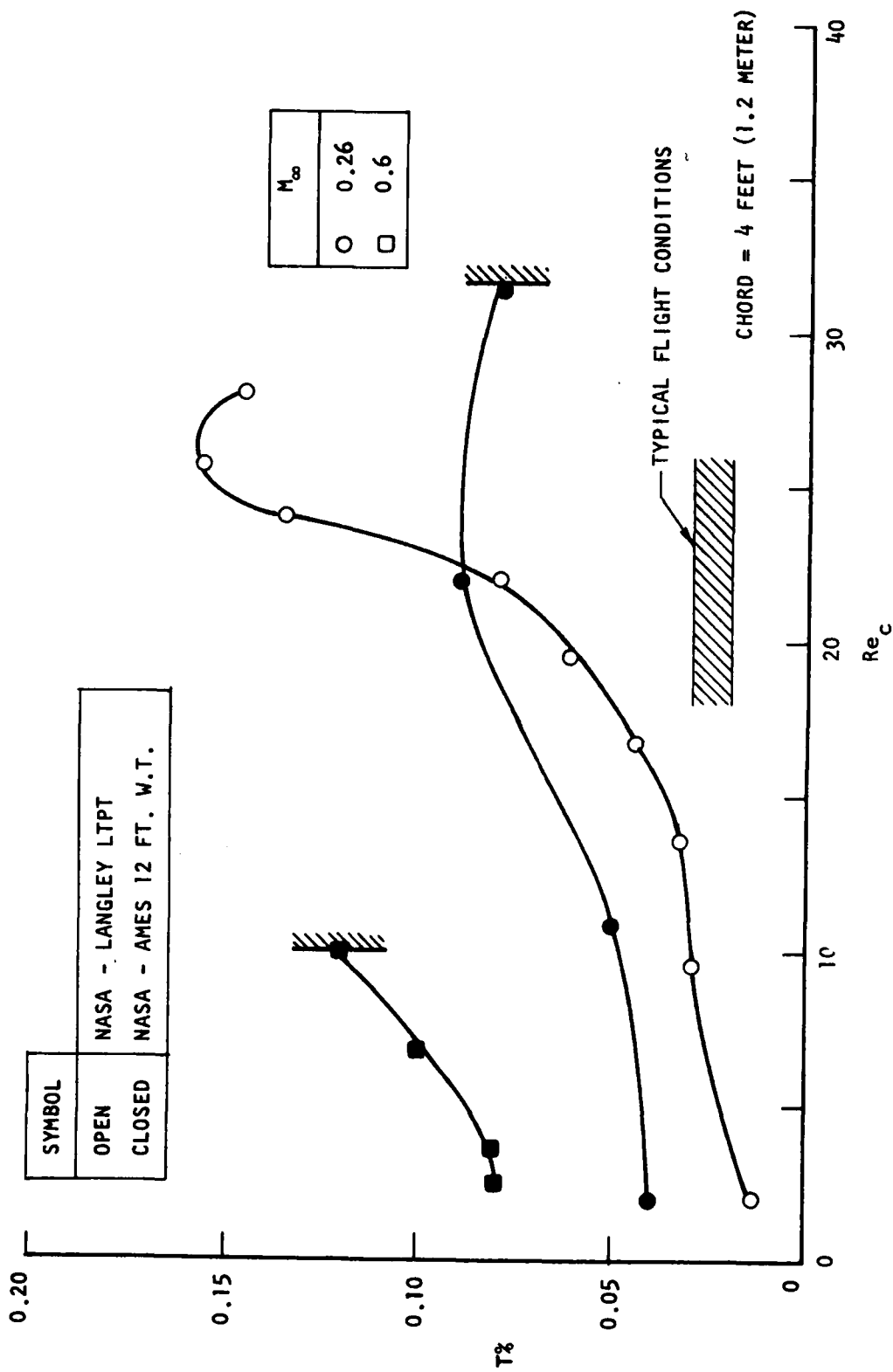
SONIC THROAT

TO ROOTS
PUMP

SMOKE
GENERATOR

BLEED
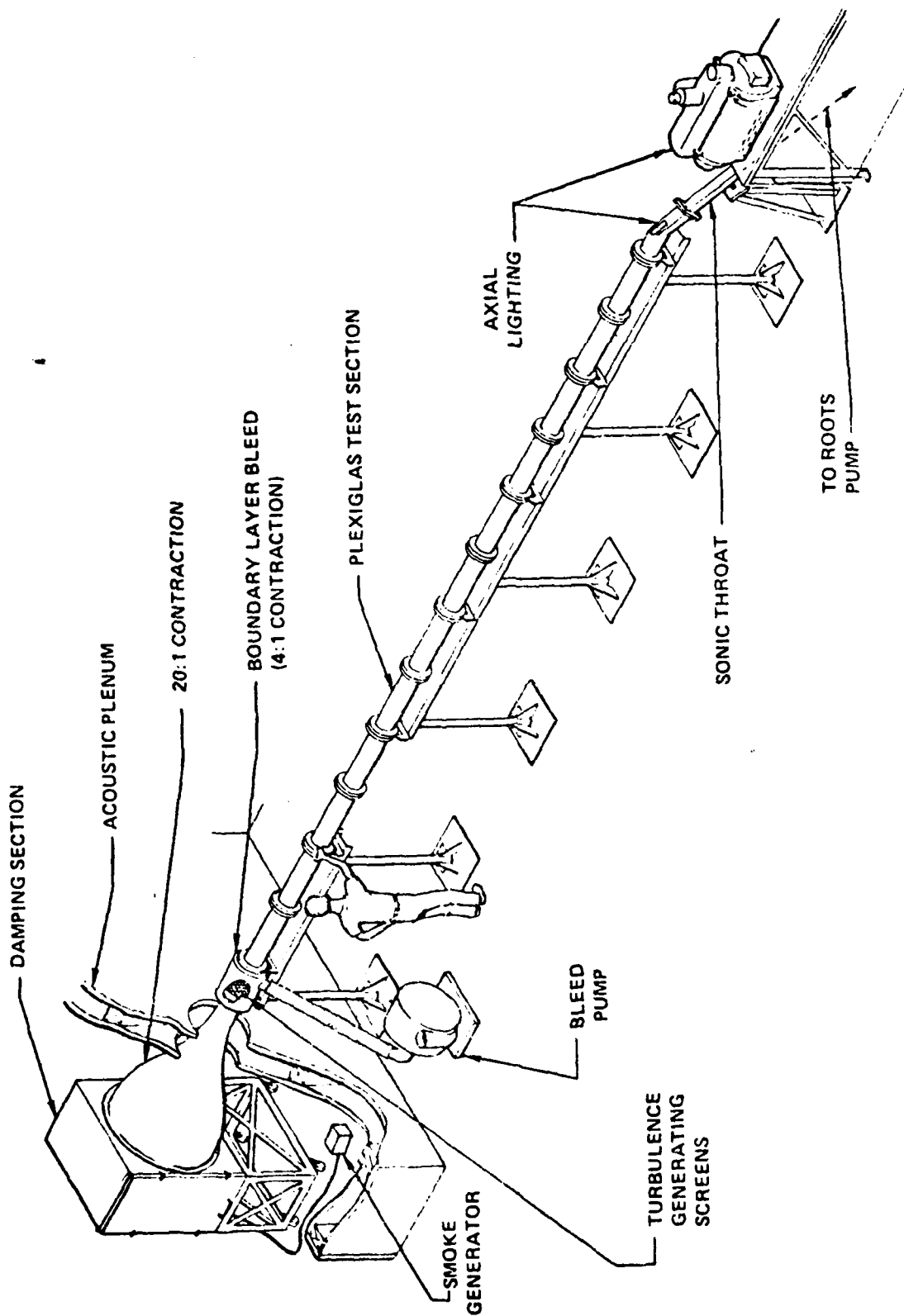PUMP

TURBULENCE
GENERATING
SCREENS

FIGURE 3-2   ATC AIR BOUNDARY LAYER TRANSITION CHANNEL.

17

was achieved. For the ATC/laminar airfoil simulation, the ABLC was designed for an exit Re_{tran} = 40×10^6 with an operating test Re_{tran} range from 25×10^6 to 50×10^6. The axisymmetric ABLC facility achieves two-dimensional (2-D) flow simulation with a contoured/machined inside diameter distribution. The test section matches a specific 2-D velocity flow field, boundary layer development, and local Reynolds number distribution when pre-established design criteria are adhered to.

The ABLC design criteria established by previous ABLC designs were utilized in the design of the ATC/laminar airfoil ABLC simulation. To insure proper simulation, design considerations for both boundary layer development/growth and initial/starting conditions are required. To insure that the laminar boundary layer development is 2-D, a minimum radius size was established from previous ABLC experiments. This minimum value was defined in terms of the boundary layer displacement thickness to radius ratio, identifying a design criterion $(\delta^*/r)_{max} \leq 0.08$. An example verifying the ABLC 2-D boundary layer development is illustrated in Figure 3-3, for the pressure gradient body simulation. The 2-D boundary layer predictions, δ^* and θ, obtained with a Cebeci and A. M. O. Smith program agree very well with the axisymmetric tube flow prediction obtained from a Karman-Pohlhausen program.[9,20] This close agreement illustrates the ABLC capability of properly simulating a 2-D boundary layer development. For the ATC/laminar airfoil ABLC simulation, a very conservative radius design value $(\delta^*/r)_{max} \leq 0.035$ to 0.048 was used to insure 2-D simulation. In addition to insuring 2-D laminar boundary layer development/growth, the physical geometry limits of the ABLC require design consideration of initial/starting boundary layer conditions. To initialize the starting boundary layer in the ABLC, a suction slot was substituted for the airfoil 2-D stagnation point. Due to concern for the influence of initial boundary layer perturbations on the laminar boundary layer stability, an evaluation was made with the TAPS program, Figure 3-4. The analysis was performed for the previous ABLC pressure gradient simulation and indicated no adverse effect on the maximum spiral amplification envelope due to the suction slot substitution for the stagnation point.[19] The simulation of the 2-D boundary layer development/growth and flow stability can be insured in the ABLC facility when proper design considerations are adhered to.

The ABLC is a quiet facility utilizing the benefits of the sonic throat at the channel exit to eliminate pump noise and an acoustic plenum at the inlet to eliminate inlet disturbances, Figure 3-2. The test section freestream turbulence level is reduced by the 14-20 screens located in the entrance of the ABLC followed by the 20:1 contraction section. The suction slot substitution for the stagnation point is located at the

SOLID LINES - CEBICI AND SMITH COMPUTER ROUTINE (FROM "TAPS") - 2-D PREDICTION

SYMBOLS - KARMAN-POHLHAUSEN - AXISYMMETRIC TUBE PREDICTION

AXISYMMETRIC LAMINAR
FLOW BODY SIMULATION

$Re_{s_{exit}} = 27 \times 10^6$

$(\delta^*/r)_{max} \leq 0.05$
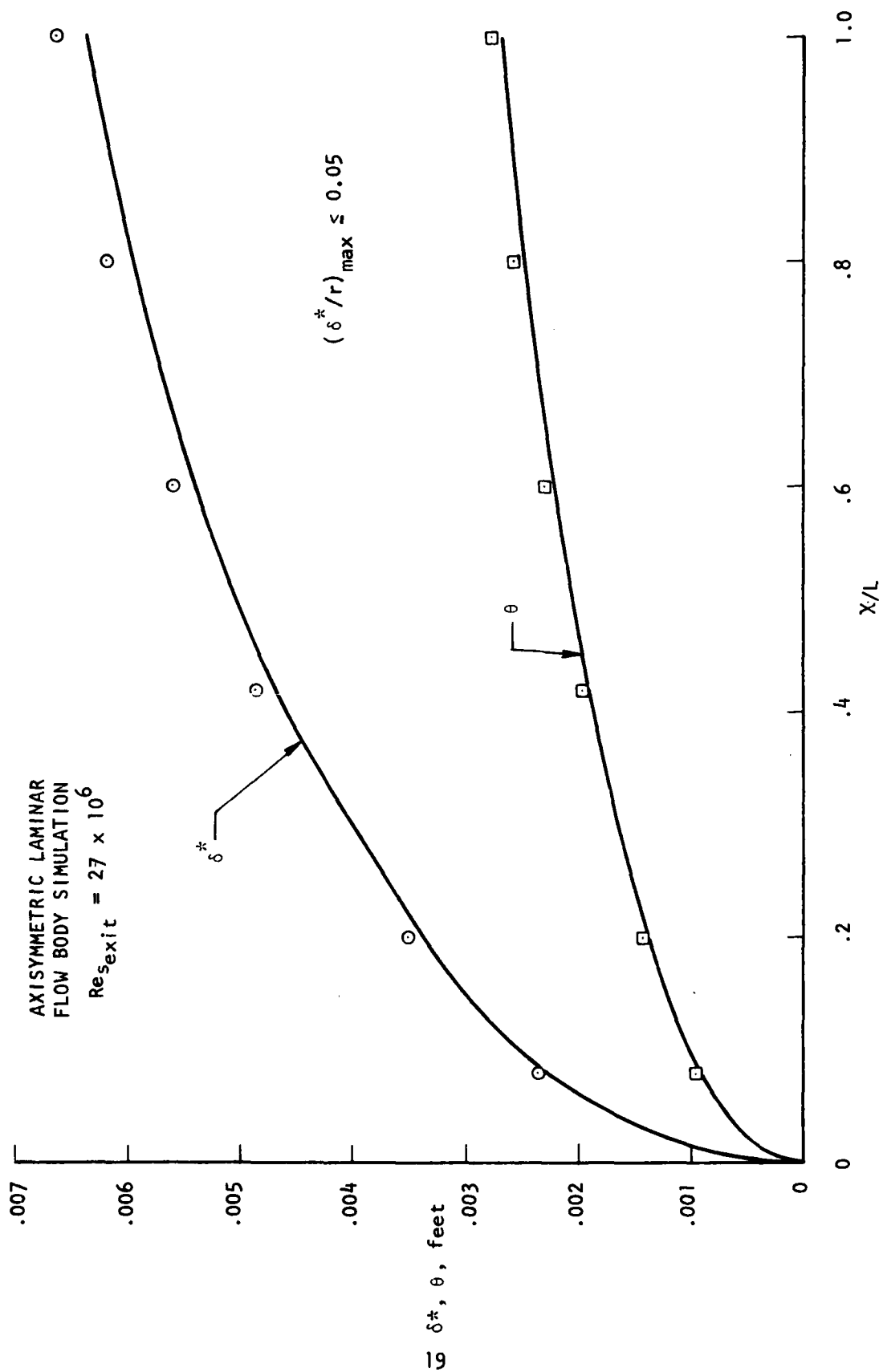
δ^*, θ, feet

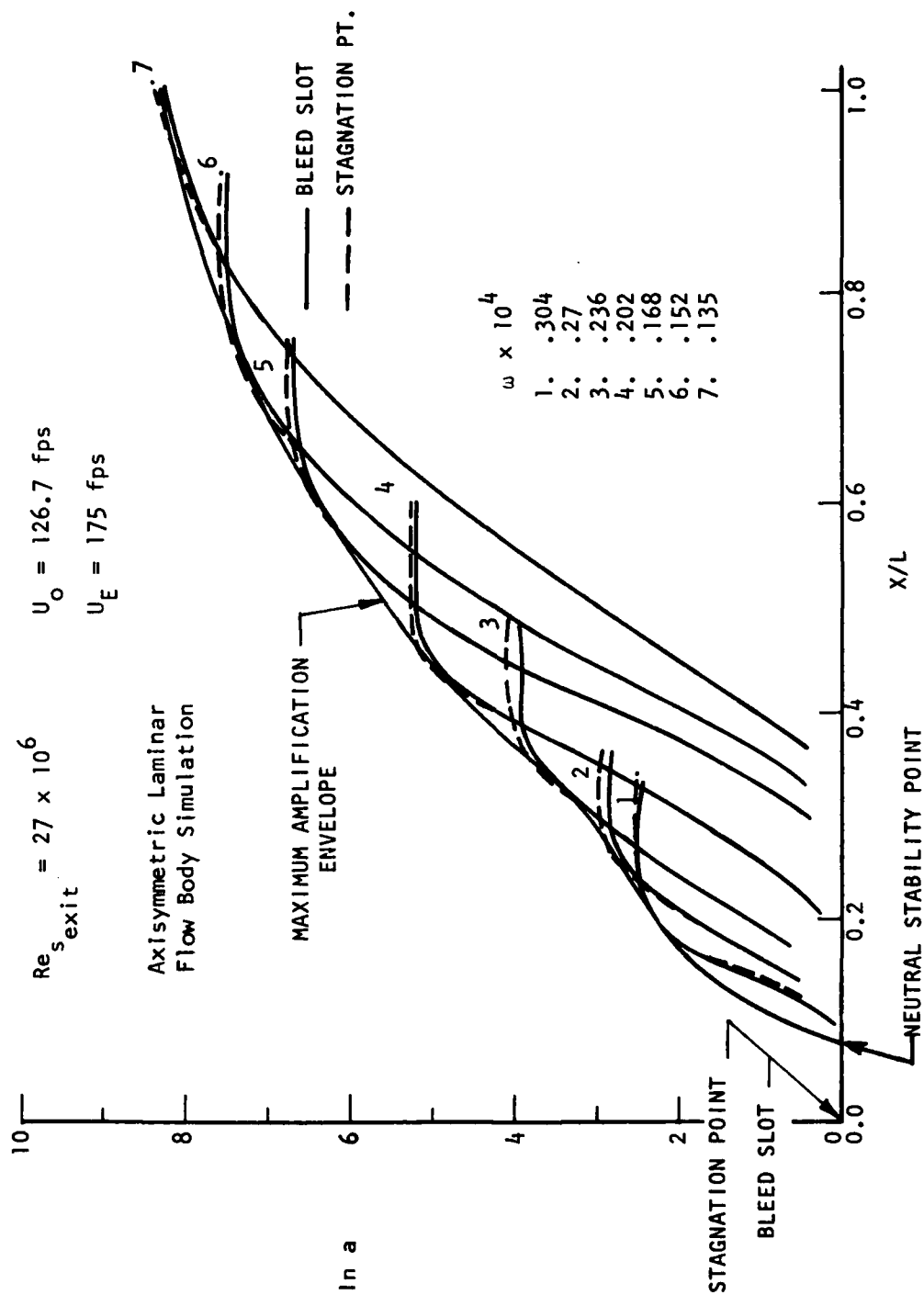FIGURE 3-3   ABLC BOUNDARY LAYER PREDICTIONS

19

FIGURE 3-4 ABLC 2-D SIMULATION - STAGNATION POINT VS. SUCTION SLOT

test section at a $U/U_\infty = 0.85$. To duplicate the airfoil velocity ratio distribution in the ABLC facility, the inside diameter distribution was contoured as shown in Figure 3-5. This contour was defined with the aid of an in-house computer program which uses the input velocity distribution to identify the corresponding radius requirements, accounting for viscous corrections. The test section was manufactured from twelve transparent plexiglas sections approximately 25 inches in length. The overall length of the ABLC test section is 304.5 inches (773.43 cm). The inside diameter varies in size from 3.66 inches (9.31 cm) at the suction slot, to 2.8 inches (7.11 cm) at the exit, Figure 3-5. The errors in surface mis-match at the joints were held to ±0.0002 inches with a surface waviness of less than ±0.0001 inches/inch. Located at the exit of the ABLC is a hot wire probe, Figure 3-6, used to measure the freestream and transition onset information.

3.2 SIMULATION EXPERIMENTS

Three major ATC/laminar airfoil simulation experiments were performed in the ABLC facility: (1) full scale Reynolds number validation; (2) freestream turbulence intensity influence; and (3) discrete roughness and gap/slot transition tests.

The initial test was to validate the design point passive laminar flow stabilization Re$_{tran}$ = 4×10^7 and identify maximum Re$_{tran}$ capability at minimal ABLC freestream turbulence intensity. The design point Re$_{tran}$ = 4×10^7 was achieved, Figure 3-7, and at the lowest turbulence intensity level of 0.02 - 0.03%, referenced to exit velocity conditions, a transition Reynolds number of 48×10^6 was realized. Validation of larger values was, however, limited by the maximum flow capability of the ABLC pump. The laminar flow, prior to Re$_{tran}$ = 48×10^6, was very stable and repeatable as demonstrated by its insensitivity to local vibrations produced by tapping on the test section and vibration transmitted through the structure from the pump located outside of the building. The maximum amplification ratio value, at S/C = 0.8, corresponding to the maximum ABLC validation Re$_{tran}$ was identified with the TAPS program.[9] This prediction was performed for a maximum Re$_{tran}$ = 49×10^6, slightly larger than the ABLC validation value of 48×10^6, Figure 3-8. The maximum amplification value at the ABLC exit (S/C = 0.8) is 7.2, slightly below the transition onset criteria of 9. This safety margin was representative of the high Reynolds number flow repeatability and insensitivity to local vibrations. Hence, justification for using e^9 to define transition onset now has a much stronger basis at the higher Reynolds numbers. If the pump limits had not been reached, potential validation of Re$_{tran}$ > 55×10^6 could have been obtained in the ABLC facility.
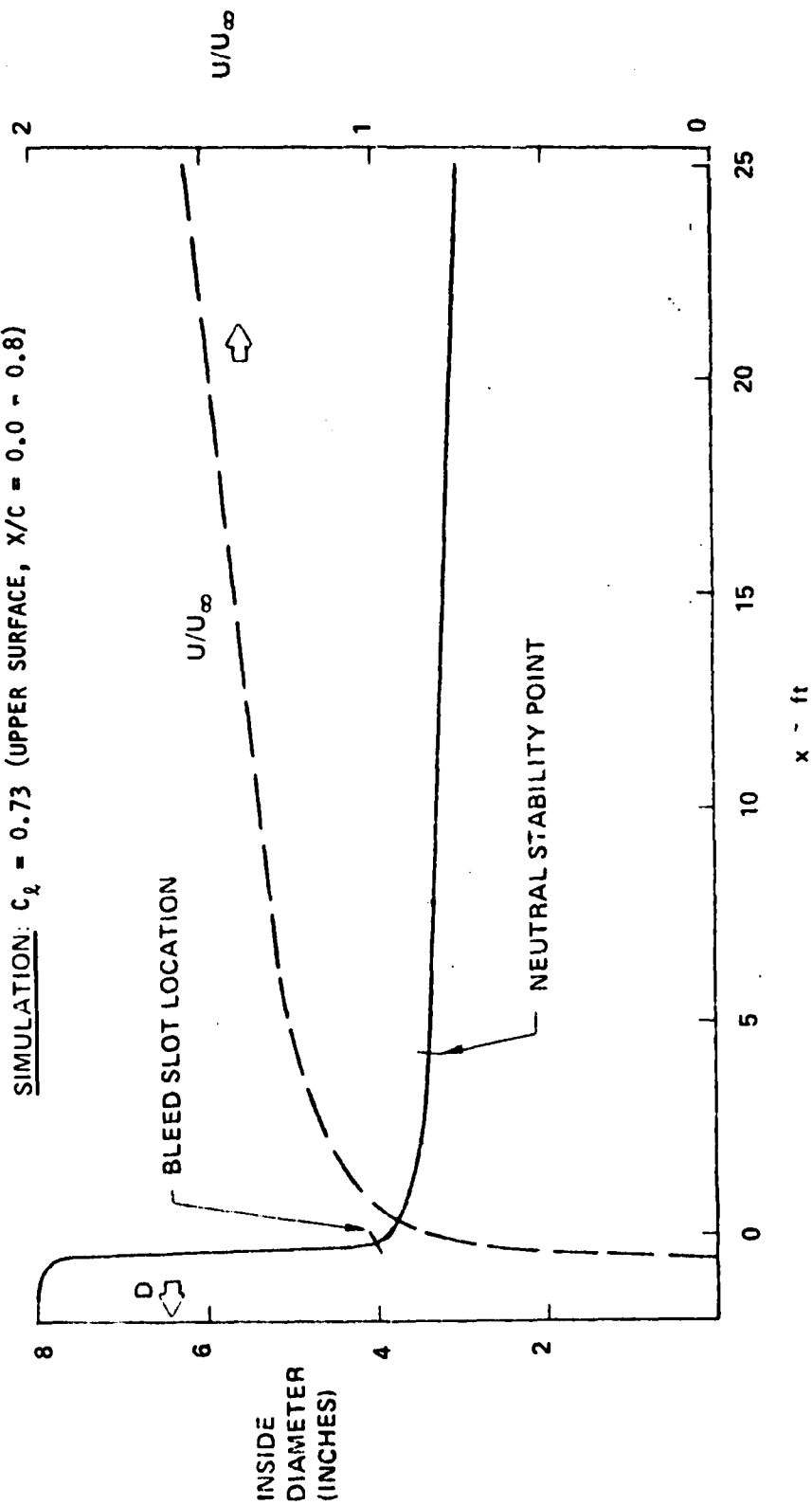
FIGURE 3-5 CHANNEL DESIGN FOR ATC/LAMINAR AIRFOIL SIMULATION.

22

SIDE VIEW

PROBE SUPPORTS

TRANSITION SECTION

HOT WIRE SENSOR

TEST SECTION

FLOW

TO ANEMOMETER

FRONT VIEW

PROBE SUPPORT
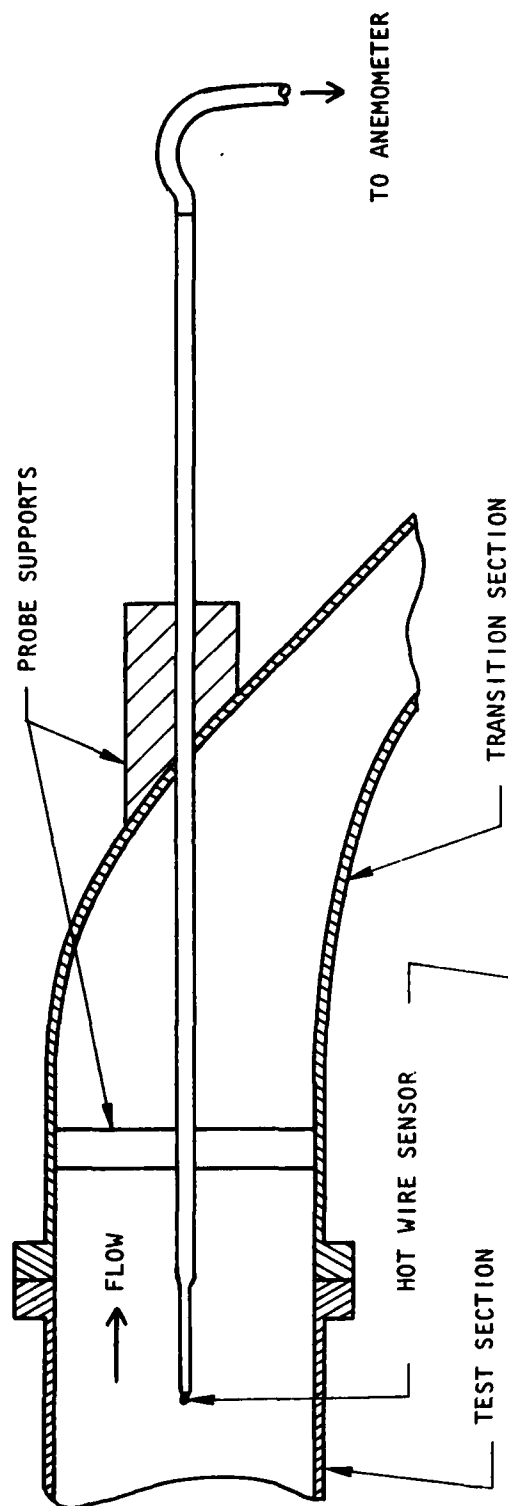
FIGURE 3-6   TEST SECTION EXIT HOT WIRE PROBE

23

FIGURE 3-7 AIR BOUNDARY LAYER CHANNEL VELOCITY DISTRIBUTION COMPARISON
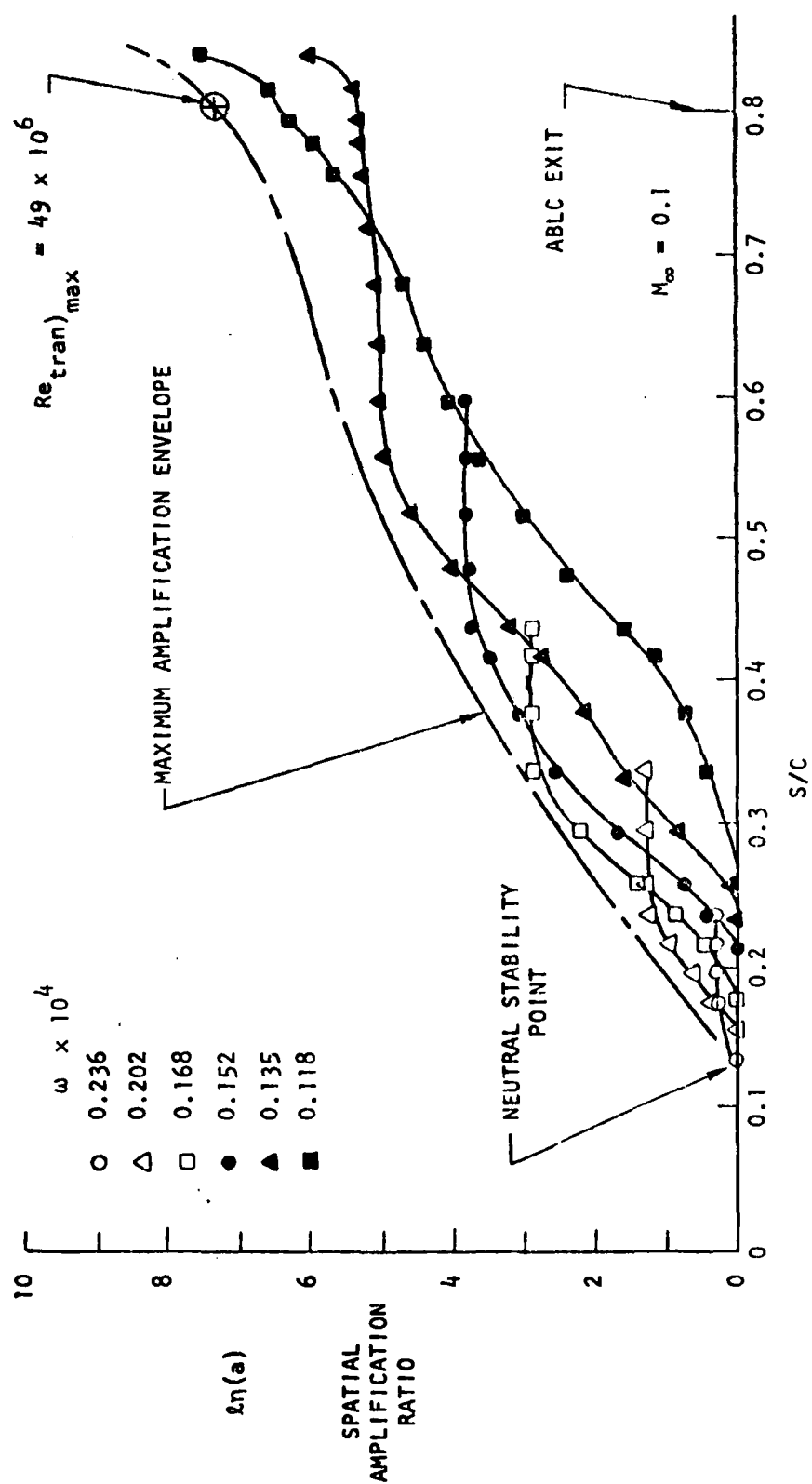
FIGURE 3-8 AIR BOUNDARY LAYER CHANNEL STABILITY ANALYSIS - SIMULATING ATC/LAMINAR AIRFOIL UPPER SURFACE VELOCITY DISTRIBUTION, C_ℓ = 0.73.

The objective of the second test was to determine the influence of turbulence intensity, typical of tunnel turbulence levels 0.04% to 0.2%, on transition Reynolds number degradation. To identify the influence of turbulence intensity experimentally on maximum Re_{tran}, the number of screens and the size of the wire grids were changed in the entrance of the ABLC. The turbulence intensity measurements were obtained with a hot wire located at the exit of the ABLC. The results of this experiment are shown in Figure 3-9, where the turbulence intensity is referenced to the local exit velocity. The experimental data identifies a strong influence of real flow turbulence intensity on maximum Re_{tran}. As turbulence intensity increases, the maximum Re_{tran} decreases rapidly. Examination of the turbulence intensity influence on the airfoil design point performance is discussed in Section 4.3, with off-design considerations, subject to tunnel environment, presented in Section 5.3.

Discrete roughness and gap/slot tests were performed to identify critical surface tolerances and critical static pressure orifice size. The discrete roughness test consisted of a 0.25 inch (0.635 cm) diameter cylinder which was varied in height to determine critical values. The gap/slot width test was achieved by displacing two sections of the ABLC and inserting a spacer creating a sealed gap around the c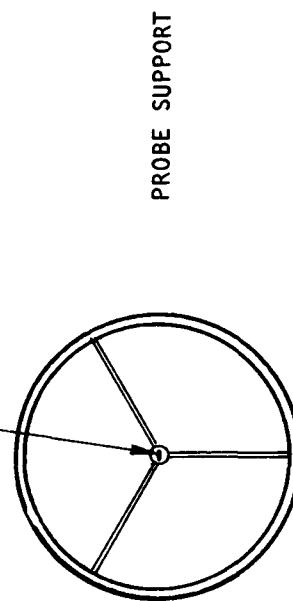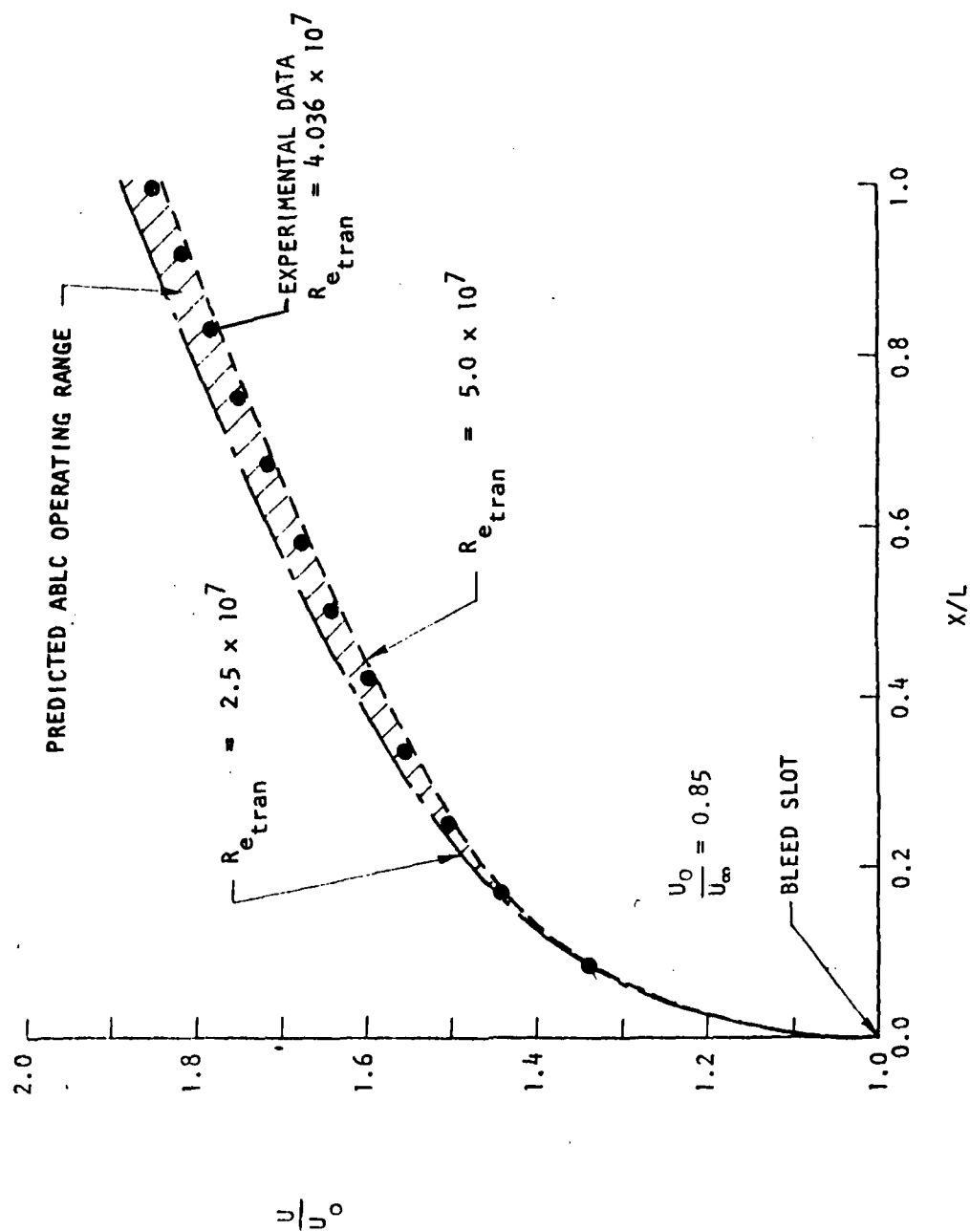ircumference of the test section. The results for the discrete roughness height test performed at a ABLC location X/L = 0.176 is illustrated in Figure 3-10. For an exit Re_{tran} = 4 x 10^7, the critical height was 0.0075 inches (0.01905 cm) with a critical roughness Reynolds number $Re_K = U_K K/\nu = 141$. The discrete roughness test identified a critical Re_K value range from 100 to 200. These values are at least four times larger than the critical value for hydraulic smoothness, $Re_K = 25.$[21] The hydraulic smoothness value defines the lower limit for which any roughness will generate transition. The results for the critical gap/slot width test is illustrated in Figure 3-11. At a Re_{tran} = 4 x 10^7 the critical width, at a X/L = 0.183, was 0.152 inches (0.386 cm) with a critical Re_K = 44,000. The critical Re_K values for the gap/slot width ranged from 20,000 to 45,000. This experimental data identified critical slot width values at a factor of 20 larger than the critical height values at the same test conditions, Re_{tran} = 4 x 10^7 and X/L ≈ 0.18. This information was used to identify the wind tunnel model fabrication tolerances for a 4-foot (121.92 cm) chord model, discussed in Section 6.1.
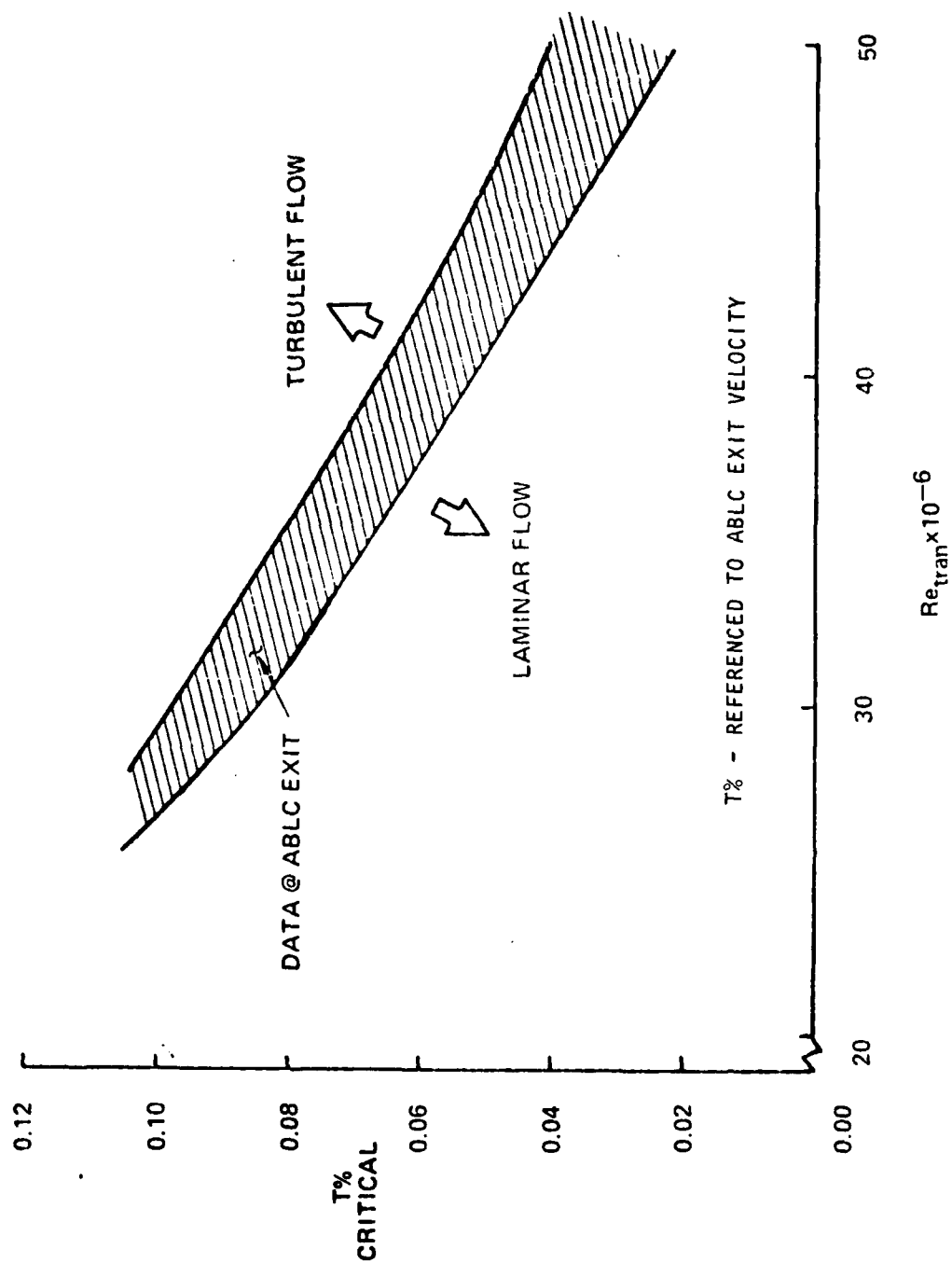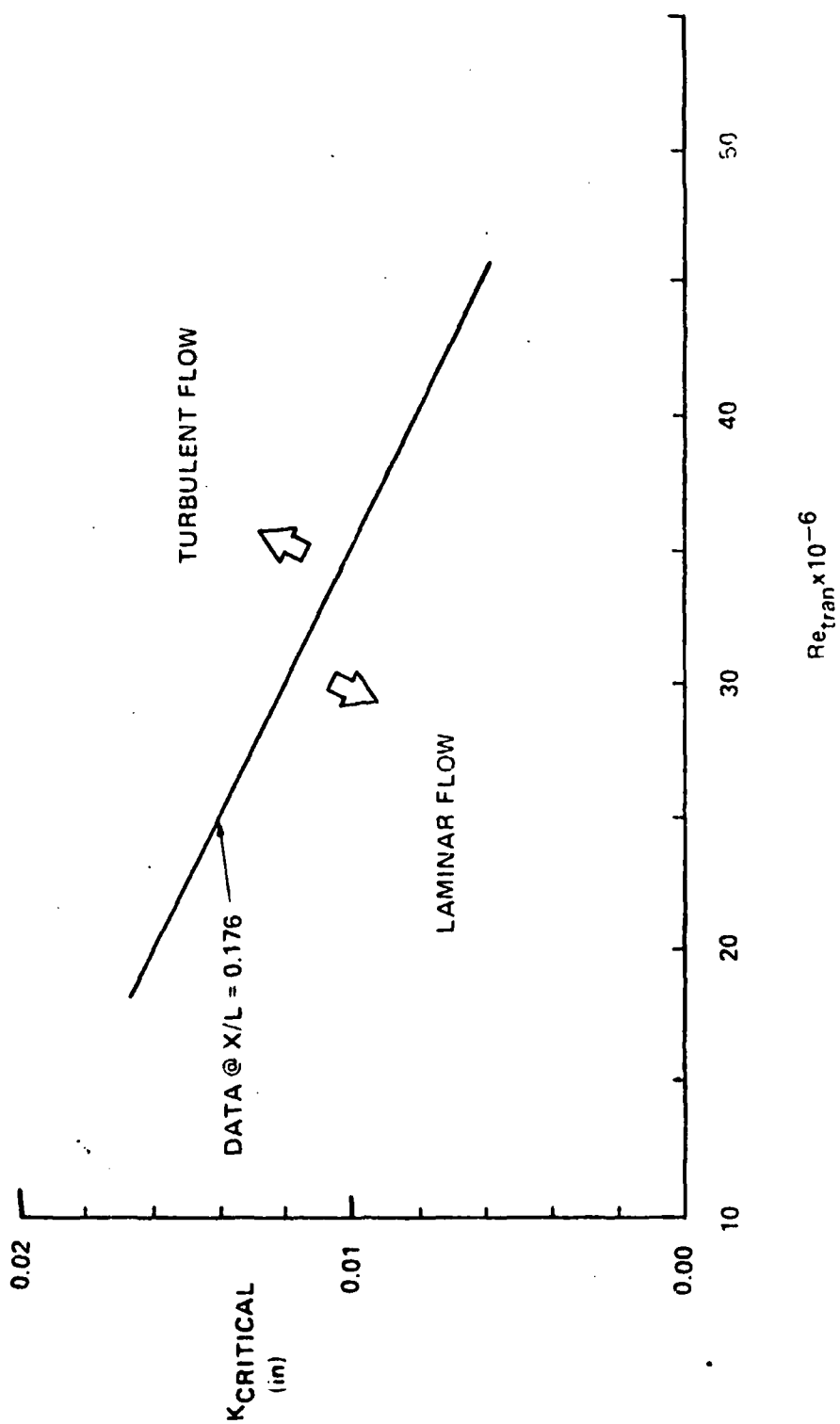
FIGURE 3-9 FREESTREAM TURBULENCE INFLUENCE.

27

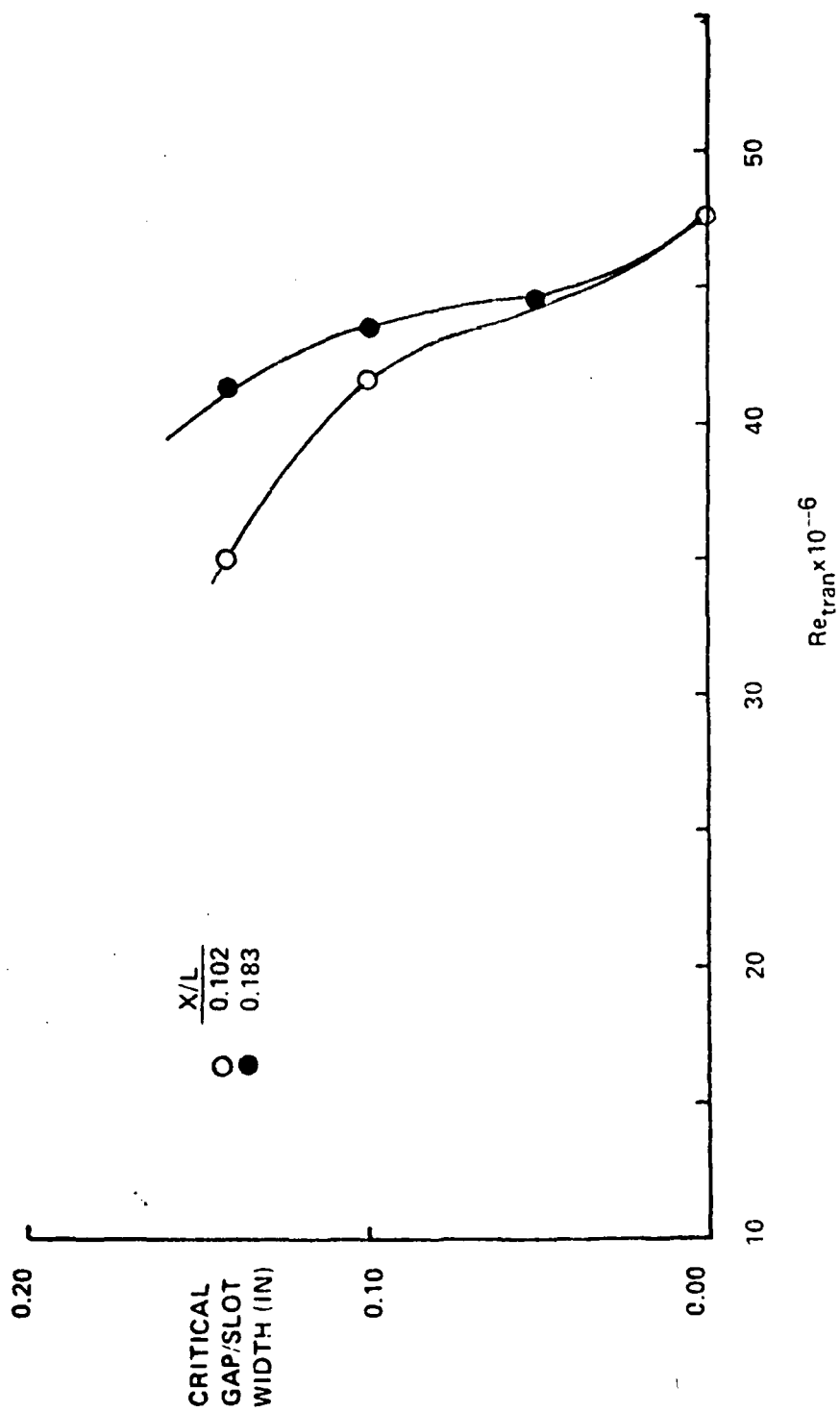FIGURE 3-10 DISCRETE ROUGHNESS - TRANSITION TEST.

28

FIGURE 3-11 GAP/SLOT - TRANSITION TEST

29

4.0 ENVIRONMENT INFLUENCE ON PASSIVE LAMINAR FLOW STABILIZATION

In addition to the passive laminar flow stabilization experiments an analysis was performed to define additional environment influence on the passive laminar flow stabilization concept. This analysis included identifying unit Reynolds number, model/freestream temperature, freestream turbulence, and crossflow influence on the laminar boundary layer stability.

4.1 UNIT REYNOLDS NUMBER INFLUENCE

The two major concerns related to unit Reynolds number (Re^*) is its effect on; (1) transition location, and (2) critical roughness K_{crit}. At present no analytical method exists for correctly identifying the Re^* influence on transition, however, its influence on K_{crit} is established and can be related to local boundary layer parameters. An attempt was made to identify an appropriate method for evaluating the Re^* influence on transition location.

The current approach identifies Re^* influence on transition in terms of Re_{tran}.[22] This approach has had some conflicting results with pressure gradient data and cannot be related to a criteria for predicting transition location. It is proposed that the appropriate method for evaluating Re^* influence on transition location be correlated with a transition onset criteria e^a. Utilizing an e^a relationship, predictions could be performed for a variety of applications. The experimental data presented in A.M.O. Smith's report,[23] was used to develop an e^a correlation with Re^*. The results of the analysis are illustrated in Figure 4-1. The data includes the test results for two airfoils, tested in the NASA-Langley Low Turbulence Pressure Tunnel, and an axisymmetric body, tested in the NASA-Ames 12 foot Pressure tunnel. The $\ln(a)_{tran}$ correlation with experimental transition data identifies an e^a independent of Re^*. The data for the NACA-0012 airfoil did indicate some variation at the lower Re^* values, which can be attributed to the decreased turbulence intensity at the lower Re^* values, Figure 3-1. In general the transition onset criteria e^a is not influenced by Re^*. For the evaluation of the ATC/laminar airfoil performance, the assessment of Re^* influence was eliminated because of the e^a insensitivity. The major Re^* consideration, however, is directed at surface tolerance requirements which is discussed in Section 6.1.

4.2 MODEL/FREESTREAM TEMPERATURE

In a real flow validation environment (tunnel/flight), the ATC/laminar airfoil surfaces will most likely be nonadiabatic. Because of the potential temperature gradient that may exist between the model and the validation environment, an analysis
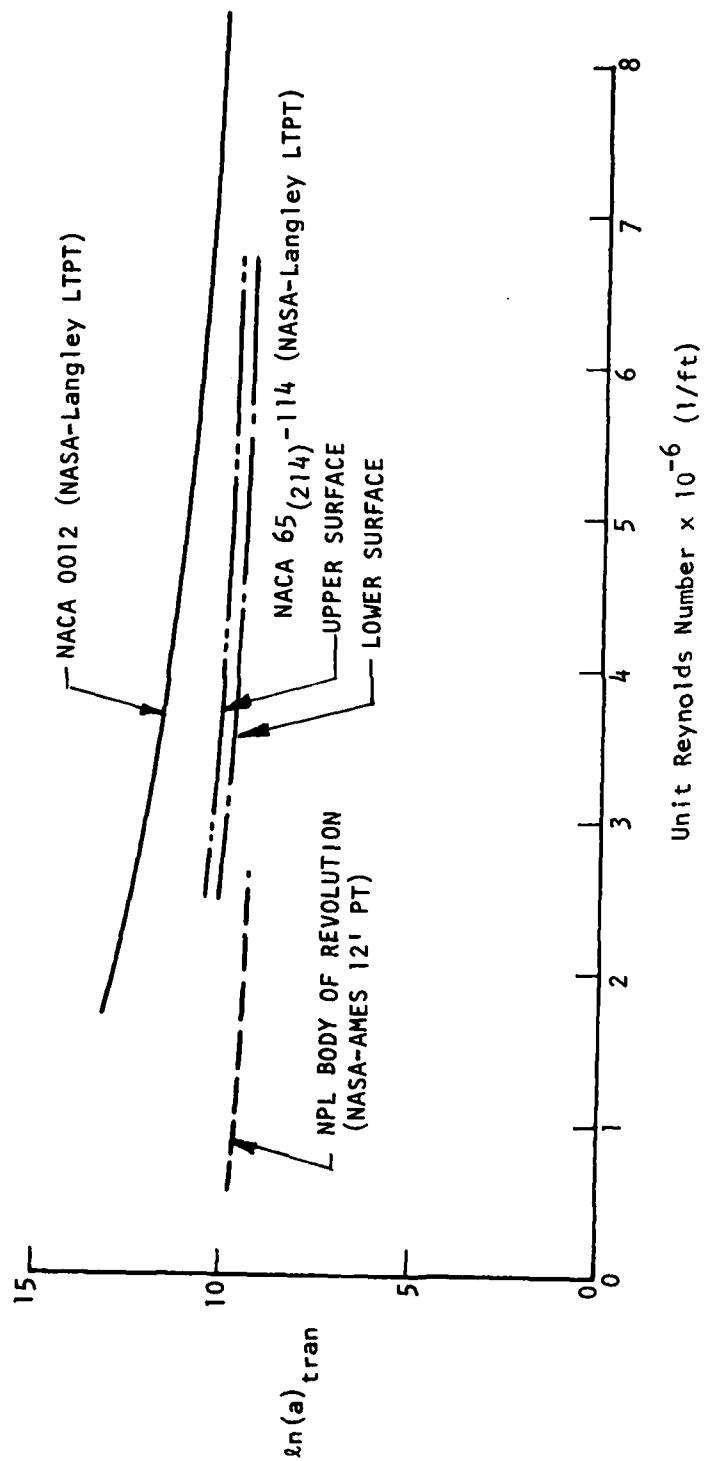
FIGURE 4-1   UNIT REYNOLDS NUMBER EFFECT ON TRANSITION $\ell n(a)$

31

was performed with the TAPS program to identify model/freestream temperature differences on the laminar flow stability.[9] Three wall temperature conditions were evaluated for the airfoil upper surface at the design point C_ℓ = 0.73, M_∞ = 0.6 and Re_c = 4 x 10^7, Figure 2-4. A wall temperature delta of ±40°R on the freestream temperature (518°R) was used in the analysis, Figure 4-2. As was expected, the prediction showed that the cold wall was very effective in reducing laminar flow instabilities. For the heated wall condition the instabilities increased, however, the increment was not as large as the cold wall case. The heated wall case did not indicate any severe growth in the spatial amplification envelope. The heated wall case maximum amplification ratio, at S/C = 0.8 increased from 4.5, adiabatic wall, to 5, still well below the transition onset criteria of 9. The cold wall was very effective in reducing the maximum spatial amplification ratio from 4.5, adiabatic wall, to 1.5. Because of these two effects the ATC/laminar airfoil design concept could provide additional design benefits. These benefits could include; (1) Using heat for de-icing/frost without influencing the laminar boundary layer stability, and (2) using the fuel stored in the wing as a medium for cooling the surfaces providing additional flow stabilization benefits.

4.3 FREESTREAM TURBULENCE

The ABLC experiments demonstrated that the passive laminar flow stabilization was sensitive to freestream turbulence. The experiments identified a strong dependence of maximum Re_{tran} on the level of turbulence intensity, Figure 3-9. In the process of evaluating the influence of turbulence intensity on Re_{tran} a method for predicting the turbulence intensity influence was developed.

Recall that the ABLC turbulence intensity data, shown in Figure 3-9, was obtained at the ABLC exit and was referenced to local velocity conditions. To relate the Re_{tran} degradations to freestream velocity conditions a transformation of the experimental data is required. This transformation was performed with a method developed by M. Tucker.[24] The method utilizes tube flow convergence theory to identify the change in the turbulence vorticity in an accelerated tube flow, representative of the ABLC facility. The transformed data is illustrated in Figure 4-3. The experimental data defines a zone for which transition location is stable at X/C = 0.775. If the turbulence intensity increases beyond the critical value, transition location will move forward of X/C = 0.775. The relative high values of critical turbulence intensities, example; Re_{tran} = 4 x 10^7, T = 0.32%, required to transition the flow is attributed to the large stable safety margin, represented by the difference between the predicted maximum amplification
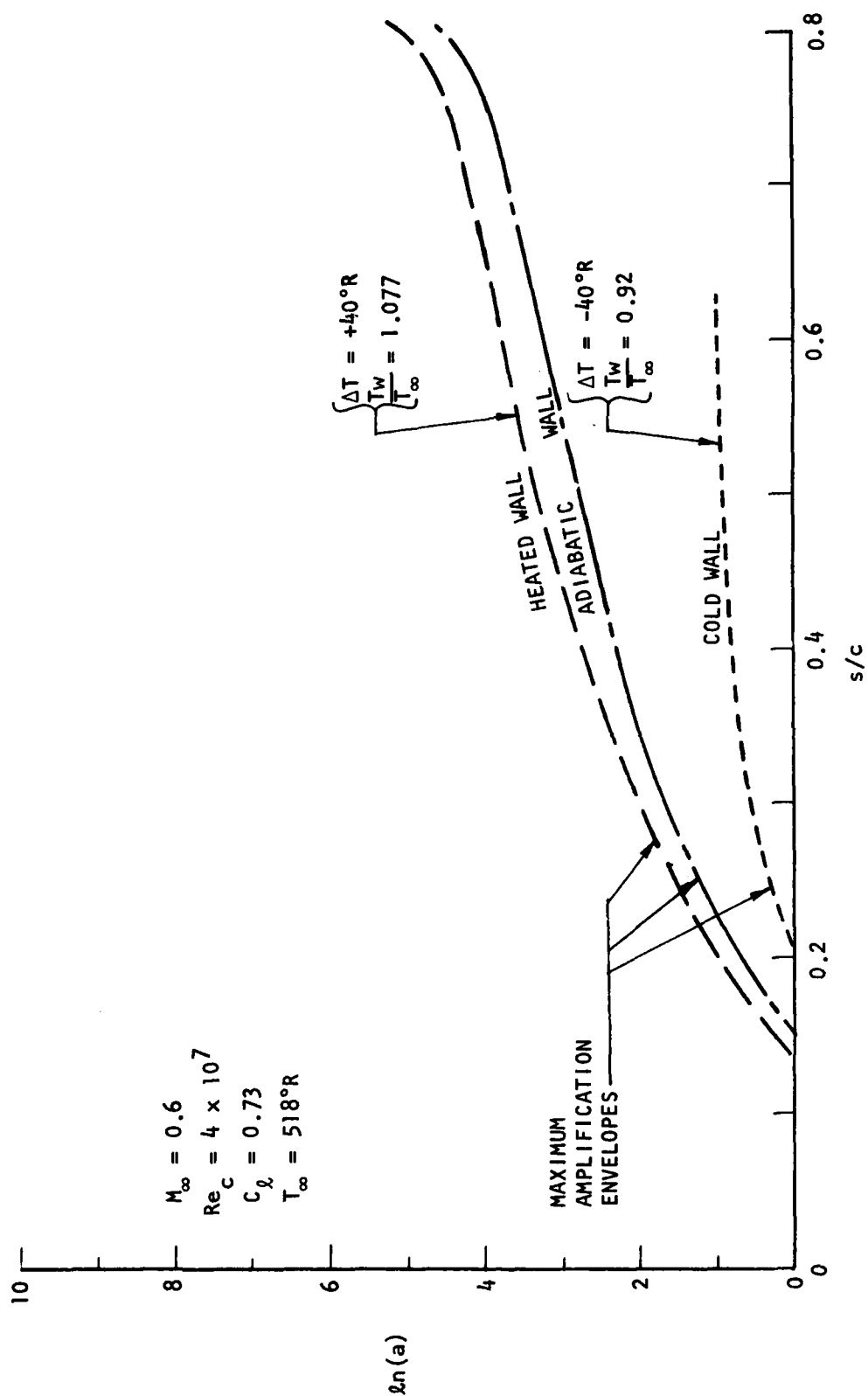
32

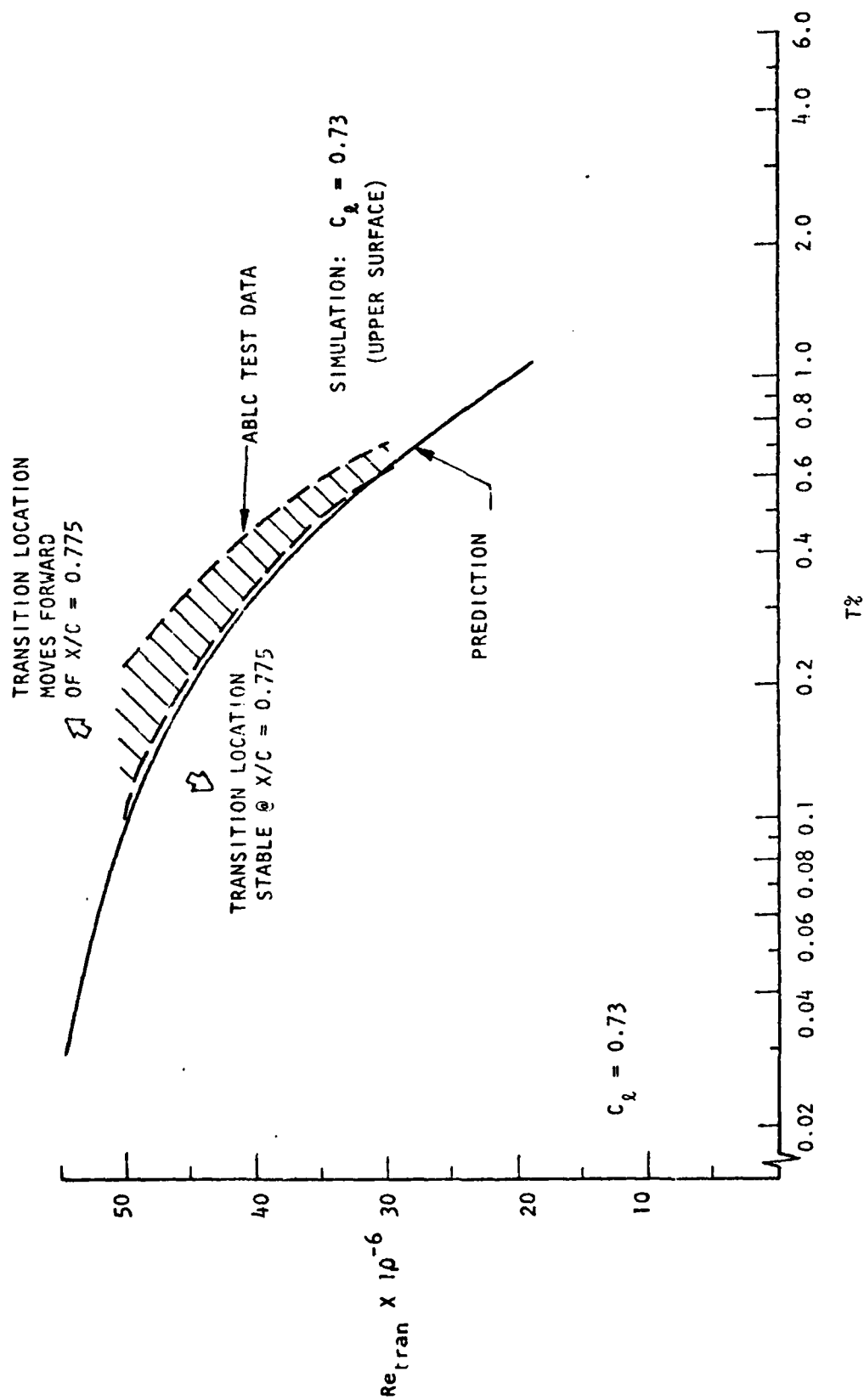FIGURE 4-2   WALL TEMPERATURE EFFECTS ON FLOW STABILITY
(UPPER SURFACE)

33

FIGURE 4-3 MAXIMUM TURBULENCE INTENSITY - Re_{tran} FOR DESIGN POINT $C_\ell = 0.73$.

34

ratio, at S/C = 0.8, and transition onset criteria discussed in Section 2.3.
As a result of these high critical levels, the ATC/laminar airfoil design point
$C_\ell(0.73)$ at Re_c (4×10^7) is relatively insensitive to flight test environment
(T = 0.02% - 0.03%) and to some tunnels with turbulence levels less than T = 0.2%.

Plotted with the experimental data, illustrated in Figure 4-3, is a theoretical
curve which agrees very well with the experimental data. This theoretical prediction
was derived from the author's extrapolation of Mack's theoretical prediction of
turbulence intensity influence on laminar flow stability for constant Hartree β
velocity distributions.[25] Modifications were made to Mack's analytical results
by correlating the analytical predictions more closely to an e^9 transition onset
criteria, Figure 4-4. The curves in Figure 4-4 define the degradation of maximum
Re_{tran} with increasing turbulence intensity values for constant Hartree β velocity
distributions. For example, a flat plate laminar boundary layer ($\beta = 0$) defines
a maximum Re_{tran} decrease from 3.25×10^6, at flight conditions, to 2×10^6, at
turbulence intensity levels representative of the Ames 12-foot pressure tunnel at
$M_\infty = 0.26$. If an airfoil β distribution is known, the maximum Re_{tran} can be
identified for different turbulence levels from the curves in Figure 4-4. An example
utilizing Figure 4-4 to define transition degradation with increasing turbulence
intensities is illustrated in Figure 4-5. The example is the ATC/laminar airfoil
upper surface design point $C_\ell(0.73)\beta$ distribution with a local Re at S/C = 0.8 equal
to 50×10^6, slightly higher than the ABLC maximum validation $Re_{tran} = 48 \times 10^6$.
Note as the turbulence levels increase the transition location, defined by the
intersection of critical values with the airfoil β distribution, moves forward on
the airfoil surface. To maintain laminar flow at X/C = 0.8, representing
$Re_{tran} = 50 \times 10^6$, the turbulence intensity must be less than 0.08%. The method
seems to agree very well with the ABLC data and as a result future analysis and
experimental examination of the method is anticipated. A discussion of the method
as applied to the ATC/laminar airfoil off-design M_∞, C_ℓ and Re_c is presented in
Section 5.3. The method proved very useful in identifying candidate tunnel
validation envelopes.

4.4 CROSSFLOW

In addition to the evaluation of test environment influences on the ATC/laminar
airfoil concept, an analytical examination of three-dimensional crossflow boundary
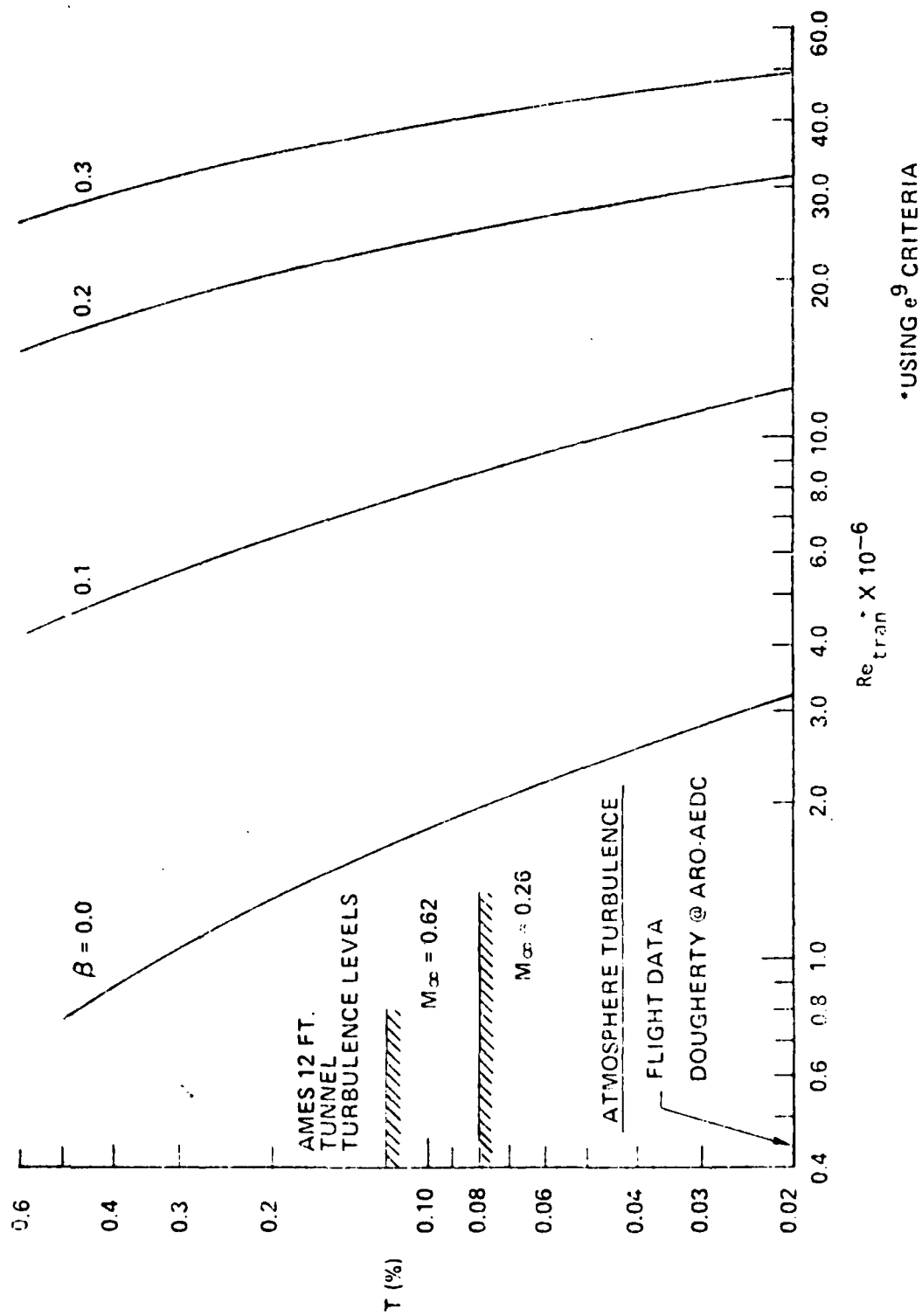layer effects on passive laminar flow stabilization was made. In general the

35

FIGURE 4-4   INFLUENCE OF TURBULENCE INTENSITY ON TRANSITION, $M_\infty = 0.0$.
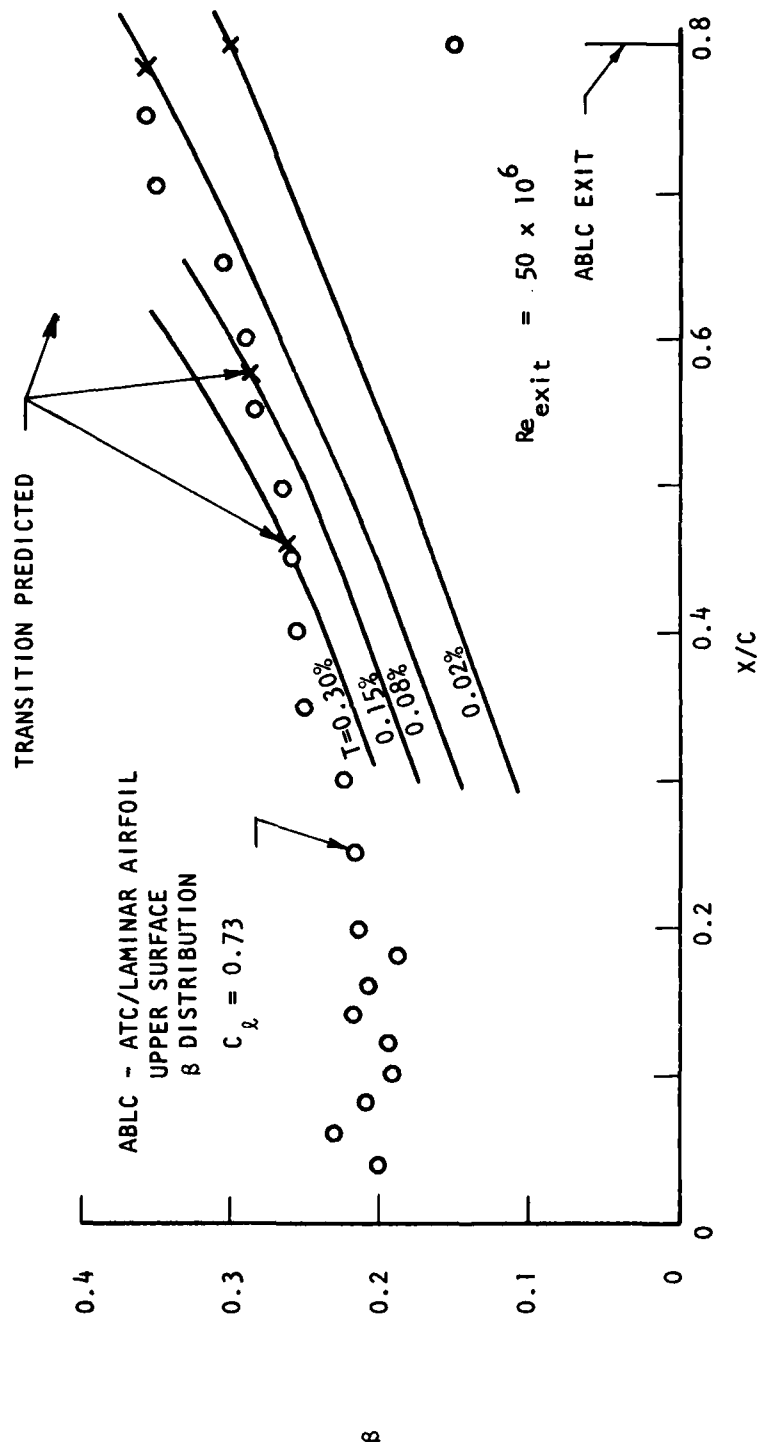
*USING e^9 CRITERIA

FIGURE 4-5 INFLUENCE OF TURBULENCE INTENSITY ON TRANSITION LOCATION

crossflow effects are generated by sweeping the wing with reference to the freestream flow direction. The primary reason for sweeping a wing is to increase the wing drag divergence Mach number and reduce the wave drag. The ATC/laminar airfoil was not designed for transonic Mach numbers and as a result would not offer noticeable wave drag improvements by sweeping the wing. However, because of the interest in the crossflow influences on the passive laminar flow stabilization performance, a swept ATC/laminar wing analysis was made at a cruise $M_\infty = 0.6$. The analysis applied the 2-D pressure distributions directly to an infinite swept wing, assuming that a 3-D section geometry could be identified to produce the 2-D pressure distribution. The crossflow stability calculations were performed with the NASA stability code, SALLY.[26] The analysis was performed for the upper surface of the ATC/laminar airfoil at sweep angles from 0° to 20° or until forward movement of transition location, from $X/C_{tran} = 0.775$ was identified. The influence of pressure gradient and Reynolds number on crossflow instabilities was identified for the design point $C_\ell(0.73)$ and off design $C_\ell(0.85)$ distributions in Figure 2-7.

At the design point conditions ($M_\infty = 0.6$, $C_\ell = 0.73$ and $Re_c = 4 \times 10^7$) the growth of the crossflow instabilities were identified at various sweep angles (γ), Figure 4-6. From $\gamma = 0°$ to $\gamma = 5°$ the maximum spatial amplification ratio did not change appreciably. With further increases in sweep, the crossflow instability increases rapidly predicting transition onset at $S/C = 0.35$ for $\gamma = 10°$. By decreasing the operating Reynolds number from 4×10^7 to 2×10^7 the growth of the crossflow instabilities is reduced, stabilizing the laminar flow to $S/C = 0.75$ for $\gamma = 10°$, Figure 4-7. A summary of the effects of crossflow instabilities on the design point $C_\ell(0.73)$ are illustrated in Figure 4-7.

To reduce the 2-D Tollmien-Schlichting instabilities, as discussed in Section 2.0, strong pressure gradients are required. However, to reduce crossflow instabilities a decrease in pressure gradient is required, producing a conflict in passive laminar flow stabilization design objectives. To identify the influence of pressure gradient on crossflow instabilities, an analysis was made for a reduced pressure gradient condition at $C_\ell = 0.85$, Figure 4-8. For a swept wing of $\gamma = 10°$, the reduced pressure gradient strongly influenced the growth of crossflow instabilities by moving the transition onset from $S/C = 0.35$ to 0.52. Therefore for a swept transonic wing configuration, crossflow would be one of the major considerations in the design. It should be noted also that the above results are all for sweeping of a constant section geometry. Spanwise tailoring of section geometries for maximum chordwise laminarization opens new possibilities for optimization.

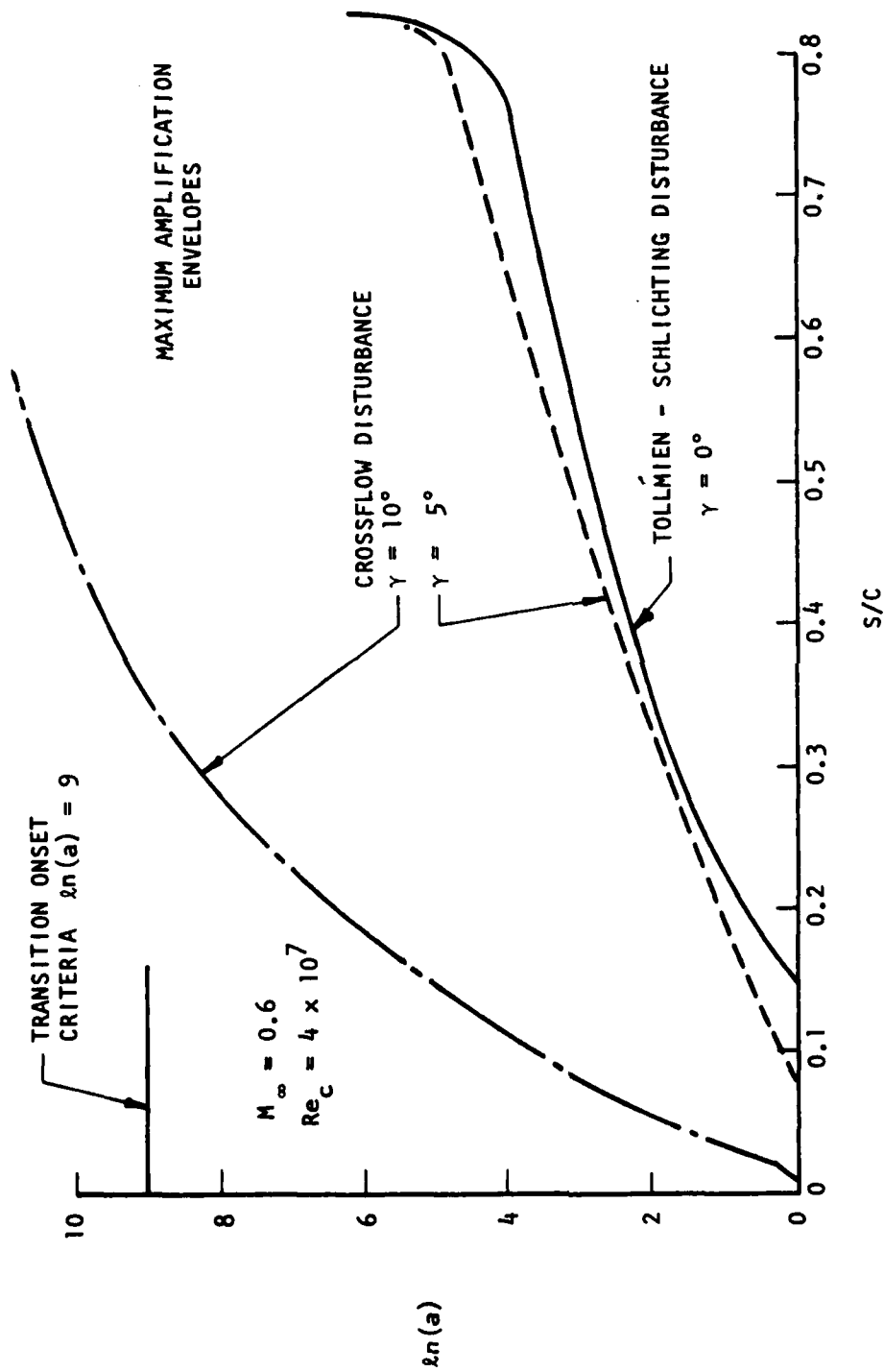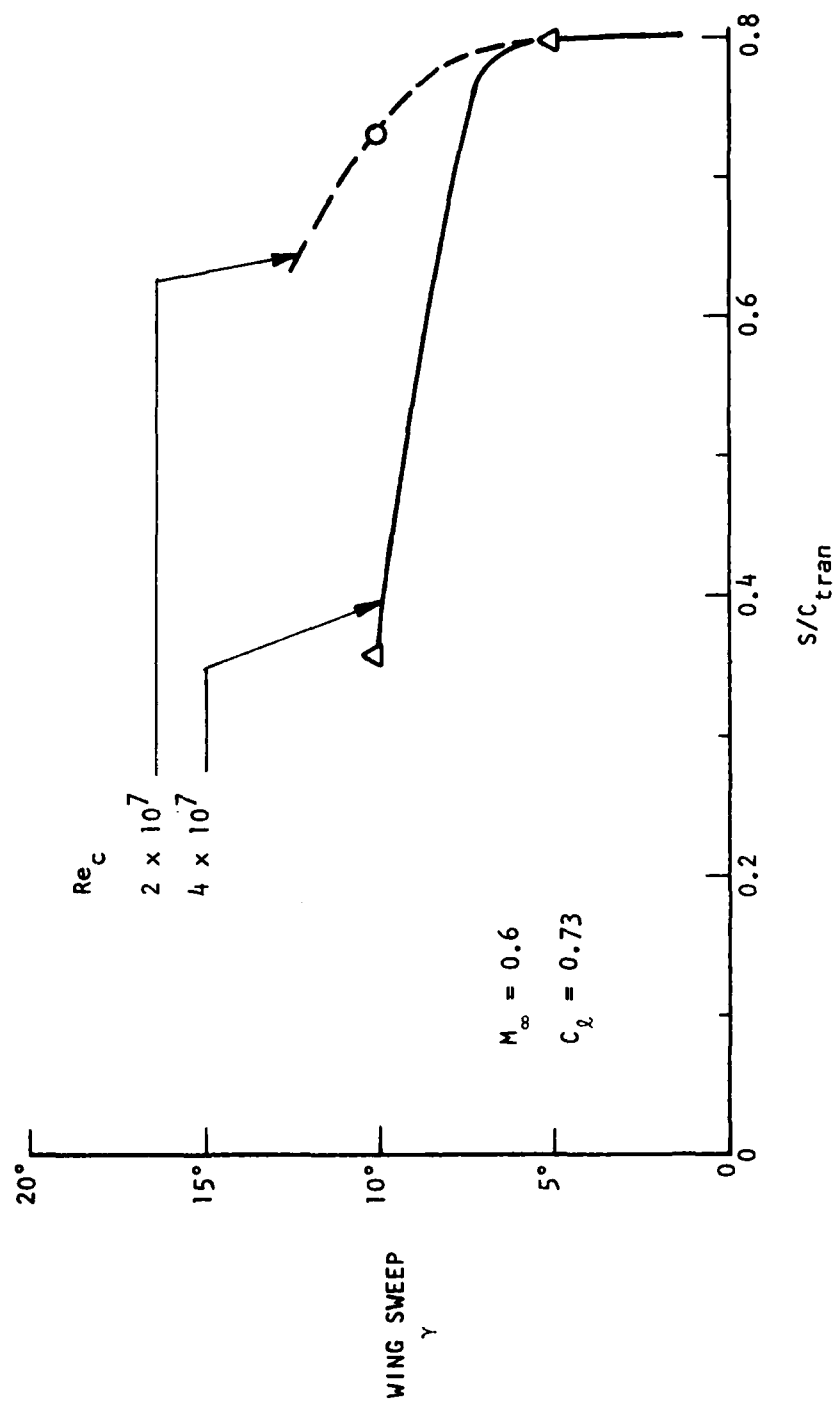FIGURE 4-6 UPPER SURFACE CROSSFLOW STABILITY ANALYSIS, $C_\ell = 0.73$

39

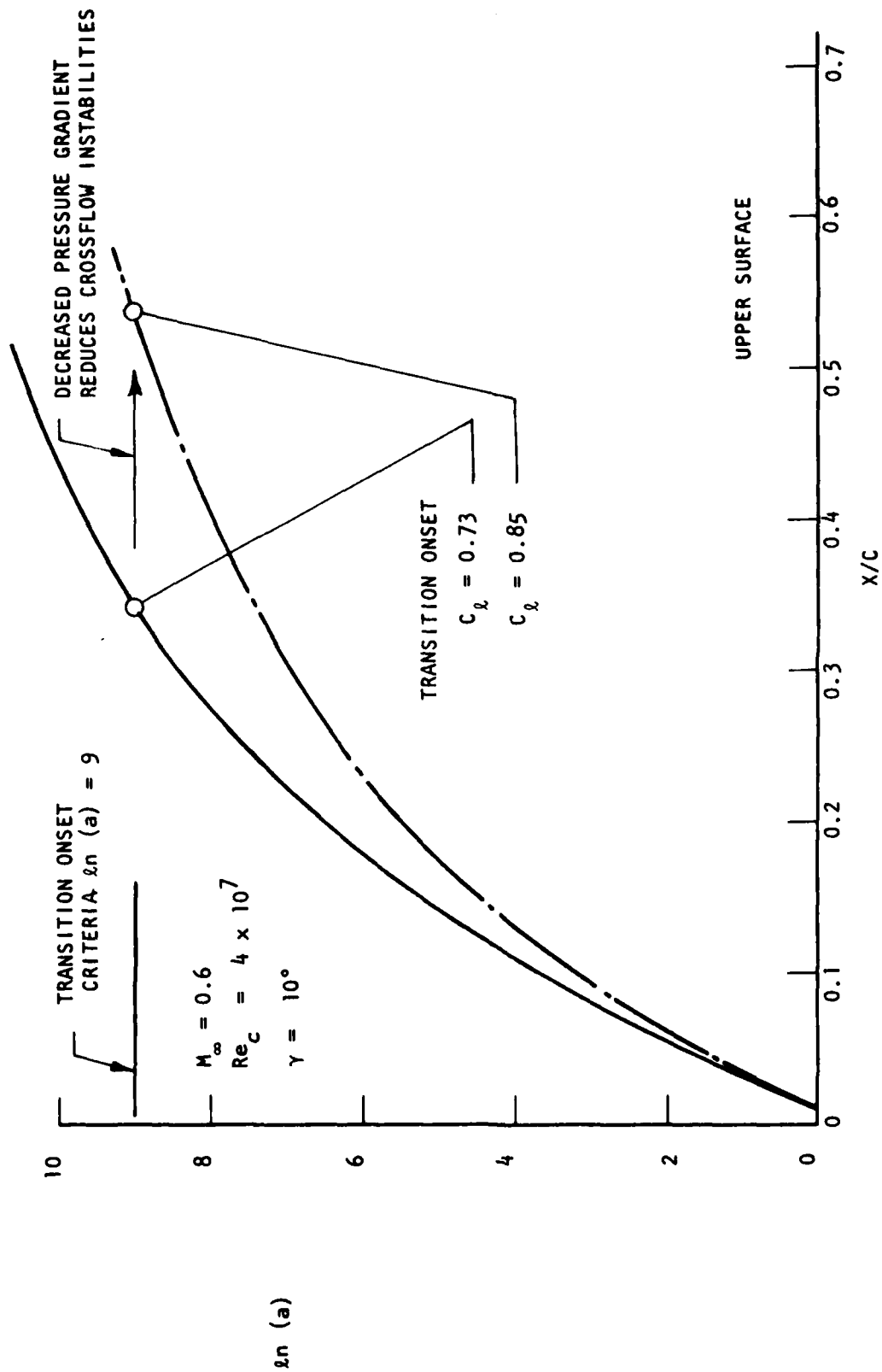FIGURE 4-7   INFLUENCE OF WING SWEEP ON UPPER SURFACE TRANSITION LOCATION

FIGURE 4-8 COMPARISON OF CROSSFLOW INSTABILITIES FOR DIFFERENT C_ℓ AT $M_\infty = 0.6$

41

5.0 WIND TUNNEL VALIDATION ASSESSMENT

An assessment was made of potential test facilities and their compatibility
with the ATC/laminar airfoil design and off-design validation requirements. The
primary requirement is that the tunnel test environment is suitable for laminar flow
testing, quiet with a very low turbulence intensity level. The additional tunnel
requirements include test compatibility at the airfoil design and off-design Mach
numbers and Reynolds numbers and an auxiliary high pressure air source for the
wall jet. A Vought in-house survey of university, industry and government owned
test facilities identified a limited number of candidate facilities. Of them,
the Ames 12 foot Pressure Tunnel appeared to be the best suited for the validation
of the ATC/laminar airfoil concept.[15] The alternate facility was the Langley
Low Turbulence Pressure Tunnel.[16] The following sections discuss the candidate
tunnel operating ranges and test environment, examine the ATC/laminar airfoil
off-design performance subject to candidate tunnel operation limits, identify
tunnel environment influences on performance,and define the tunnel validation
envelopes.

5.1 TEST FACILITY EVALUATION

A detailed examination of the candidate Ames 12 foot Pressure Tunnel test
environment and operating envelope was performed to identify the ATC/laminar
airfoil validation compatibility. The examination identified; (1) freestream
turbulence intensity levels, (2) limitation to the design point high Reynolds
number passive laminar flow validation with alternate off-design validation
considerations, and (3) model support/trunnion limits.

The candidate Ames tunnel and the alternate Langley tunnel offer the
best suited facility environments for the high Reynolds number passive laminar flow
validation. The test environment of the candidate Ames tunnel was recently
evaluated by NASA-Langley's personnel to determine its suitability for laminar
flow wing testing.[15] These tests included measurements of turbulence, acoustic,and
vibration intensities along with their corresponding spectrum. The results of the
tunnel turbulence intensity measurements are shown in Figure 3-1, including the
values from the Langley tunnel and flight data.[16,17] In general the tunnel turbu-
lence intensities are at a much higher level than the flight environment. Note
also that the level of turbulence intensity increases as the tunnel Re_c, M_∞ increase.

Examination of the tunnel turbulence intensity influence on the airfoil performance is discussed in Section 5.3.

The operating envelopes of the candidate Ames tunnel presents limits on the validation of the ATC/laminar airfoil design concept. The major limitation of the tunnel is the limited unit Reynolds number capability, Figure 5-1. At the airfoil design point M_∞ (0.6) the maximum Re_c is limited to 10^7, for a 4 ft (1.2 m) chord model, well below the desired validation $Re_c = 4 \times 10^7$. To validate the high Reynolds number passive laminar flow concept, M_∞ tradeoffs were considered. An off-design validation $M_\infty = 0.3$ was selected because of the tunnel High Reynolds number capability, $Re_c = 3.5 \times 10^7$. Examination of the ATC/laminar airfoil performance at the off-design M_∞ and Re_c are discussed in Section 5.2.

The Ames tunnel model support/trunnion load limits were obtained from NASA-Ames personnel. The lift load limits are -4,000 lbs (-1,800 kg) and +20,000 lbs (+9,000 kg). The drag load limit is 10,000 lbs (4,500 kg). The pitching moment limits are ±12,000 ft-lbs (±4,860 m-kg). These load limits are utilized in Section 5.4 to identify the maximum C_ℓ limits.

5.2 AIRFOIL OFF-DESIGN EVALUATION

The major full scale validation constraint imposed by the tunnel facility is the maximum Reynolds number limitation, previously discussed in Section 5.1. To determine the full scale Reynolds number validation potential of the passive laminar flow concept, off-design predictions were made at $M_\infty = 0.3$ for two different Re_c (2 x 10^7 and 3 x 10^7) within the tunnel test envelope. At the off-design M_∞ (0.3) an example pressure distribution for $C_\ell = 0.5$ is shown in Figure 5-2. The general shape of the off-design M_∞ (0.3) and C_ℓ (0.5) pressure distribution is representative of the design point C_ℓ (0.73) and M_∞ (0.6) pressure distribution, Figure 2-4. The reduced pressure gradient , at $M_\infty = 0.3$, over the forward section of the airfoil, Figure 5-2, is related to the decrease in compressibility effect. This decrease in pressure gradient influences the passive laminar flow stability and reduces the level of C_ℓ and Re_c at which the full potential of passive laminar flow stabilization can be verified. For the off-design $C_\ell = 0.5$, validation of the high Reynolds number passive laminar flow concept can be obtained for $Re_c = 3 \times 10^7$, neglecting any flow environment degradations. At this $C_\ell = 0.5$, controlled trailing edge diffusion was predicted, without requiring auxiliary C_μ, predicting a $C_d = 0.00338$ with a L/D = 150. The stability analysis of off-design C_ℓ (0.5) at $Re_c = 3 \times 10^7$ is
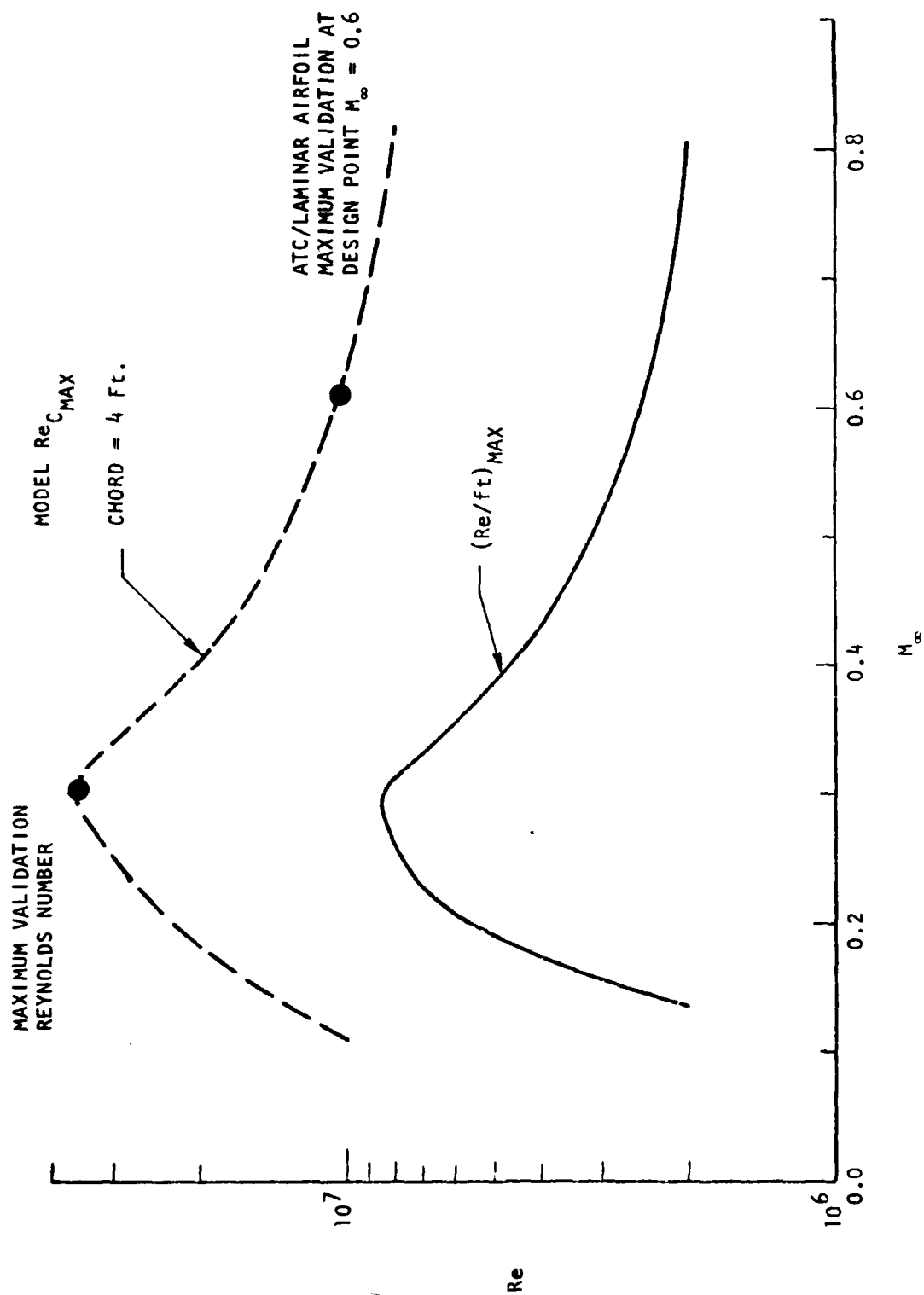
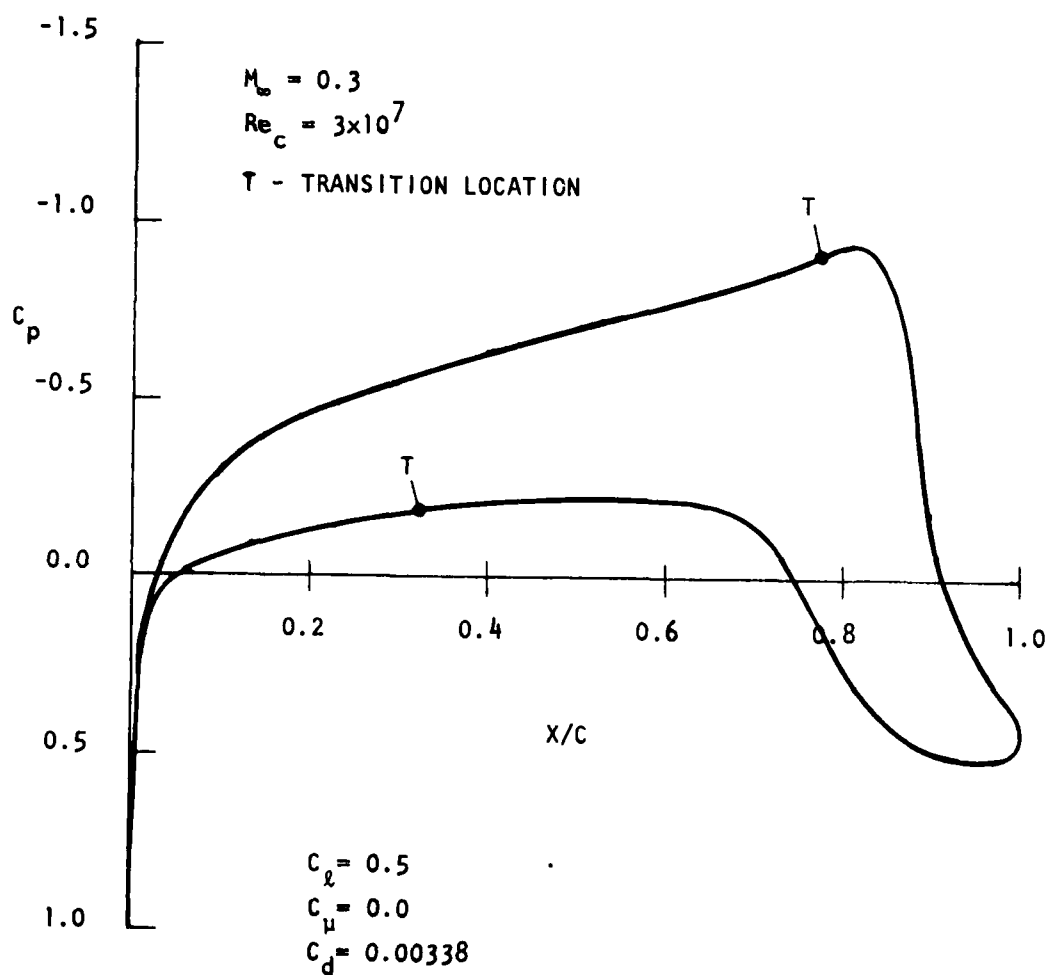FIGURE 5-1 AMES 12 FOOT PRESSURE TUNNEL, REYNOLDS NUMBER - M∞

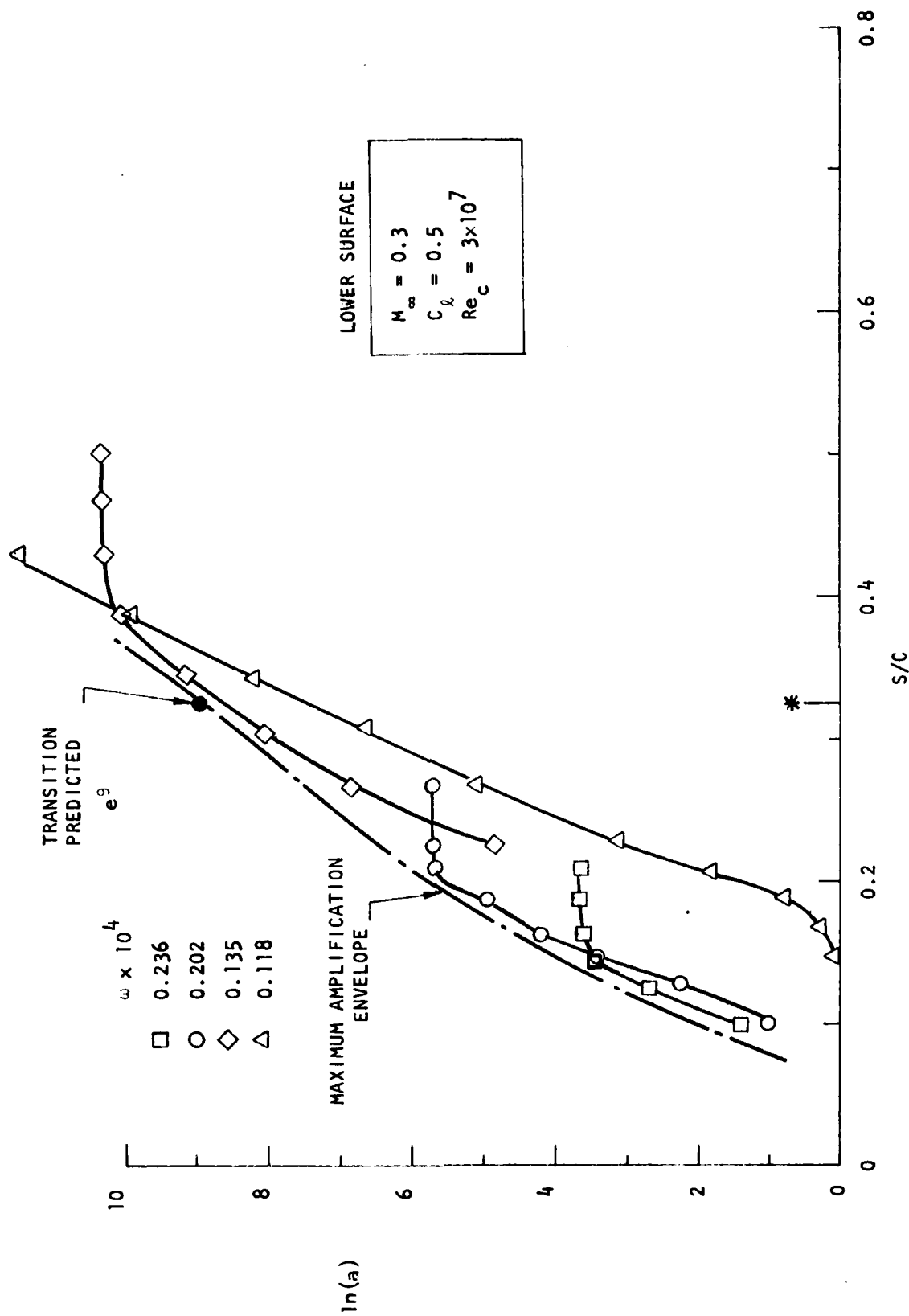FIGURE 5-2   ATC LAMINAR AIRFOIL PRESSURE DISTRIBUTION, C_ℓ = 0.5

FIGURE 5-3 ATC/LAMINAR AIRFOIL STABILITY ANALYSIS, C_ℓ = 0.5
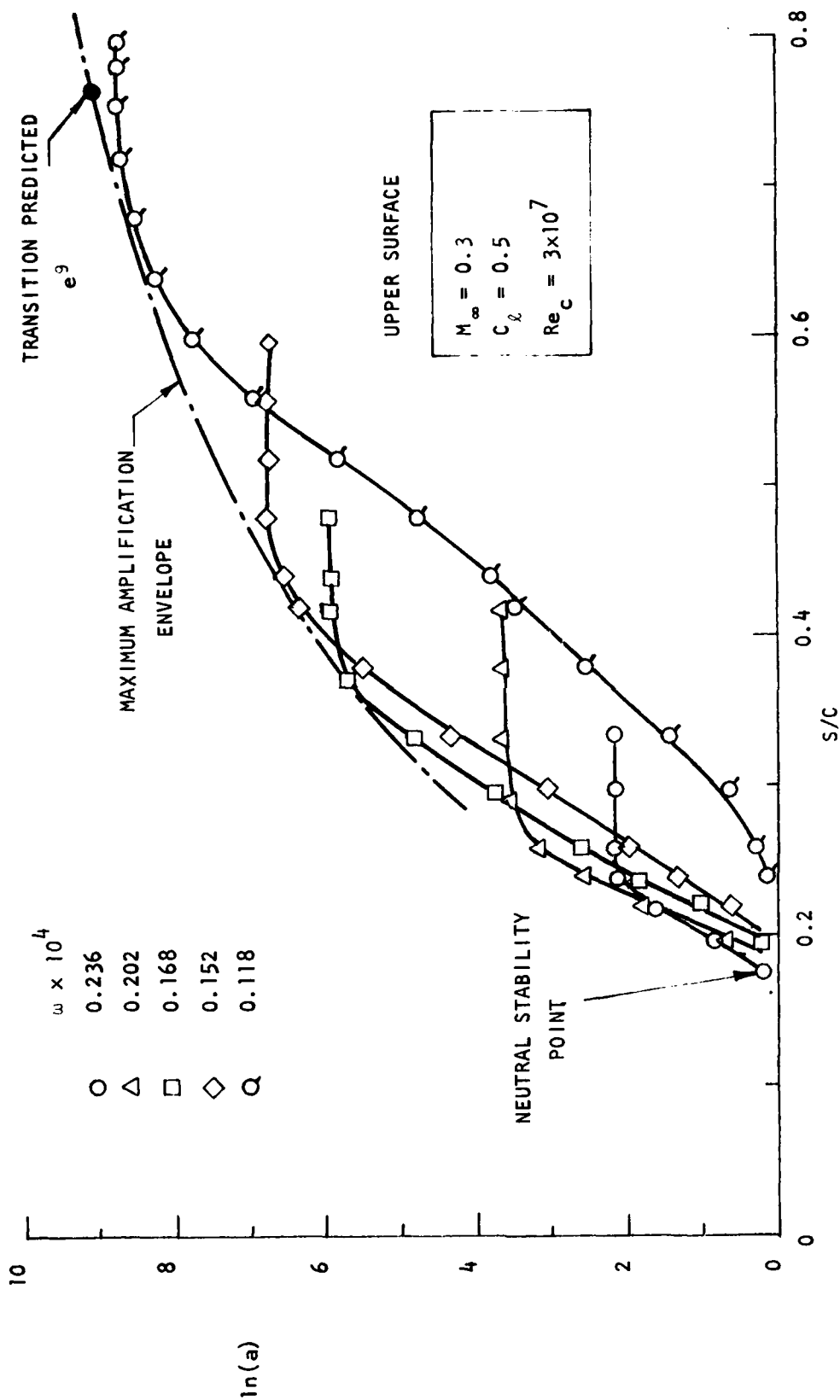
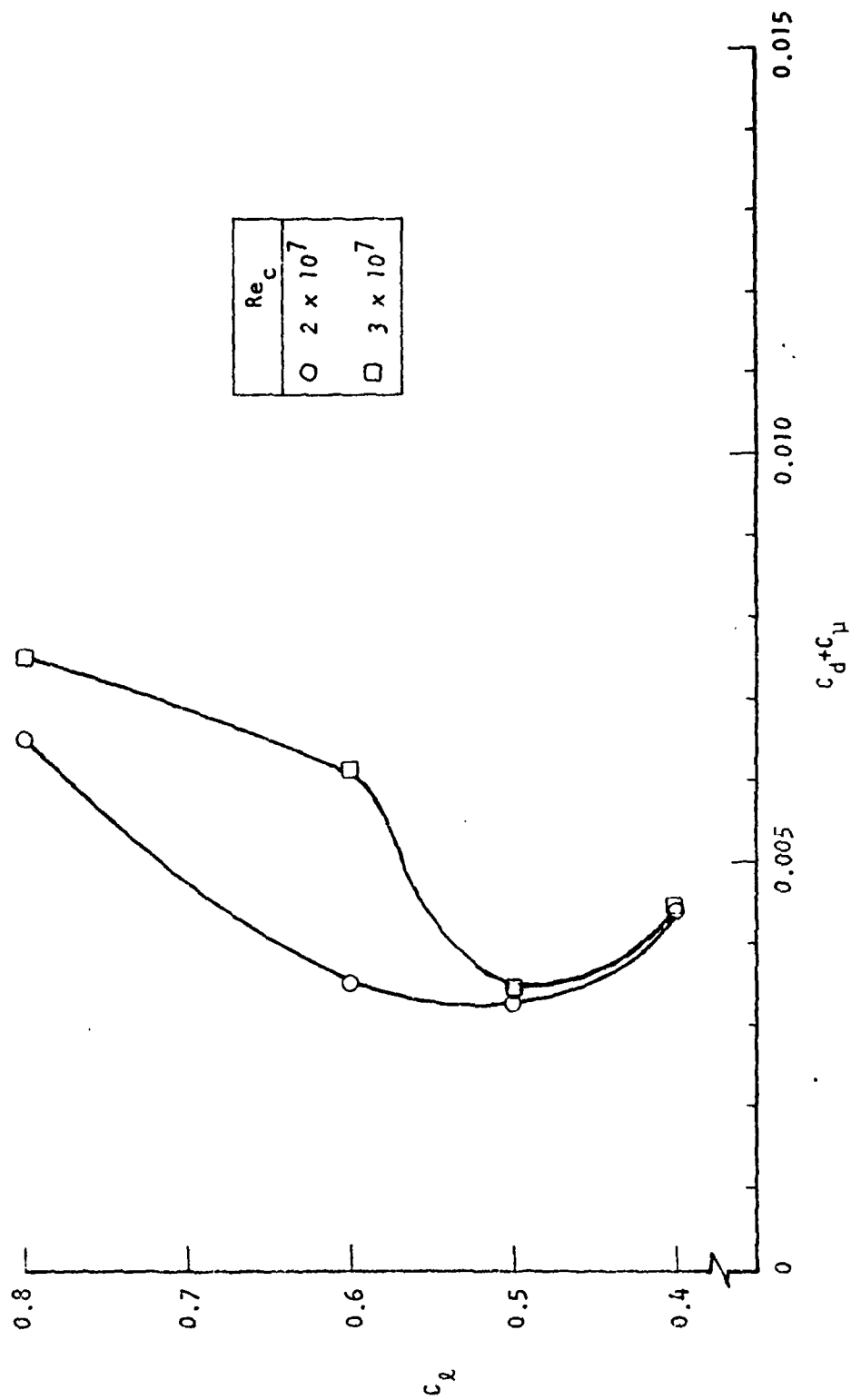FIGURE 5-4 ATC/LAMINAR AIRFOIL STABILITY ANALYSIS, $C_\ell = 0.5$

FIGURE 5-5   PREDICTED DRAG POLARS FOR $M_\infty = 0.3$

shown in Figures 5-3 and 5-4, identifying upper and lower surface transition
locations at S/C = 0.75 and 0.34, respectively. The performance of the ATC/laminar
airfoil design at the off-design M_∞ (0.3) was identified using the same approach
discussed in sections 2.2 and 2.3. The resultant off-design drag
at M_∞ = 0.3 for Re_c = 2 x 10^7 and 3 x 10^7 (Figure 5-5), identify the passive laminar
flow off-design performance subject to tunnel validation constraints. At the lower
Re_c (2 x 10^7) a large drag bucket is identified and as expected with increasing
Re_c (3 x 10^7) the size of the drag bucket is reduced. The C_μ requirement predicted
for M_∞ = 0.3 identified an optimum level, related to a wing with partial laminar
flow, and a maximum blowing requirement defined by a fully turbulent wing, Figure
5-6. The maximum C_μ prediction is related to anticipated forced transition
experiments.

An analysis was also performed for the design point M_∞(0.6) constrained to
the tunnel maximum Re_c = 10 x 10^6 capability. The drag polar prediction at this
low Re_c identified a very large drag bucket with a maximum drag bucket $C_\ell \approx 1.2$
with a L/D = 200, Figure 5-7. The low Re_c (10 x 10^6) reduced the favorable pressure
gradient requirement for maintaining stable laminar flow and permitted the low drag
levels to be obtained at the larger C_ℓ's. The shift in the minimum drag level from
the reference design point Re_c = 4 x 10^7 case is a Reynolds number effect and not a
movement in transition location.

5.3 TUNNEL ENVIRONMENT INFLUENCE ON PERFORMANCE

Analysis of the environment influence on the design point passive laminar flow
stabilization, discussed in Section 4.0, identified several parameters which had
some or no influence on the laminar flow stability. Of these parameters the free-
stream turbulence intensity posed the greatest potential for degrading the 2-D
laminar flow stability. In veiw of the moderate turbulence intensity levels of the
candidate Ames 12 foot pressure tunnel (Figure 3-1), potential validation limits
are posed. To identify these performance degradations, associated with the tunnel
turbulence levels, calculations were made with the turbulence intensity influence
method discussed in Section 4.3. This analysis was performed for the off-design
cases discussed in Section 5.2.

At the off-design tunnel M_∞ = 0.3 the predicted airfoil performance, defined
in Figure 5-5, was reevaluated for the tunnel turbulence intensity level associated
with Re_c = 2 x 10^7 and 3 x 10^7. Two examples illustrating the calculations of
tunnel turbulence intensity influence on C_ℓ = 0.5 are shown in Figure 5-8 and 5-9
for Re_c = 2 x 10^7 and 3 x 10^7, respectively. The transition location is identified
by the intersection of the airfoil β distribution with the critical turbulence
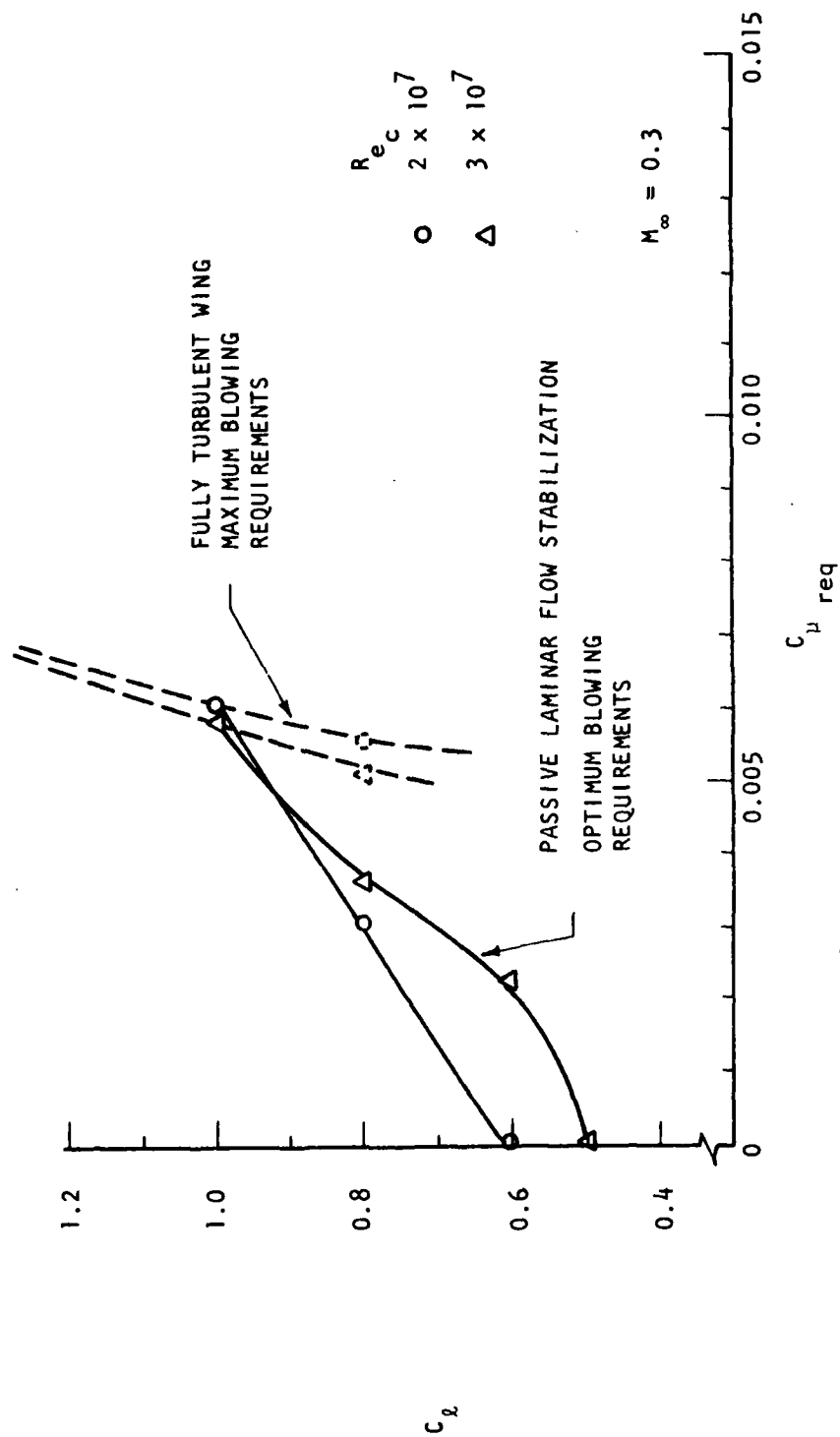
49

FIGURE 5-6 TUNNEL VALIDATION C_μ REQUIREMENTS, $M_\infty = 0.3$
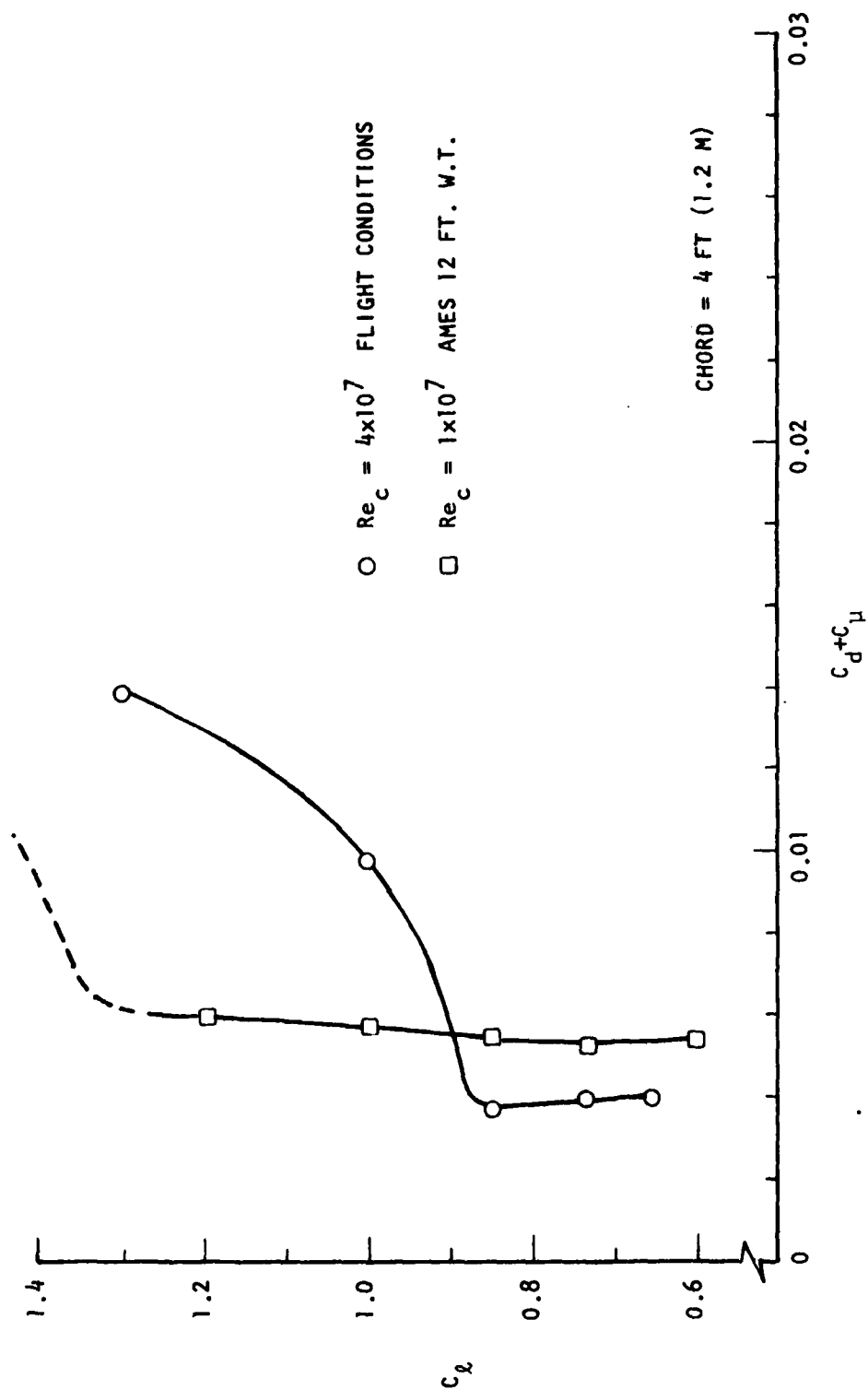
50

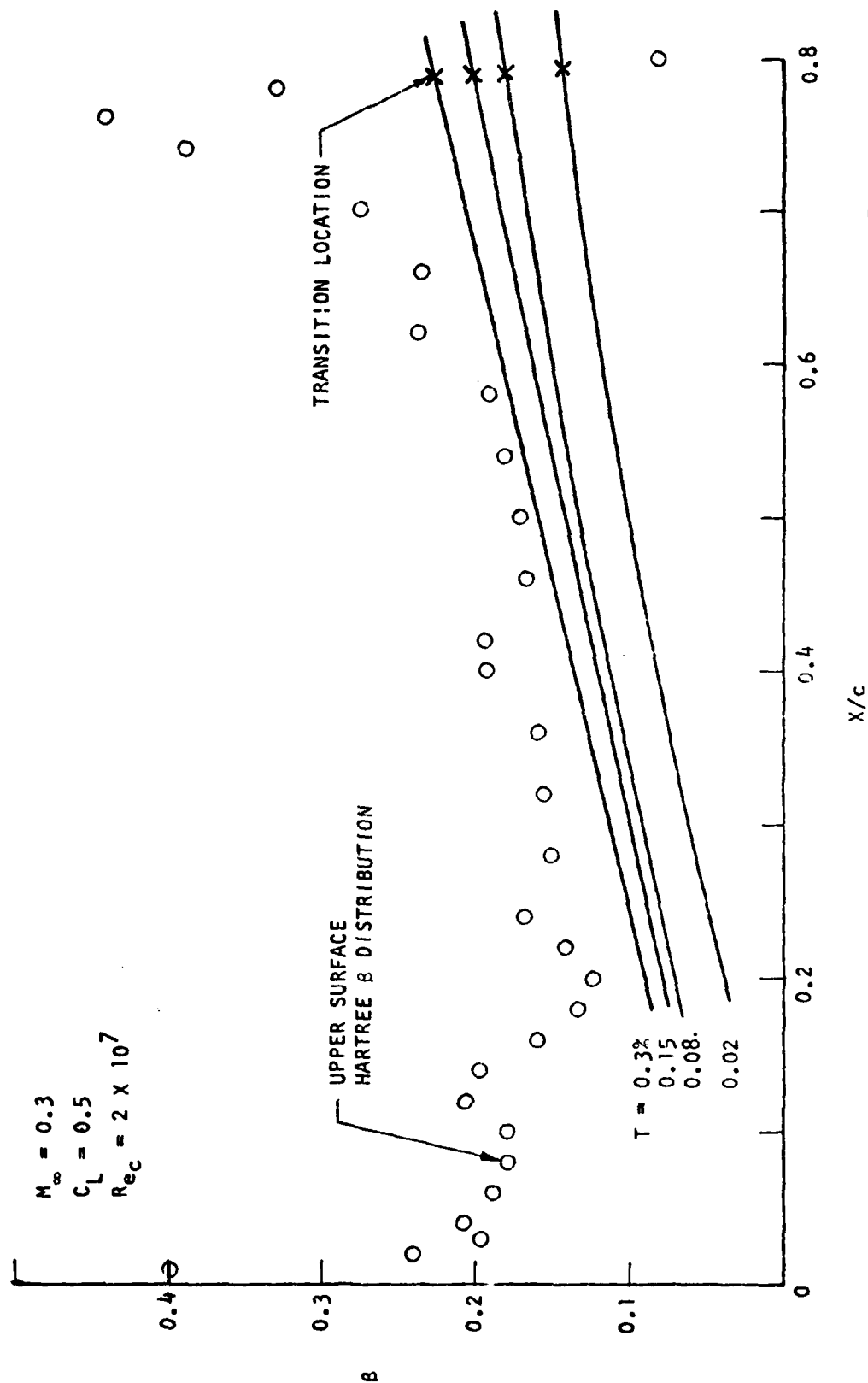FIGURE 5-7 PREDICTED DRAG POLARS FOR M_∞=0.6 TEST ENVIRONMENT

FIGURE 5-8 TURBULENCE INTENSITY EFFECT ON TRANSITION LOCATION, $Re_c = 2 \times 10^7$
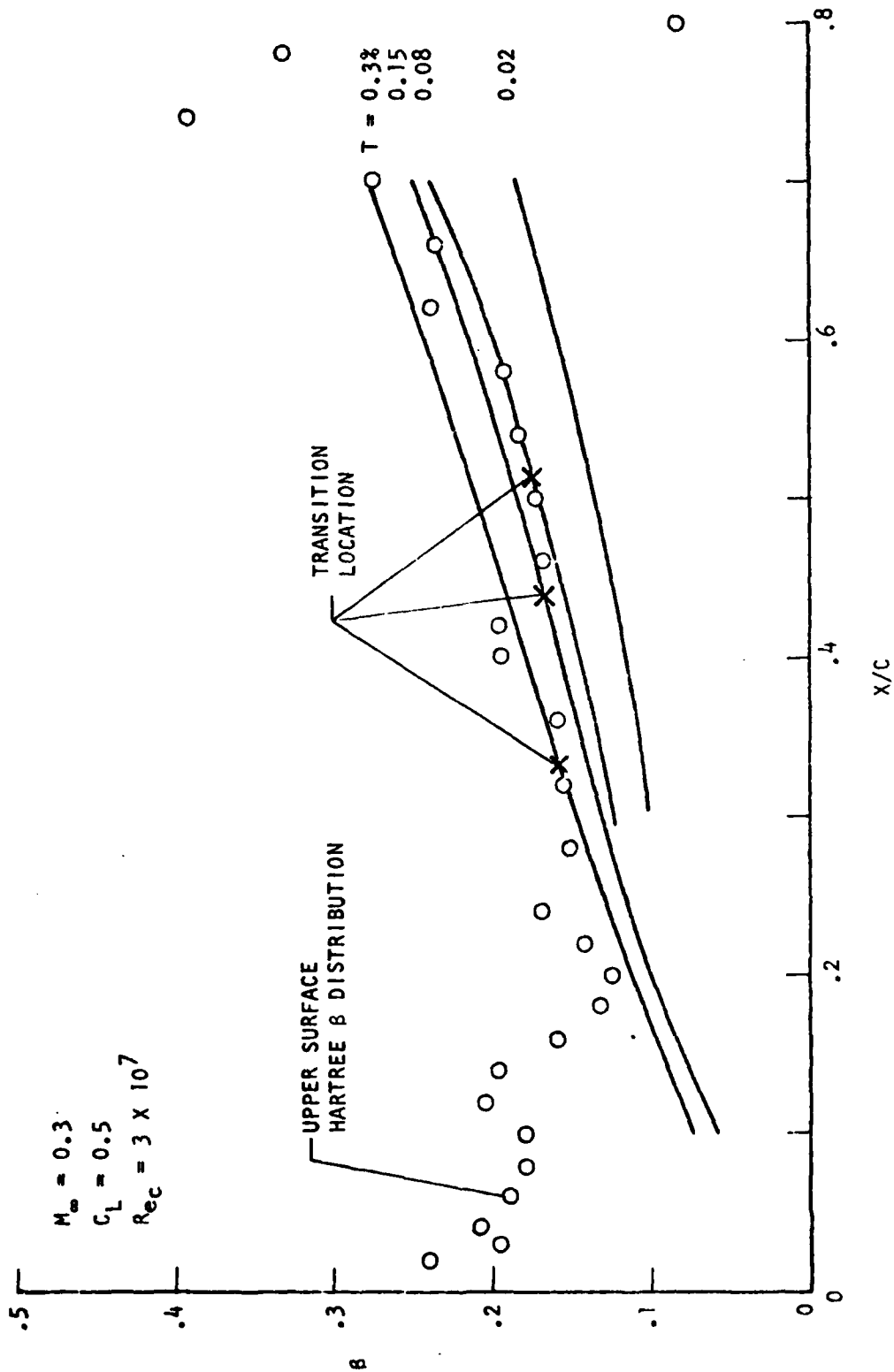
FIGURE 5-9 TURBULENCE INTENSITY INFLUENCE ON TRANSITION LOCATION, $Re_c = 3 \times 10^7$

intensity values. For a $Re_c = 2 \times 10^7$, the tunnel turbulence intensity, T = 0.08% (Figure 3-1), did not effect the predicted transition location at X/C = 0.8. At $Re_c = 3 \times 10^7$, the tunnel turbulence intensity, T = 0.08%, transitioned the flow at X/C = 0.52. This information and additional calculations were input into the boundary layer analysis to identify the drag polars with the tunnel turbulence intensity effects, Figure 5-10. The turbulence intensity strongly influenced the performance of the ATC/laminar airfoil. The tunnel turbulence level at $Re_c = 3 \times 10^7$ completely eliminated the drag bucket and greatly reduced the size of the drag bucket at $Re_c = 2 \times 10^7$. To obtain a validation of the passive laminar flow concept at high Re_c (3×10^7), the validation would have to be limited to upper surface validation only at $C_\ell < 0.4$. At C_ℓ greater than 0.4, the transition location would be forward of X/C = 0.8.

The analysis was also performed for the design point M_∞ (0.6) at the limited $Re_c = 10 \times 10^6$. The results of the analysis indicated that the predicted performance, illustrated in Figure 5-7, was unchanged. Although the tunnel turbulence intensity, T = 0.12%, was higher the reduced Re_c made the laminar flow extremely stable and the effect of the turbulence intensity did not influence the performance.

5.4 TUNNEL VALIDATION POTENTIAL

The purpose of a wind tunnel validation test will be to demonstrate and document the ATC laminar airfoil design concept. Because of the limitations of the test facilities, NASA-Ames 12 foot pressure tunnel and alternate tunnel NASA-Langley LTPT, full scale validation of the design point $C_\ell = 0.73$ at $Re_c = 4 \times 10^7$ and $M_\infty \sim 0.6$ cannot be obtained. However, potential validation of the concept at lower Mach numbers ($M_\infty = 0.3$) is possible at significant Re_c, Figure 5-11. Shown in Figures 5-11 and 5-12 are the operation limits of the Ames tunnel and model trunion support load limits. These limits define the maximum Re_c capability of the Ames tunnel at M_∞ and C_ℓ. Plotted in Figure 5-11 is the Re_c - M_∞ validation envelope defining potentials and marginal validation regions. For $M_\infty = 0.3$ maximum passive laminar flow validation is possible for $Re_c = 2-2.5 \times 10^7$ and at higher Reynolds number passive laminar flow validation is possible for the airfoil upper surface only at the tunnel limits ($Re_c \sim 3.5 \times 10^7$) for $C_\ell < 0.4$. For $M_\infty = 0.6$ the validation of the ATC laminar airfoil concept is not limited in C_ℓ, however the maximum tunnel Re_c is limited to 1×10^7.

For comparison, S-3 and P-3 operation regions were plotted against tunnel full scale validation envelopes, Figures 5-11 and 5-12. The S-3 cruise/on station operation, at $M_\infty = 0.6 - 0.64$, is very near the full scale Re_c capability of the
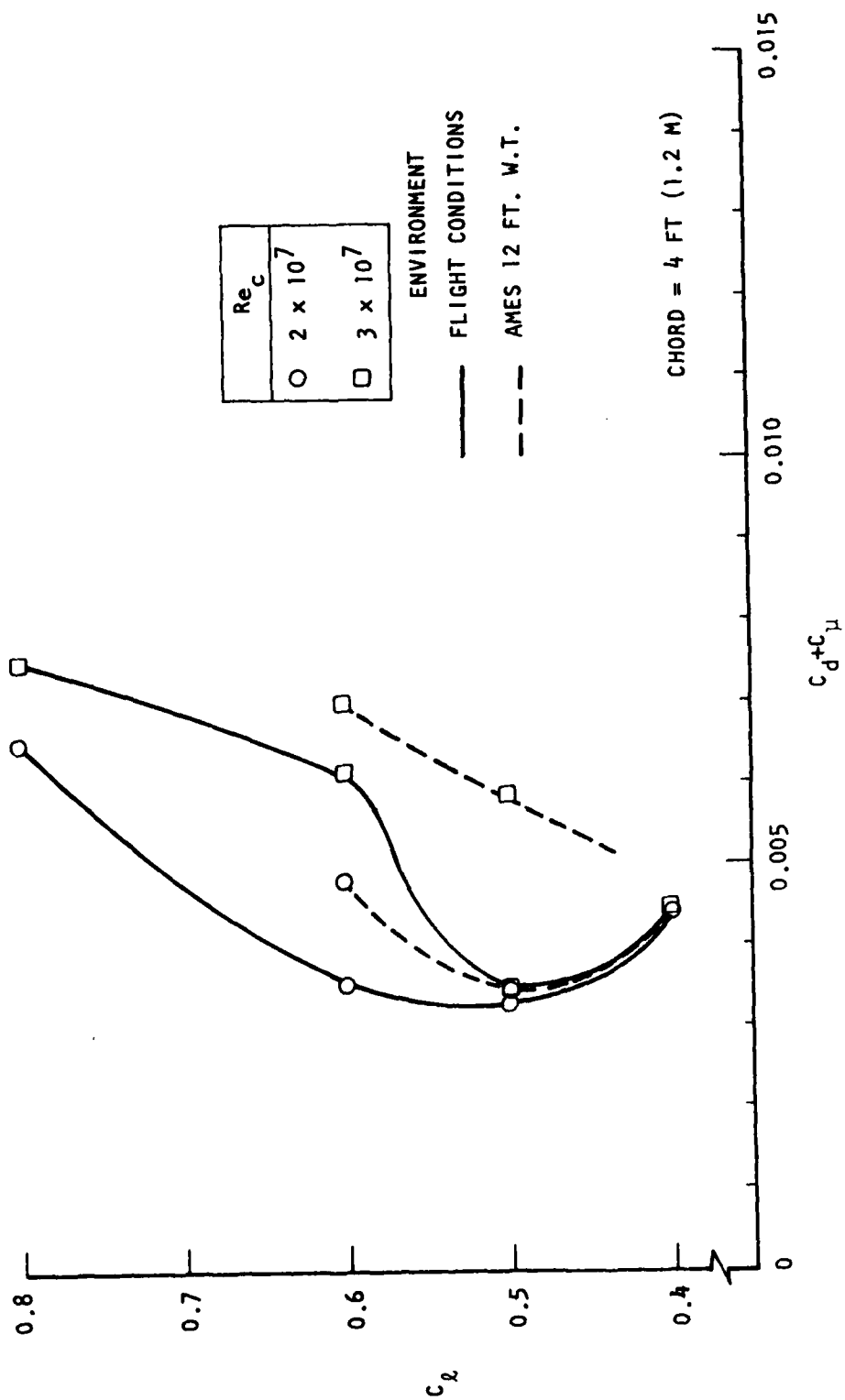
54

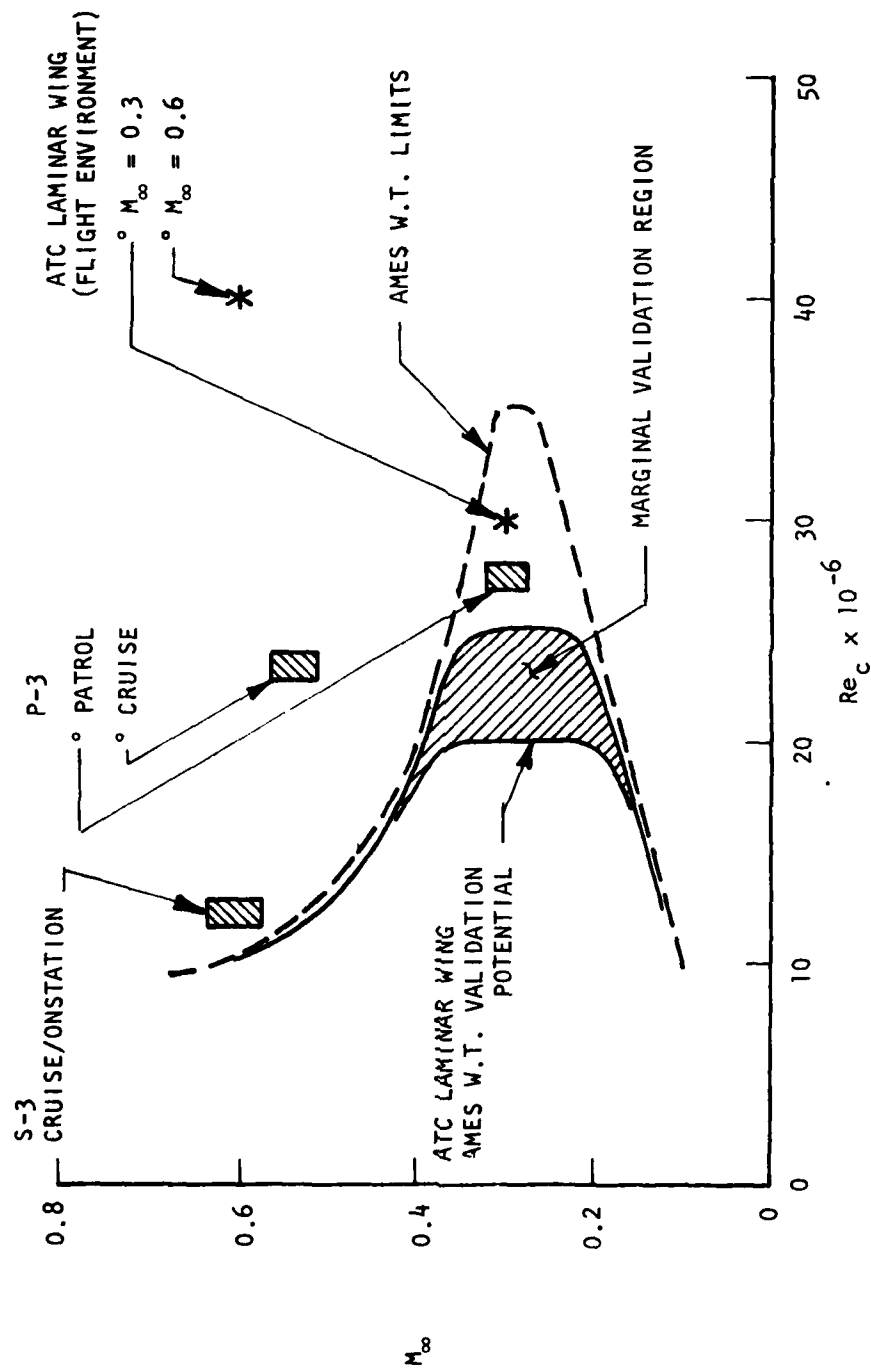FIGURE 5-10   PREDICTED DRAG POLARS FOR $M_\infty=0.3$ TEST ENVIRONMENT

FIGURE 5-11   FULL SCALE M_∞–Re_c VALIDATION POTENTIAL/LIMITATION/APPLICATION
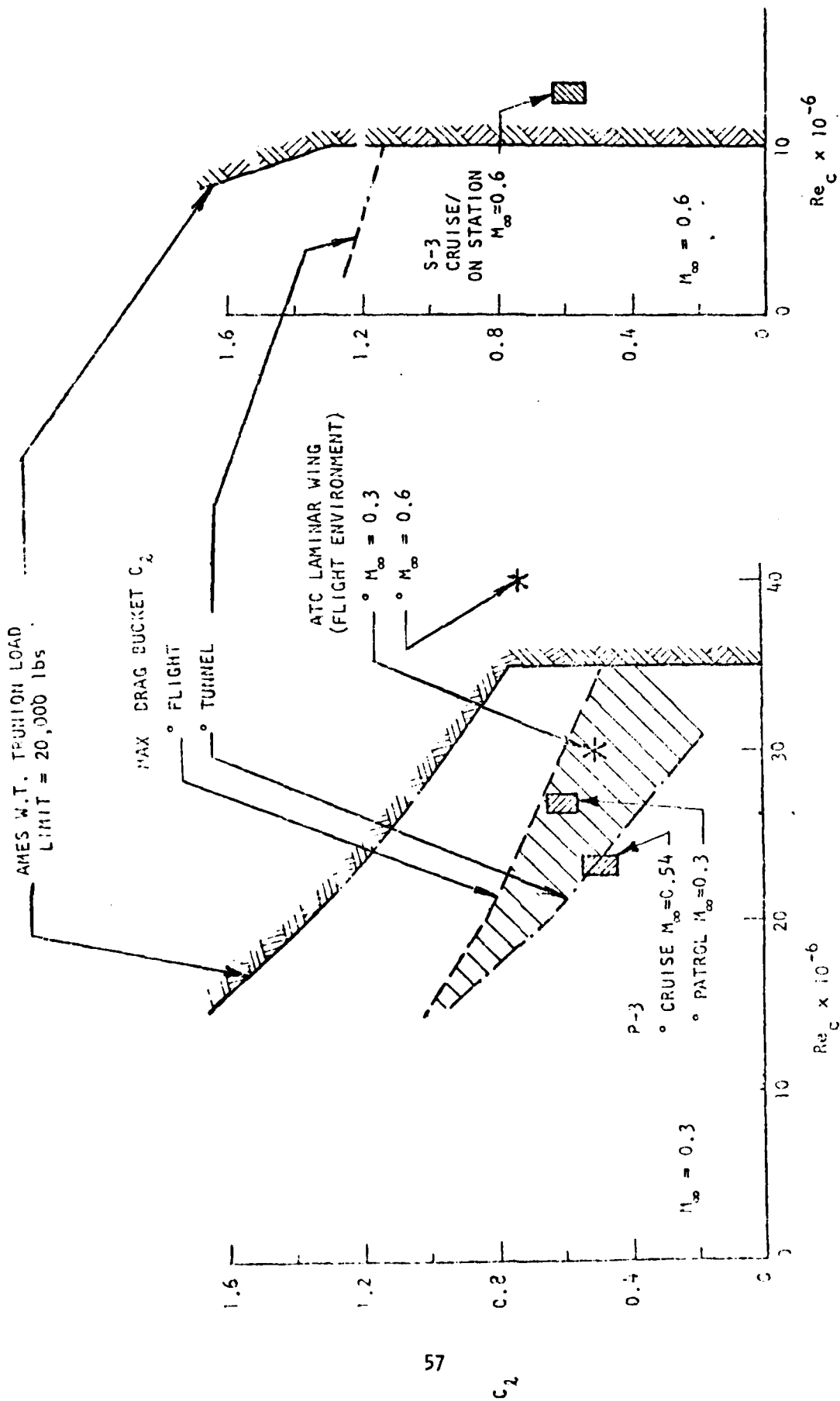
FIGURE 5-12   FULL SCALE C_ℓ-Re_c VALIDATION POTENTIAL/LIMITATION/APPLICATION

57

C_ℓ

tunnel. For the P-3, the cruise point is outside of the tunnel validation capa-
bilities however, the patrol requirements are within the tunnel operating envelope.
Hence, the potential exists for direct application of full scale tunnel validation
tests of the ATC laminar wing concept, to an aircraft configuration. Although the
tunnel validation performance is degraded and limited, portions of the validation
envelopes predicted for the ATC laminar wing address S-3 and P-3 application require-
ments over the range of M_∞. Flight test validation of an ATC/laminar wing/wing glove
configuration is a foreseeable extension to the tunnel validation and examination
of the design/off design performance.

5.5 TEST PRIORITIES

From the tunnel validation assessment, priorities were defined for a proposed
wind tunnel test. The test priorities are:

PRIORITY I: Validate the ATC high Reynolds number laminar flow design concept
(M_∞ = 0.3, 0.6) within tunnel Re_c limits.

o Validate the airfoil predicted performance C_ℓ, C_d, C_μ and C_p distributions.

o Validate passive laminar flow design integrations with active trailing
edge boundary layer control.

o Validate laminar stability theoretical predictions for high Reynolds
number laminar flow.

o Define transition location on upper and lower surface
(Monitor RMS signals from individual pressure transducers.)

o Determine change in tunnel turbulence intensity level with model present.
(Turbulence intensity measurements taken in the tunnel by Harvey
of NASA Langley, will be used as the data base.)

o Define model vibration RMS level/spectrum.

o Define C_ℓ and C_d degradations for forced transition at design/off design C_μ.

PRIORITY II: Demonstrate off design performance (M_∞ = 0.4, M_{DD})

o Define cruise drag divergence Mach number M_{DD}.

o Examine intermediate Mach number performance.

PRIORITY III: Examine laminar boundary layer stability for alternate trailing
edge camber. (M_∞ = 0.3, 0.6, M_{DD})

o Define transition performance at cruise conditions with a different
pressure gradient associated with the change in trailing edge camber.

o Define increases in cruise M_{DD} performance with decreased trailing edge camber.

A proposed test plan to achieve the above validation is shown in Table I. Each run is identified by an angle of attack scan. Priority I test plan consists of 47 runs with Priority II and III containing a total of 24 runs. Priority I tests will be concerned with detailed laminar boundary layer transition effects on performance, while Priority II and III tests are concerned with general performance characteristics.

TABLE I

ATC LAMINAR AIRFOIL PRELIMINARY TEST PLAN

PRIORITY I

MACH NUMBER	REYNOLDS NUMBER x10^{-6}	C_μ	NO* RUNS	TEST DESCRIPTION
0.3	20	0.005	1	CHECKOUT
↓ 0.6 →	34, 30, 25, 20 15, 10	0.0, 0.002, 0.005 0.010, 0.02	30	LOW MACH NUMBER VALIDATION
	30, 20	0.002, 0.010	4	FORCED TRANSITION
	10, 8	0.0, 0.002, 0.005 0.010	8	HIGH MACH NUMBER VALIDATION
	10, 8	0.002, 0.010	4	FORCED TRANSITION

PRIORITY II

0.4, M_{DD}	MAX, INTERMEDIATE	0.002, 0.005, 0.010	12	INTERMEDIATE M_∞/M_{DD} VALIDATION

PRIORITY III

0.3, 0.6, M_{DD}	MAX, INTERMEDIATE	0.002, 0.005	12	OFF DESIGN CAMBER VALIDATION

* Each Run is a Full Angle of Attack Scan (-5° to Stall).

60

6.0 MODEL DESIGN/INSTRUMENTATION

6.1 MODEL DESIGN

A preliminary two-dimensional (2-D) ATC/laminar airfoil model design was defined directed toward follow-on entry in the Ames 12 foot pressure tunnel. A sketch of the proposed model installation is shown in Figure 6-1. The proposed 2-D model is mounted horizontally in the tunnel spanning the width of the test section, 11 feet 3 inches (3.429 m), with a 4 foot (1.2 m) chord. The model is mounted on the center line of the tunnel with a center of rotation near mid chord. A traversing wake rake, required for the drag data acquisition, is to be located approximately 1.5 chord lengths aft of the model trailing edge.

A sketch of the 2-D ATC/laminar airfoil model assembly and segmented views are shown in Figures 6-2 and 6-3. The general features of the model design include; blowing plenum/jet with an adjustable lip for controlling C_μ, trailing edge section with flap capability for off-design testing, and storage areas for instrumentation and high pressure air lines. The model blowing plenums are divided into 3 sections, providing model/end plate turbulent boundary layer control independent of an instrumented center span blowing section. The outboard plenums have a span of approximately 3 feet (0.914 m) with a center span plenum having a length of 5 feet (1.52 m). Two separate high pressure auxiliary air lines are piped to the two different types of plenums. To route the high pressure air from the source, at the tunnel outer pressure chamber, to the model would require· additional equipment. A sketch identifying the auxiliary equipment is shown in Figure 6-4. The high pressure air is piped through each end of the model support into the model as illustrated in Figures 6-4 and 6-5.

The model fabrication tolerances were identified from the correlation obtained in the ABLC experiments for the prevention of transition onset. To insure that the model surface maintains laminar flow, the hydraulic smoothness criteria, $Re_K = 25$, was used to identify the K_{crit} for the surface perturbations. Note however this Re_K (25) value is a conservative value in terms of the ABLC test results for the discrete roughness, $Re_K = 100-200$. The model K_{crit} values for the tunnel maximum operating conditions at $M_\infty = 0.3$ and 0.6 are identified in Figure 6-6. The maximum allowable surface K_{crit} value is established by the high Re_c (3×10^7) low M_∞ (0.3) test case. To identify the model critical static pressure orifice size, needed for pressure measurements, a K_{crit} factor of 20 identified by the ABLC roughness and gap/slot test results was used. The factor of 20 was applied to the

61

FIGURE 6-1   NASA-AMES 12 FOOT PRESSURE TUNNEL - TEST SECTION

BLOWING JET

TRAILING EDGE WITH
FLAP CAPABILITY

ADJUSTABLE LIP

BLOWING PLENUM

CHORD = 4 ft (1.2 m)
SPAN = 11 ft, 3 in (3.393 m)

UPPER SURFACE PANEL

INSTRUMENTATION
STORAGE AREA

HIGH PRESSURE AIR HOSES

LOWER SURFACE PANEL
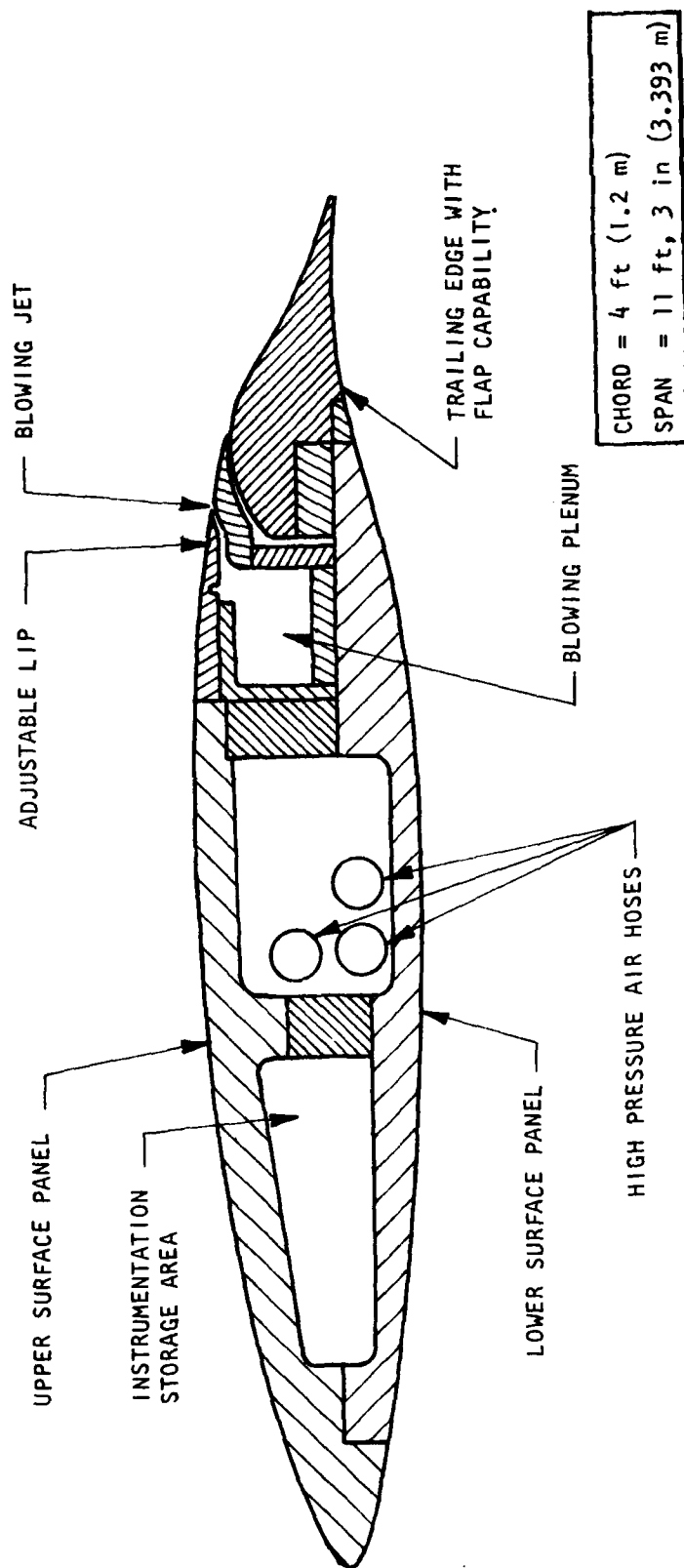
FIGURE 6-2 PRELIMINARY ATC AIRFOIL MODEL DESIGN

① UPPER SURFACE PANEL
② LOWER SURFACE PANEL
③ BLOWING PLENUM/LIP
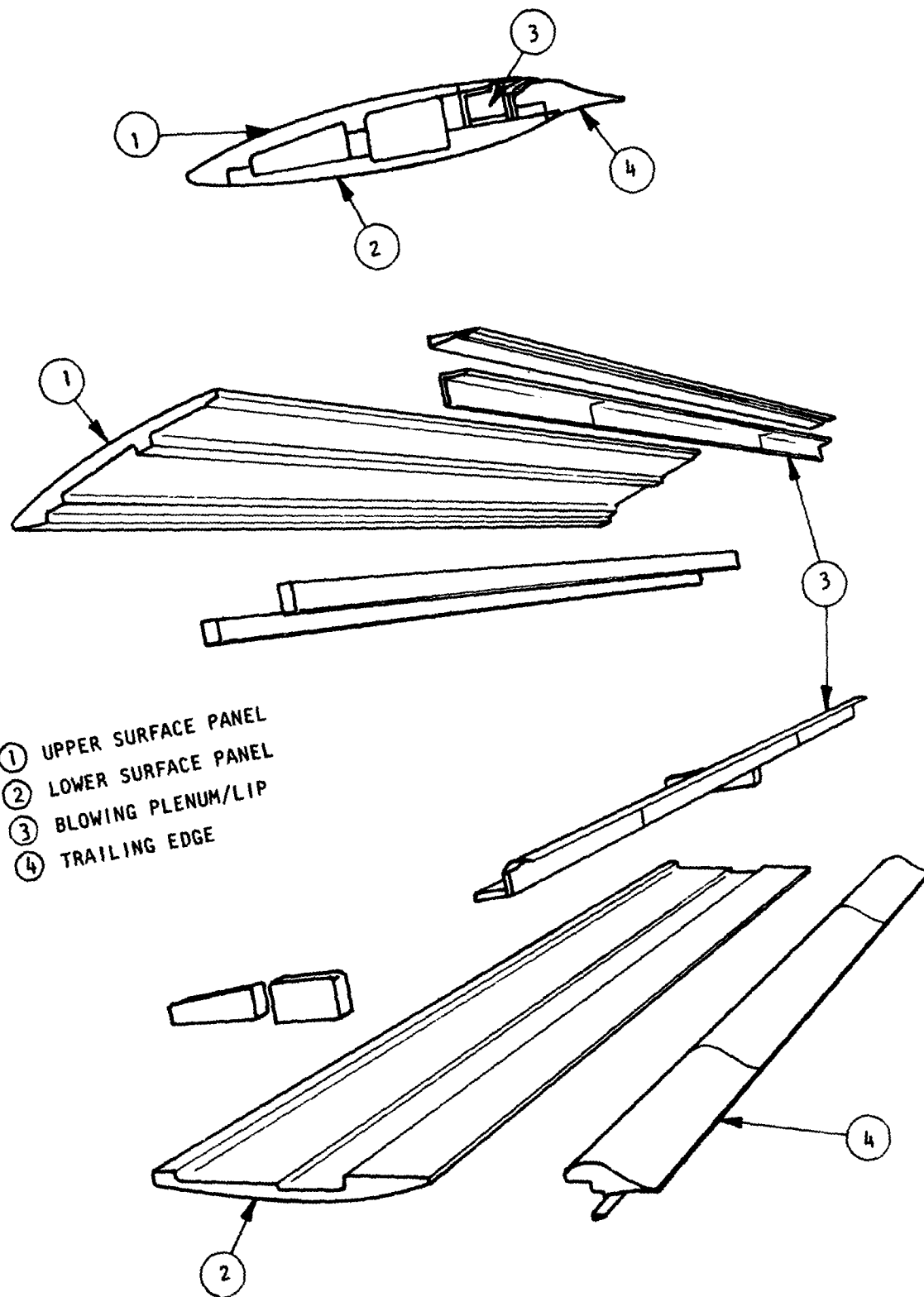④ TRAILING EDGE
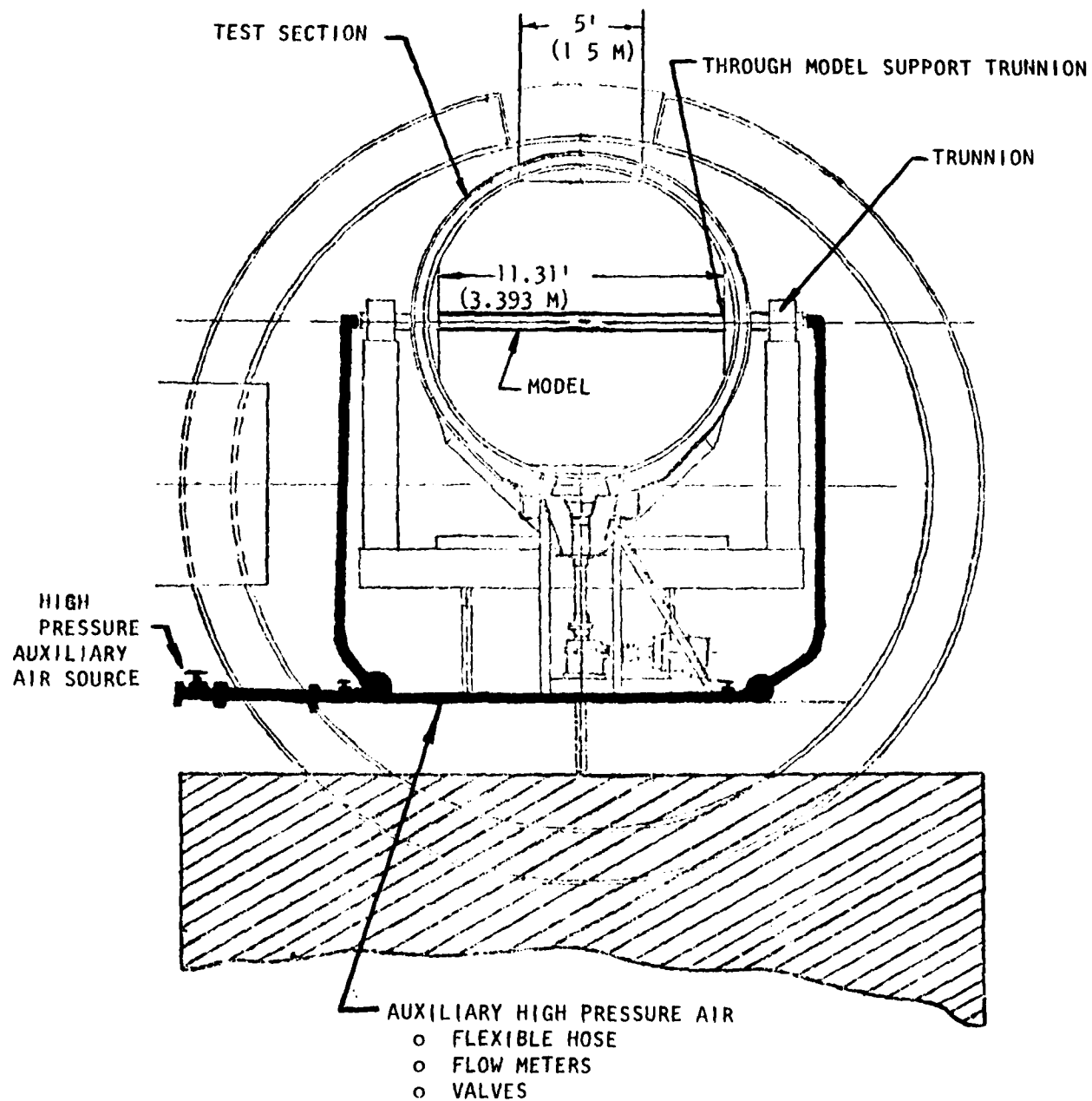
FIGURE 6-3 ATC AIRFOIL ASSEMBLY

FIGURE 6-4   NASA-AMES 12 FOOT PRESSURE TUNNEL - TEST SECTION
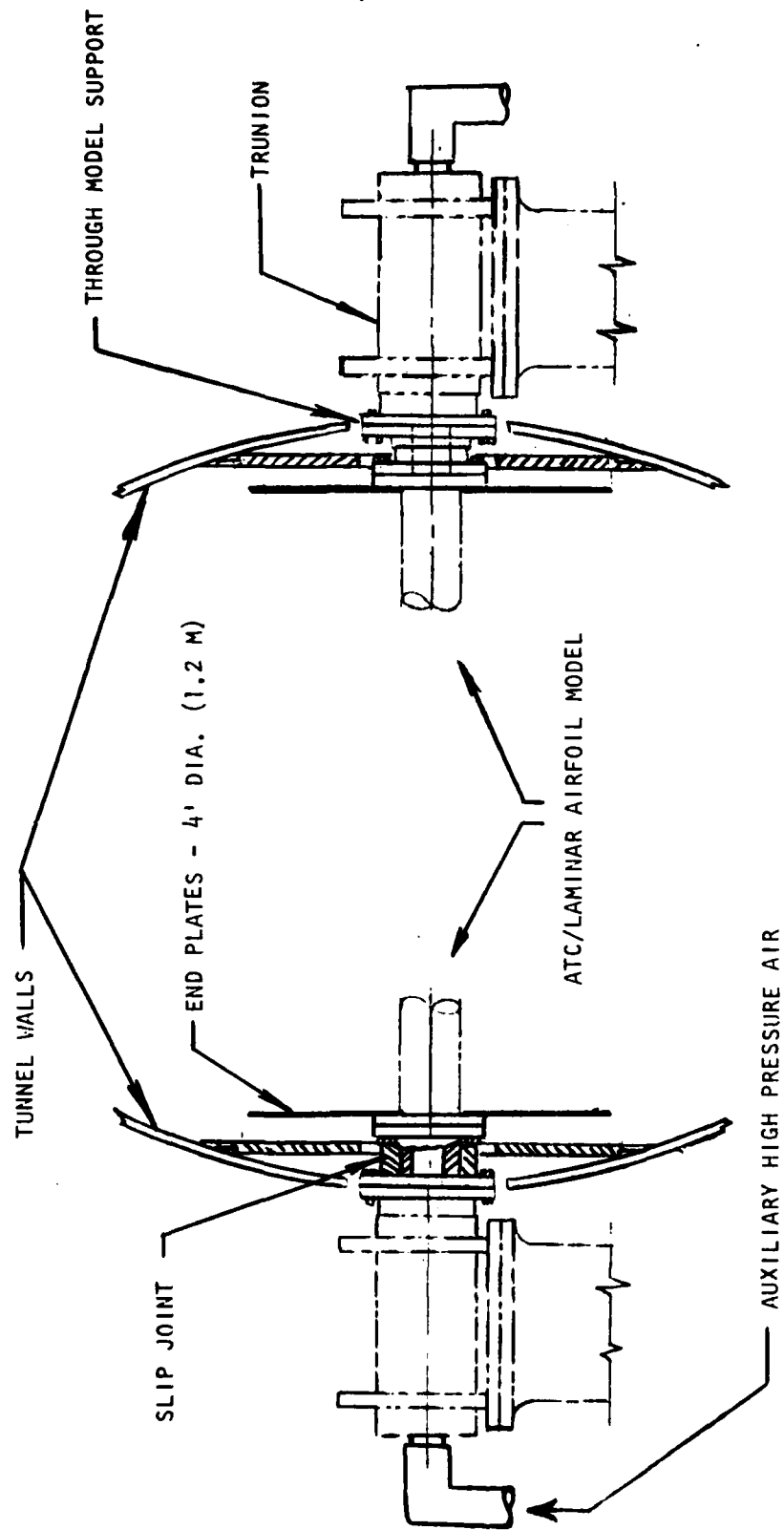
FIGURE 6-5   NASA-AMES 12 FOOT PRESSURE TUNNEL - TRUNNION MODEL SUPPORT

66
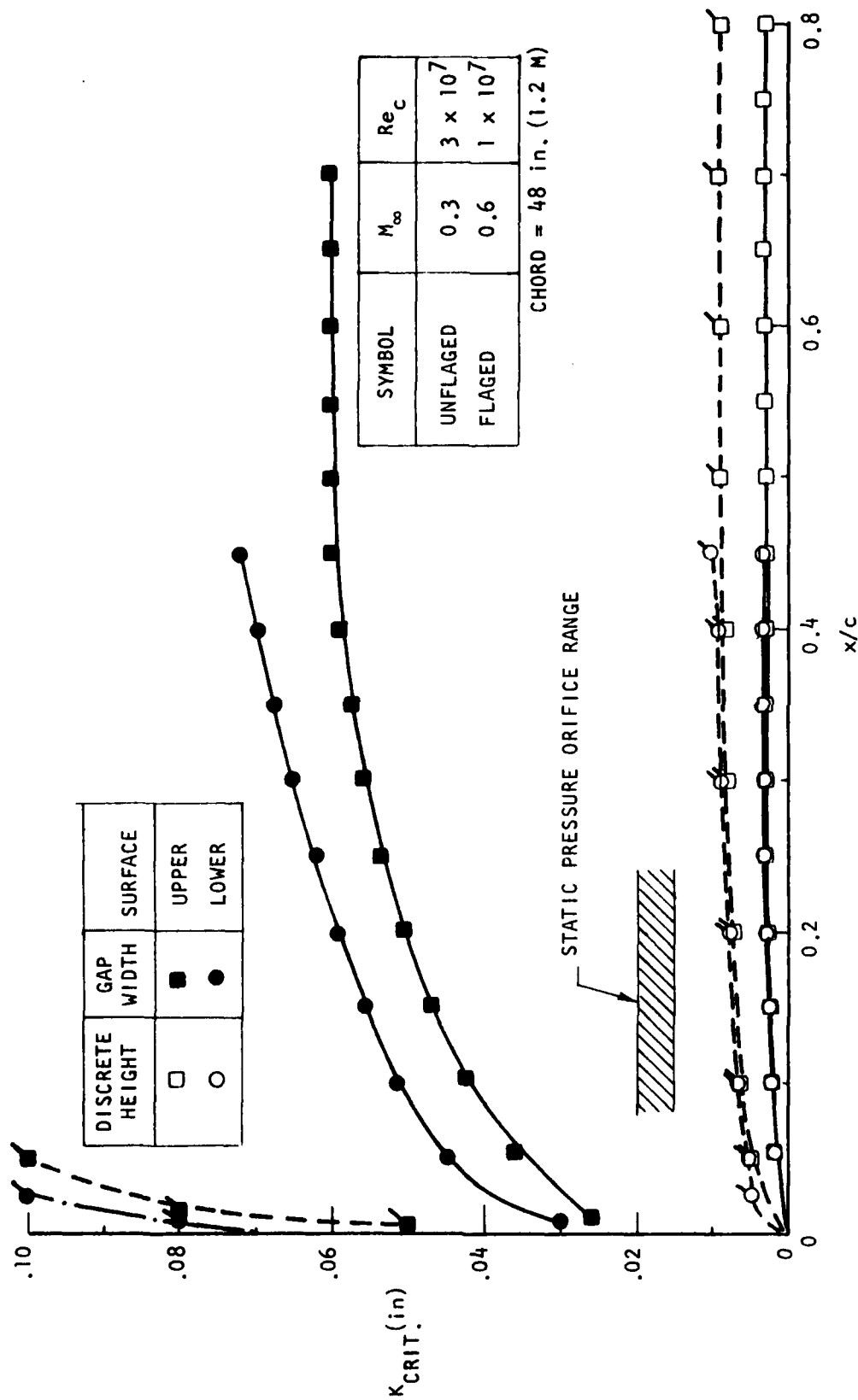
FIGURE 6-6. MODEL CRITICAL ROUGHNESS

conservative discrete roughness values defined by the $Re_K = 25$. For a static pressure orifice diameter range of 0.015 to 0.02 inches (0.0381 - 0.05 cm) a safety margin of 2-3 is predicted for the most critical test case.

6.2 TEST SUPPORT INSTRUMENTATION

The instrumentation required for the proposed tunnel validation test is illustrated in Figure 6-7. Some of the specific equipment and requirements of the instrumentation and test support facility are listed below:

1. <u>Lift/Drag Performance</u> - Priority I Testing

    A. Wake rake

        o Need the capability of flow alignment with model wake flow field while a test is in progress.

        o Approximate size; 30 static pressures and 150 total pressure probes.

    B. Scanning-type pressure valves for the wing and wake rake.

        o Wing - C_p

            (1) Static pressures - (75 taps)

            (2) Total pressures (inside high pressure air plenum) - (4 probes)

        o Wake Rake

            (1) Static pressure - (30)

            (2) Total pressure - (150)

2. <u>Transition Information</u> - Priority I Testing

    A. Tunnel turbulence intensity measurements

        o Hot wire system - (1 channel)

    B. Laminar boundary layer transition definition

        o Pressure transducers, conditioners and power supply   -(10-14 channels)

        o Multiple channel signal amplifier/conditioner   -(10-14 channels)

        o Multiple channel scanner true RMS meter   -(10-14 channels)

        o Spectro Analyzer

        o Real time paper trace read out of RMS signal   -(10-14 channels)

    C. Model Vibration

        o Accelerometer   - (1 unit)

Wake Rake

Scanie Valve

PLOTS

o C_p vs X/C
o C_d vs Y/C

DC Power Supply

Scanie Valve

Pressure Transducers & Conditioners

REAL TIME OUTPUT

o Integrated C_ℓ Value
o Integrated C_d Value
o C_μ Value
o C_p & C_d Distribution

Tunnel Hot Wire (Turbulence Intensity)

Tunnel Mic

Accelerometer

Mic

High Pressure Air Supply

Signal Conditioner Amplifiers

FM Multi-Track Recorder

True RMS/Spectro Analyzer

Real Time RMS Paper Trace

FLOW METERS

o Mid Section
o Outboard Sections

FIGURE 6-7 ATC/LAMINAR AIRFOIL INSTRUMENTATION

69

3. <u>High Pressure Air Supply</u> - Priority I Testing

   A. Air Supply Requirements
      o $(Po_J/Po_\infty)_{Max} = 2.5$
      o $\dot{m}_{Jmax} = 0.03$ lbm/sec

   B. High pressure air flow meters and appropriate instrumentation
      (pressure transducers and temperature sensors)   (2 units)

4. <u>Additional Instrumentation</u> (Lower Priority)

      o FM multiple track recorder - (18 channels)
      o Acoustic measurements in tunnel/model - (2 units)

7.0 CONCLUSIONS

A high chord Reynolds number ATC/laminar airfoil geometry was defined providing a high L/D potential. The airfoil design point corresponds to a $C_\ell = 0.73$ at a $M_\infty = 0.6$ and $Re_c = 4 \times 10^7$ with a L/D = 240. The ATC/laminar airfoil design concept is an integration of passive laminar flow stabilization with active diffusion control to provide a highly energy efficient concept. At the design point C_ℓ (0.73), the laminar flow region extends to 80 and 44 percent of the upper and lower surfaces, respectively. The corresponding stability analysis of the large upper surface laminar region exhibits a very stable passive laminar flow design. This is demonstrated by the low value of maximum spatial amplification ratio of 4.5, up to the wall jet, well below the transition onset criteria of 9. An additional benefit of the ATC laminar airfoil concept is the potential for off-design high maneuvering lifts obtained with the integration of blowing and trailing edge camber. The ATC/laminar airfoil concept is a simple geometry configuration providing the "best of two worlds"; (1) low drag cruise design C_ℓ (0.73), M_∞ (0.6) and Re_c (4×10^7), at a high L/D = 240, and (2) high maneuvering lifts at low drag levels associated with C_p roof-top loading and BLC.

Full scale high Reynolds number passive laminar flow stabilization experiments were conducted in an Air Boundary Layer Channel (ABLC) simulating the airfoil upper surface velocity distribution from X/C = 0.0 to 0.8. Three major experiments were conducted in an Air Boundary Layer Channel (ABLC). Three major experiments were performed; (1) validation of the passive laminar flow concept, (2) examination of real flow freestream turbulence intensity influence, and (3) identification of fabrication tolerance. Validation of the ATC/laminar airfoil upper surface passive laminar flow concept was obtained at the design point $Re_{tran} = 40 \times 10^6$ and was extended to a $Re_{tran} = 48 \times 10^6$. The tests were very stable and repeatable for the entire high Reynolds number operating range from 40×10^6 to 48×10^6. Examination of the real flow freestream turbulence intensity influence identified a strong dependency of maximum Re_{tran} performance on the level of intensity. For the design point Reynolds number (4×10^7) the stable margin between maximum spatial amplification ratio of 4.5 and transition onset of 9 represents the transition onset resistance to real flow influences. This is demonstrated by a critical turbulence intensity value of 0.1%, at $Re_{tran} = 4 \times 10^7$, approximately 4-5 times larger than the flight environment. The ATC/laminar airfoil critical fabrication tolerances were identified from discrete roughness height and gap/slot width transition onset tests. The critical $Re_K = U_k K/\nu$ values for the discrete roughness data ranged from 100 to 200,

while the gap-slot width data ranged from 20,000 to 45,000. This quantified the importance of protuberances in design considerations. Applying these critical values to full scale aircraft configurations identifies tolerance levels well within the capabilities of present day composite wing technology. The ABLC proved to be a unique facility for performing full scale laminar flow/transition experiments and controlling the test environment.

An analytical examination was performed of real flow perturbation parameters which potentially influence the airfoil design point performance. These parameters included unit Reynolds number scaling, model/freestream temperature difference, freestream turbulence, and crossflow disturbances. It was determined that unit Reynolds number does not influence the transition onset correlation (e^9), but does directly influence the local boundary layer parameters which govern the critical surface tolerances. Examination of model/freestream temperature difference identified potential trade-offs for the ATC/laminar airfoil design concept. For example, a heated wing stability analysis, representative of a de-icing requirement, does not appear to degrade the airfoil design point performance while the alternative of cooling the wing surfaces indicates substantial improvement in laminar flow stabilization. Examination of three-dimensional crossflow effects identified passive laminar flow design considerations for swept wing configurations. Although a swept wing configuration is not required for the subsonic design point M_∞ (0.6), the prospect of extending the concept applications to higher transonic Mach numbers opens new possibilities for low drag spanwise optimization.

A detailed examination of the ATC/laminar airfoil performance, subject to candidate wind tunnel and flight test environments and operating envelopes, verified the test validation potential. Even with the strong coupling in a wind tunnel facility between M_∞, Re_c, and freestream turbulence, all critical features of the concept can be demonstrated. The high Re_c ($\geq 35 \times 10^6$) characteristics of the upper surface stabilization can be validated at $M_\infty = 0.3$ and low angle of attack. Overall high Re_c results for design/off-design airfoil stabilization and blowing can be simulated at $M_\infty = 0.3$ and $Re_c \sim 25 \times 10^5$. Compressibility effects can be determined by testing at $M_\infty = 0.6$, $Re_c = 10 \times 10^6$. Measured C_ℓ, C_d, C_μ, and C_p distributions, along with flow disturbance data, perturbation analysis, and performance predictions from the present effort, will

provide for a high confidence level wind tunnel validation of both conceptual and
predictive approaches. Preliminary design studies of test hardware/accessory re-
quirements reinforce the practicality of the wind tunnel tests. The present study
also indicates flight testing to be a viable direct validation candidate, sub-
sequent to preliminary tunnel testing to ascertain flying quality limits.

8.0 RECOMMENDATIONS

The present contract has provided a firm design and evaluation data base for
the ATC/laminar airfoil concept and has provided supportive experimental results
from Air Boundary Layer Channel simulations. Two specific recommendations for
additional study follow from this data base; (1) wind tunnel validation of the
design concept, and (2) extension of the concept to transonic swept wing configura-
tions. A two-dimensional wind tunnel validation of the ATC/laminar airfoil
concept, as discussed in Section 7.0, would provide the necessary data for
evaluating optimum performance of the integrated design. The tunnel test would
also provide validation of prediction methods and empirical correlations and
lay the groundwork for subsequent flight testing. Extension of the ATC/laminar
wing concept to transonic speeds, lower chord Reynolds numbers, and swept wing
configurations has the potential for new flexibility in low drag flight vehicle
optimization. An analytical design study for a three-dimensional finite swept
wing configuration incorporating the features of passive stabilization and coupled
active diffusion control would be the initial step. Use would be made of super-
critical results from validations already performed for active diffusion control
airfoils.[5,6] This effort would lead into full scale wind tunnel/flight demonstra-
tions of the passive-diffusion control coupling.

9.0 REFERENCES

1. Allison, Dennis O. and Dagenhart, John R., "Design of a Laminar-Flow-Control Supercritical Airfoil for a Swept Wing," NASA CP-2036, N78-27069, June 1978.

2. Frenninger, W., Reed, Helen L., and Dagenhart, J. R., "Design Considerations of Advanced Supercritical Low Drag Suction Airfoils," presented at the Symposium on Viscous Drag Reduction, Dallas, Texas, November 1979.

3. Haight, C. H., "Design Procedures for a Transonic Airfoil Employing Active Diffusion Control," ATC Report No. B-94300/6TR-2, January 1976.

4. Mask, R. L., and Krall, K. M., "Low Speed Wind Tunnel Test of an ATC Optimized High Lift Wing," ATC Report No. B-94300/4TR-34, August 1974.

5. Haight, C. H., and Spangler, J. G., "Test Verification of a Transonic Airfoil Design Employing Active Diffusion Control," ATC Report No. B-94300/5CR-34, June 13, 1975, NADC Contract No. N62269-74-C-0517.

6. Haight, C. H., and Mask, R. L., "Validation of a Transonic Maneuver/Cruise Airfoil Design Employing Active Diffusion Control - Final Report," ATC Report No. B-91100/8CR-84, December 1977, NADC Contract No. N62269-76-C-0318.

7. Bauer, F., Garabedian, P., Korn, D. and Jameson, A., Supercritical Wing Sections II, Lecture Notes in Economics and Mathematical Systems, Springer-Verlag, New York, 1975.

8. Bauer, F., Garabedian, P. and Korn, D., Supercritical Wing Section III, Lecture Notes in Economics and Mathematical Systems, Springer-Verlag, New York, 1977.

9. Gentry, A. E. and Wasson, A. R., "The Transition Analysis Program System," Volume I and II, Report No. NDC J7255/02, June 1976, NASC Contract N00024-75-C-7205.

10. Smith, A. M. O. and Gamberoni, N., "Transition, Pressure Gradient, and Stability," Proc. Int. Congr. Appl. Mech., 9th Brussels, Belgium 4, 234. Also, AD125559, 1956.

11. Stratford, B. S., "The Prediction of Separation of the Turbulent Boundary Layer," J. Fluid Mechanics, Vol. 5, pp. 1-16, 1959.

12. Stratford, B. S., "An Experimental Flow with Zero Skin Friction Throughout its Region of Pressure Rise," Vol. 5, J. Fluid Mechanics, pp. 17-35, July 1958.

13. McNally, William D., "Fortran Program for Calculating Compressible Laminar and Turbulent Boundary Layers in Arbitrary Pressure Gradients," NASA TN-DD-5681, May 1970.

14. Cebeci, T., and Smith, A. M. O., Analysis of Turbulent Boundary Layers, Academic Press, New York, 1974.

15. Owen, F. K., Stainback, P. C., and Harvey, W. D., "Evaluation of Flow Quality Measurements in Two NASA Transonic Wind Tunnels," AIAA 12th Fluid and Plasma Dynamics Conference, 79-1532, July 1979.

16. vonDoenhoff, A. E., and Abbott, F. T., Jr., "The Langley Two-Dimensional Low-Turbulence Pressure Tunnel," NACA-TN-1283, May 1947.

17. Dougherty, S., Verbal communication of flight test data, ARO-AEDC, October, 1978.

18. Wells, C. S. and Spangler, J. G., "A Facility for Basic Boundary Layer Experiments," Report No. 0-71000/2R-32, November 1962.

19. Wallace, D. B. and Spangler, J. G., "Disturbance Effects on Boundary Layer Transition in the Presence of a Strong Favorable Pressure Gradient," Final Report Contract No. N000140-76-C-6627, ATC Report No. B-94300/7CR-53, June 1977.

20. Schlichting, H., Boundary Layer Theory, McGraw-Hill Book Company, New York, 1968.

21. Smith, A. M. O. and Clutter, D. W., "The Smallest Height of Roughness Capable of Affecting Boundary-Layer Transition," Journal of Aero/Space Sciences, April, 1959.

22. Potter, J. L., "The Unit Reynolds Number Effect on Boundary-Layer Transition, Dissertation, Vanderbilt University, 1974.

23. Jaffe, N. A., Okamura, T. T., and Smith A. M. O., "Determination of Spatial Amplification Factors and their Application to Predicting Transition," AIAA Journal, page 301-308, February 1970.

24. Tucker, Maurice, "Combined Effect of Damping Screens and Stream Convergence on Turbulence," NACA-TN-2878, June 1953.

25. Mack, Leslie M., "Transition and Laminar Instability," JPL Publication 77-15, NASA-CP-153203, May 15, 1977.

26. Srokowski, A. J., Sally Level II User's Guide, Langley Research Center, January 1979.

27. Leehey, P., "The Influence of Environment in Laminar Boundary Layer Control," presented at the Symposium on Viscous Drag Reduction, Dallas, Texas, November 1979.